AD-A129 757 ROTOR NOISE DUE TO BLADE-TURBULENCE INTERACTION(U) 1/2
PENNSYLVANIA STATE UNIV UNIVERSITY PARK APPLIED
RESEARCH LAB K ISHIMARU 25 JAN 83 ARL/PSU/TM-83-27
UNCLASSIFIED N00024-79-C-6043 F/G 20/1 NL

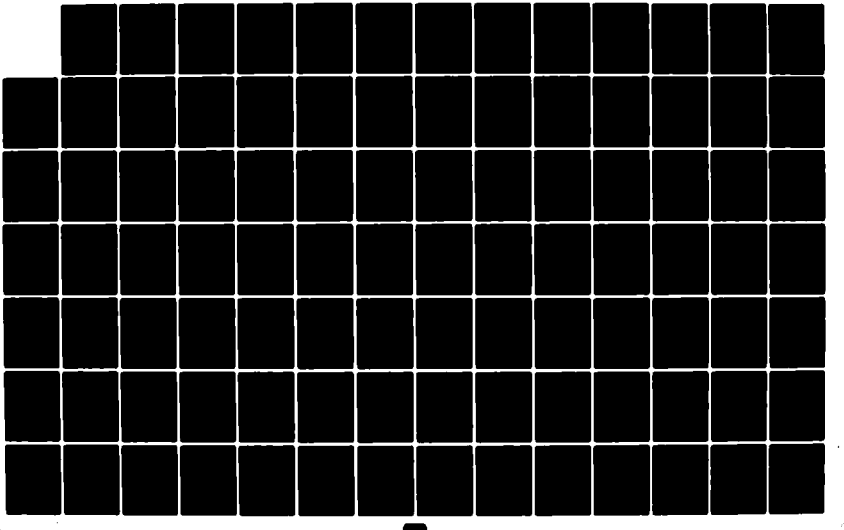

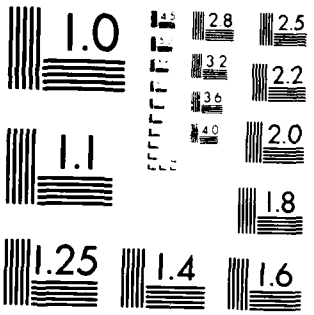

ROTOR NOISE DUE TO BLADE-TURBULENCE INTERACTION

K. Ishimaru

Technical Memorandum
File No. TM 83-27
January 25, 1983
Contract No. N00024-79-C-6043

Copy No. 23

The Pennsylvania State University
Applied Research Laboratory
Post Office Box 30
State College, PA 16801

Approved for Public Release

Distribution Unlimited

NAVY DEPARTMENT

NAVAL SEA SYSTEMS COMMAND

UNCLASSIFIED

SECURITY CLASSIFICATION OF THIS PAGE *(When Data Entered)*

REPORT DOCUMENTATION PAGE	READ INSTRUCTIONS BEFORE COMPLETING FORM
1. REPORT NUMBER: 83-27	2. GOVT ACCESSION NO.: AD-A129 757
	3. RECIPIENT'S CATALOG NUMBER:
4. TITLE *(and Subtitle)*: ROTOR NOISE DUE TO BLADE-TURBULANCE INTERACTION	5. TYPE OF REPORT & PERIOD COVERED: Ph.D., Thesis, May 1983
	6. PERFORMING ORG. REPORT NUMBER: 83-27
7. AUTHOR(s): Kiyoto Ishimaru	8. CONTRACT OR GRANT NUMBER(s): N00024-79-C-6043
9. PERFORMING ORGANIZATION NAME AND ADDRESS: The Pennsylvania State University, Applied Research Laboratory, P.O. Box 30, State College, PA 16801	10. PROGRAM ELEMENT, PROJECT, TASK AREA & WORK UNIT NUMBERS:
11. CONTROLLING OFFICE NAME AND ADDRESS: Naval Sea Systems Command, Department of the Navy, Washington, DC 20362	12. REPORT DATE: January 25, 1983
	13. NUMBER OF PAGES: 108 pages
14. MONITORING AGENCY NAME & ADDRESS*(if different from Controlling Office)*:	15. SECURITY CLASS. *(of this report)*: Unclassified, Unlimited
	15a. DECLASSIFICATION DOWNGRADING SCHEDULE:
16. DISTRIBUTION STATEMENT *(of this Report)*: Approved for public release, distribution unlimited, per NSSC (Naval Sea Systems Command), 12 April 1983	
17. DISTRIBUTION STATEMENT *(of the abstract entered in Block 20, if different from Report)*:	
18. SUPPLEMENTARY NOTES:	
19. KEY WORDS *(Continue on reverse side if necessary and identify by block number)*: rotor, noise	

20. ABSTRACT *(Continue on reverse side if necessary and identify by block number)*

The time-averaged intensity density function of the acoustic radiation from rotating blades is derived by replacing blades with rotating dipoles. This derivation is done under the following turbulent inflow conditions: turbulent ingestion with no inlet strut wakes, inflow turbulence elongation and contraction with no inlet strut wakes, and inlet strut wakes.

Dimensional analysis reveals two non-dimensional parameters which play important roles in generating the blade-passing frequency tone and its multiples.

DD FORM 1 JAN 73 1473 EDITION OF 1 NOV 65 IS OBSOLETE

UNCLASSIFIED

SECURITY CLASSIFICATION OF THIS PAGE *(When Data Entered)*

The elongation and contraction of inflow turbulence has a strong effect on the generation of the blade-passing frequency tone and its multiples. Increasing the number of rotor blades widens the peak at the blade-passing frequency and its multiples. Increasing the rotational speed widens the peak under the condition that the non-dimensional parameter involving the rotational speed is fixed. The number of struts and blades should be chosen so that (the least common multiple of them)·(rotational speed) is in the cutoff range of Sears' function, in order to minimize the effect of the mean flow deficit on the time averaged intensity density function. The acoustic intensity density function is not necessarily stationary even if the inflow turbulence is homogeneous and isotropic. The time variation of the propagation path due to the rotation should be considered in the computation of the intensity density function; for instance, in the present rotor specification, the rotor radius is about 0.3 m and the rotational speed Mach number is about 0.2.

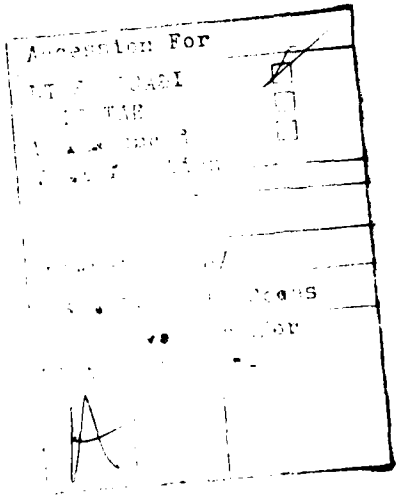

ABSTRACT

The time-averaged intensity density function of the acoustic radiation from rotating blades is derived by replacing blades with rotating dipoles. This derivation is done under the following turbulent inflow conditions: turbulent ingestion with no inlet strut wakes, inflow turbulence elongation and contraction with no inlet strut wakes, and inlet strut wakes.

Dimensional analysis reveals two non-dimensional parameters which play important roles in generating the blade-passing frequency tone and its multiples. The elongation and contraction of inflow turbulence has a strong effect on the generation of the blade-passing frequency tone and its multiples. Increasing the number of rotor blades widens the peak at the blade-passing frequency and its multiples. Increasing the rotational speed widens the peak under the condition that the non-dimensional parameter involving the rotational speed is fixed. The number of struts and blades should be chosen so that (the least common multiple of them)·(rotational speed) is in the cutoff range of Sears' function, in order to minimize the effect of the mean flow deficit on the time averaged intensity density function. The acoustic intensity density function is not necessarily stationary even if the inflow turbulence is homogeneous and isotropic. The time variation of the propagation path due to the rotation should be considered in the computation of the intensity density function;

for instance, in the present rotor specification, the rotor radius is about 0.3 m and the rotational speed Mach number is about 0.2.

TABLE OF CONTENTS

LIST OF FIGURES

NOMENCLATURE

a	speed of sound
$a_n^{(p)}$	Fourier coefficient as defined in Eq. (4.42)
$b_n^{(p)}$	Fourier coefficient as defined in Eq. (4.44)
B	number of blades
c	chord length
$c_n^{(p)}$	Fourier coefficient as defined in Eq. (4.43)
d	distance between strut trailing edge and rotor leading edge
D_{mn}	distance between observer and n^{th} segment of m^{th} blade
$e_{mn}^{(p)}$	defined in Eq. (2.30)
$\vec{f}$	defined in Eq. (2.3)
$f_{mn}^{(p)}$	defined in Eq. (2.31)
$g_n(\tau)$	defined in Eq. (4.40)
$H_{mn}(\omega)$	transfer function of n^{th} segment of m^{th} blade
j	$(-1)^{1/2}$
k	integer
$\vec{k}$	wavenumber
$\vec{\ell}_{mn}(\tau)$	lift per unit span on n^{th} segment of m^{th} blade
$\ell_{mn}(\tau)$	modular of $\vec{\ell}_{mn}(\tau)$
m	integer
$M_{mn}(\tau)$	mean flow at n^{th} segment of m^{th} blade
N	number of segments

p, p_1, p_2	harmonic number
$P(r, \phi, t)$	pressure at observer
q	harmonic number
r, θ, ϕ	spherical coordinates for observer
R, ϕ, Z	cylindrical coordinates for rotor
ΔR_n	length of n^{th} segment of blade
R_T	radial position of typical segment of blade
$\mathcal{R}^{ii}_{mnk\ell}(\alpha)$	correlation function of upwash of inflow turbulence between n^{th} segment of m^{th} blade and ℓ^{th} segment of k^{th} blade
$\mathcal{R}^{qq}_{mnk\ell}(\alpha)$	correlation function of upwash of wake turbulence of q^{th} strut between n^{th} segment of m^{th} blade and ℓ^{th} segment of k^{th} blade
$\mathcal{R}^{uu}_{mnk\ell}(\alpha)$	correlation function of upwash between n^{th} segment of m^{th} blade and ℓ^{th} segment of k^{th} blade
s, s_1, s_2	harmonic number
$S^{ii}_{mnk\ell}(\omega)$	Fourier transform of $\mathcal{R}^{ii}_{mnk\ell}(\alpha)$
$S^{ww}_{mnk\ell}(\omega)$	Fourier transform of $\mathcal{R}^{qq}_{mnk\ell}(\alpha)$
$S^{uu}_{mnk\ell}(\omega)$	Fourier transform of $\mathcal{R}^{uu}_{mnk\ell}(\alpha)$
$S_{PP}(r, \phi, t, \omega)$	instantaneous intensity spectral density function
S	number of struts
t	time associated with observer
$\overline{(u^i)^2}$	mean square value of velocity fluctuation of inflow turbulence
$\overline{(u^w)^2}$	mean square value of velocity fluctuation of wake turbulence
α	time difference
β_T	stagger angle at typical segment

β_{mn}	stagger angle at n^{th} segment of m^{th} blade
γ	turbulence contraction rate
δ	turbulence elongation rate
Λ	integral length scale
$\delta(x)$	Dirac delta function
δ_{so}	Kronecker delta where o is zero
ω	angular frequency associated with sound
Ω	rotational speed of blade (rad/sec)
τ	time associated with noise source
Φ_m	$2\pi m/B$
$\langle\ \rangle$	time average over $2\pi/\Omega$ (sec)
$\mathfrak{F}(\ )$	Fourier transform
*	convolution integral

Superscripts

i	inflow turbulence
$(p),(p_1),(p_2)$	harmonic number
(q)	harmonic number
q	q^{th} strut
$(s),(s_1),(s_2)$	harmonic number
u	upwash to blade
w	wake turbulence
*	complex conjugate

Subscripts

B	B rotor blades
i	inflow
k	k^{th} blade
ℓ	ℓ^{th} segment of blade
m	m^{th} blade

n	n^{th} segment of blade
p	acoustic pressure
R	rotor
S	strut
T	typical segment

Fourier Transform Pair

$$F(\omega) = \int_{-\infty}^{\infty} f(t)e^{-j\omega t}dt$$

$$f(t) = \frac{1}{2\pi}\int_{-\infty}^{\infty} F(\omega)e^{j\omega t}d\omega$$

ACKNOWLEDGEMENTS

The author gratefully acknowledges Dr. D. E. Thompson, who suggested the thesis topic and served as chairman of his doctoral committee. His guidance and patience will always be remembered and appreciated.

The author would also like to thank Dr. S. I. Hayek, Dr. G. C. Lauchle, and Dr. F. R. Deutsch, who served as members of the author's doctoral committee.

CHAPTER I

INTRODUCTION

1.1. Statement of the Problem

This study attempts to derive the time averaged far field acoustic intensity spectral density function due to the acoustic radiation from (1) low rotational speed rotors operating in frozen, homogeneous, and isotropic turbulence, and (2) low rotational speed rotors behind inlet struts, where the rotor is assumed to be acoustically compact. For the present analysis, the dipole source due to blade/turbulence interaction, as computed by Sears' function, is assumed to be predominant over other radiation sources. A rotating dipole model is pursued so that the effect of the dipole rotation can be accounted for explicitly in the analysis. Sears' function is regarded as an impulse response function of a blade, so that the analysis is done in a time domain and in a frequency domain. There is no blade-to-blade interaction to be included, such as that developed by Kemp, et al. [1]. It is assumed that the inlet struts do not affect the sound propagation and that the distance from the rotor to the duct inlet or exit is much shorter than the sound wavelength so that duct effects on propagation are negligible.

1.2. Previous Investigations of Rotor Noise

Rigorous treatments of the effect of a solid boundary under the influence of a volume distribution of quadrupoles, as in the Lighthill

acoustic analogy approach [2], were done by Curle [3] and Doak [4] for a stationary boundary, and by Ffowcs Williams, et al. [5] for a non-stationary boundary and a rigid surface boundary of a moving body such as that of a rotating blade with a low aspect ratio. Curle derived the sound field as the sum of that generated by a volume distribution of quadrupoles and by a surface distribution of dipoles due to the diffracted wave from the quadrupole and due to the hydro/aerodynamic flow itself; but the distribution of the dipole, such as the tangential component of the dipole on the surface, is difficult to measure. Doak obtained the sound field for the same situation as did Curle, but the former's result concerning the contribution from the surface dipole is based on an easily measurable quantity. Ffowcs Williams, et al. obtained the sound field as the sum of that generated by (1) the quadrupole in a volume distribution, (2) the dipole in a surface distribution, and (3) the monopole in a surface distribution where the monopole is due to the volume displaced by a non-stationary boundary. He found also that in case (3) as for the case of the rigid surface boundary of the moving body, the monopole is broken into another quadrupole and dipole.

In the Lighthill acoustic analogy approach [2], the acoustic radiation source region is assumed to be substantially small, because the observer of the radiation is far from the source region, so that the propagation and source terms are separable and the non-linear effect is regarded as the source term in the acoustic wave equation. In other words, the source distribution does not affect the acoustic propagation or, more precisely, the region where the acoustic field is to be computed does not overlap with the source region, so that no

convection effects are involved in the acoustic wave propagation. Thus, if the linear acoustic process is isentropic, then the acoustic intensity is computed based on the acoustic pressure.

In the Lighthill acoustic analogy approach, the existence of a rigid body yields dipole and quadrupole terms in the acoustic wave equation. However, their relative importance is dependent on the rotor speed, the dimensional parameters of the rotor, and the frequency range of interest. In practice, there are situations where the dipole source dominates the acoustic radiation over that due to the quadrupole source. Ffowcs Williams, et al. [5] and Goldstein [6] showed the relative importance of the dipole source over the quadrupole source for a low speed rotor with a small number of blades, under the assumption that the dipole and quadrupole sources have similar spatial and temporal scales.

The assumption of acoustically compact blades permits replacing distributed dipole sources with a single point dipole whose strength equals the total strength of the distributed dipoles on the blade. Thus, each blade is replaced with a point dipole or multiples of a dipole. Lowson [7] derived the far field and near field acoustic pressure from a moving singular dipole source by using Lighthill's acoustic analogy approach, where the importance of the acceleration of the moving dipole was accounted for in the expression of acoustic pressure.

As there are two interpretations of the solution of the acoustic wave equation of cylindrical coordinates, i.e., a rotating pressure pattern using an exponential function for the angular variation of the pressure pattern, or a modal pressure pattern fluctuating in time

using a trigonometric function for the angular variation of the pressure pattern, the acoustically compact rotating blades can then be modeled by on-off dipoles or rotating dipoles. Homicz [8], Gutin [9], Wright [10, 11], and others pursued the on-off dipole model. Ffowcs Williams, et al. [12], Lowson, et al. [13], Morfey, et al. [14], Mani [15], and others employed the rotating dipole model.

The rotating dipole model accounts, on the one hand, for the fact that the distance between the observer and the rotating dipole varies according to the rotation of the dipole, and that the direction of the motion of the dipole varies. On the other hand, the on-off model does not account for it because the distance between the on-off dipole and the observer is fixed all the time.

There are two ways to get the dipole strength necessary to compute the acoustic radiation from rotating blades: analytically and empirically. For instance, Hanson [16] derived the far field acoustic pressure for a compact subsonic rotor based on rotating dipoles whose strength was derived from the pressure measured by a pressure sensitive transducer mounted at a specific point on the blade surface, even though the position of the transducer has a significant influence on the acoustic pressure at the observer's point. In addition, the size of the pressure transducer, i.e., the area of the transducer, influences the measured data especially at high frequencies. Homicz [8], Amiet [17], Aravamudan, et al. [18], Mani [19], Sevik [20], and other utilized a two-dimensional aero/hydrodynamic function developed by Sears [21] in order to obtain the dipole strength.

The two-dimensional aero/hydrodynamic function was developed for a two-dimensional thin airfoil having small camber under the following

assumptions: (1) the flow from the upper and lower surfaces of the blade at the trailing edge has no pressure jump, (2) a thin sheet of vorticity is shed from the sharp trailing edge (Kutta condition), (3) the thin sheet is shed along the chord line of the blade, (4) the finite thickness of the boundary layer at the trailing edge is not important, (5) no viscosity is involved although the vorticity is generated by viscous action in the airfoil boundary layer, (6) gusts to the airfoil are frozen (the frozen gust assumption implies that gusts are not distorted during the time of passage over the airfoil), and (7) the airfoil is acoustically compact.

Among the aforementioned assumptions, the Kutta, frozen gust, and compactness conditions require special care when using the two-dimensional aero/hydrodynamic function for the following reasons: although the Kutta condition has a dramatic effect on the pressure distribution on the blade surface, as shown by Kelly [22], the condition is still being investigated [23]. The frozen gust condition implies that the two-dimensional aero/hydrodynamic function is relatively valid for low values of the frequency compared with higher values. The assumption about compactness asserts that the acoustic radiation at one surface point does not affect the surface pressure at others. Thus, at high frequencies, it is meaningless to integrate the surface pressure in order to get the strength of a point dipole.

Jackson, et al. [24] compared the measured and calculated aerodynamic admittances which are associated with aero/hydrodynamic functions such as are given by Sears' two-dimensional theory, by two-dimensional strip theory, and by three-dimensional theory. The two-dimensional strip theory states that the lift of each chordwise wing

element is a function only of the local upwash fluctuations at the element, and that the lift on each strip, i.e., each element, is obtained by using Sears' two-dimensional theory. Results show that the three-dimensional theory such as that of Filotas [25] or Graham [26] gave good agreement with measurements. The two-dimensional strip theory gave gairly good agreement. Sears' two-dimensional theory overestimated for the entire reduced frequency range.

Amiet [27] showed that the two-dimensional strip theory is a good approximation for computing the far field acoustical pressure due to unsteady lift if $Mk_x d$ is large, where M, k_x, and d are a streamwise Mach number, a chordwise turbulence wave number, and a span length, respectively. The most important development in his argument is that the computed lift agrees quite well with the measured lift even when $Mk_x d = 1$. He showed that the acoustic radiation produced by the parallel gusts would be the most dominant noise source.

The two-dimensional aero/hydrodynamic function causes aliasing among different wave number gusts. This is because the two-dimensional aero/hydrodynamic function, such as Sears' function, utilized a wave number in the direction of the chord line of a thin airfoil. Therefore, even if the frozen gust is decomposed into its wave number components, each component cannot be the same among rotating blades, because the direction of the chord line of each blade is different from each other.

It should be noted that, since the two-dimensional aero/hydrodynamic function, such as Sears' function, involves one reduced frequency relating the wave number of the upwash to an airfoil to a frequency, then the interaction between blades and the flow

fluctuation can be treated in a time domain and in a frequency domain instead of a space domain and a wave number domain.

For the analysis of the acoustic radiation from rotating blades, there are three possible flow types: (1) steady uniform, (2) steady non-uniform, and (3) unsteady. Gutin [9] investigated the acoustic radiation from rotating blades under a steady uniform flow, i.e., a constant lift force. Morse, et al. [28], Lowson, et al. [13], and Wright [10, 11] tried to explain the discrepancy between Gutin's computed results and experiments, especially in the higher order harmonics of the blade-passing frequency, by introducing a steady non-uniform flow. As quoted by Lowson [29], Leverton [30] reported that no blade-passing frequency and its harmonics appeared in the spectrum of the acoustic radiation from a rotor under calm wind conditions. However, a slight change in conditions caused a blade-passing frequency and its harmonics. In a steady uniform and a steady non-uniform flow, the phase difference of the loading on different blades can be expressed deterministically by the geometrical angle position difference among blades. This is not the case for an unsteady flow.

Homicz [8] took the on-off dipole model as the representation of rotating blades operating in an unsteady flow of convected frozen turbulence by replacing a blade with a dipole at a representative radial position. Sears' function was used to compute the lift on a blade, where a reduced frequency averaged over one blade revolution was used in order to get around the aforementioned aliasing phenomenon. He showed that the total power of the acoustic radiation from rotating blades operating in homogeneous and frozen turbulence is proportional to $\overline{w^2}U^4$ where $\overline{w^2}$ and U are a mean square turbulence

velocity and a convection velocity of the turbulence, respectively. He showed further that the blade-passing frequency and its multiples occur in the frequency spectrum of the acoustic radiation when $U/(\Lambda\Omega)$ is very small where U, Ω, and Λ are an axial flow velocity, a rotational speed, and a typical length scale of the turbulence, respectively. The smallness of $U/(\Lambda\Omega)$ implies that a partially coherent turbulence is chopped by many blades so that blade-passing frequency and its multiples appear in the frequency spectrum signature.

Mani [15] investigated the noise due to the interaction of inlet turbulence with isolated stators and rotors. He assumed that the amplitude strength for each rotating dipole is equal and did not consider the phase relation of the strength of dipoles, which should occur for turbulence interaction. The blade-passing frequency and its multiples in the frequency domain were assumed due to the aerodynamic interference between moving blade rows as investigated by Kemp, et al. [1]. He showed that the sound power level increases with decreasing L/D where the turbulence is assumed to be homogeneous, isotropic, and stationary, and can be characterized by a longitudinal correlation function such as $\exp(-r/L)$ where L is the length scale of the turbulence, and D is a transverse spacing between blades. He also showed that the acoustic spectra for rotors are peaked at the blade-passing frequency and its multiples when L/D exceeds about 0.5, and that when $L/D < 0.5$ the spectra start broadening noticeably. However, the parameter L/D does not take into consideration the contribution of the rotational speed of the rotor and the axial flow velocity. That is, even if L were small, a higher rotational speed and lower axial flow velocity would create the same situation as when the length scale of

turbulence is large, together with a high axial flow velocity and lower rotational speed.

Sevik [31] derived the sound power spectrum from a rotor operating in turbulence. The noise source is the axial component of the blade lift only. The sound power is computed based on the general relation $S_x(\omega) = E\{|X(\omega)|^2\}$ where $S_{x_\infty}(\omega)$ is the power spectrum of a stochastic process x(t) satisfying $\int_{-\infty}^{\infty} \alpha R_{xx}(\alpha)d\alpha < \infty$, where $R_{xx}(\alpha)$ is the correlation function of x(t) which is assumed to be a wide-sense stationary process, and the correlation function does not account for the rotation of the blade. The assumption of the correlation function regards the rotor as being stationary. Because of the use of only the axial component of the lift, the result applies only near the centerline axis of the rotor. In Sevik's calculation of the lift of a blade, the blade is replaced by a line dipole source and the idea of a typical section is introduced, whereby the resultant velocity and chord of the various elements (or infinitesimal strips) may be represented by those of a single "typical section" located at some fraction of the span of a blade. Unfortunately, the resulting power spectrum does not predict the blade-passing frequency component and its multiples, due to the assumption of the correlation function of the upwash at the blades, although, as shown by Robbins, et al. [32], the level and general shape of the predicted spectra agree with the experimental data.

1.3. Scope of Investigation

In Chapter II, an acoustic radiation formula is obtained from the inhomogeneous acoustic wave equation with rotating dipole sources.

This leads to the integral equation, with Green's function, of the acoustic wave equation in an infinite medium. The acoustic compactness condition is introduced, so that the blade can be replaced by a point dipole. The time-averaged acoustic intensity spectral density function is developed in a general form where the effect of the rotation of the dipole is shown explicitly.

In Chapter III, the impulse response function of a blade based on two-dimensional, unsteady, thin airfoil theory is discussed so that the blade response to turbulence can be treated in a time and frequency domain. In addition, the correlation functions of the lift on blades and the lift derivative with respect to time are obtained.

In Chapter IV, the power spectrum of the upwash to the blades is obtained in the following cases: (1) the inflow turbulence is homogeneous, isotropic, and frozen, (2) the turbulence in (1) is elongated and contracted on its course to the rotor plane, and (3) there are wakes due to inlet struts in addition to the inflow turbulence. The results of Lane [33] are utilized in the derivation.

In Chapter V, the results in Chapter II, III, and IV are combined in order to obtain the time-averaged acoustic intensity spectrum. The condition for neglecting the retarded time difference among the lift of blades is introduced. Furthermore, important non-dimensional parameters are introduced so that the effect of the various turbulence properties and the rotor geometry and operating condition can be determined.

In Chapter VI, computations are done according to the results in Chapter V such as Eq. (5.16) and Eq. (5.22) by changing the number of struts and rotors, the spacing between struts and a rotor, the

observation angle, and non-dimensional parameters such as $U_3/\Lambda_i\Omega$ and R_T/Λ_i. In particular, the variation of these non-dimensional parameters are made around an axial flow velocity of U_3 = 30 m/sec, a rotor radius of R_T = 0.30 m, a rotor rotational speed of Ω = 220 rad/sec, an inflow turbulence length scale of Λ_i = 0.15 m and 0.017 m, and a wake turbulence length scale Λ_w = 0.0068 m.

CHAPTER II

ACOUSTIC RADIATION FROM ROTATING DIPOLE SOURCES

2.1. Introduction

There are two tasks necessary for analyzing the acoustic radiation from rotating blades: (1) obtaining the lift on the blades due to the interaction between the rotating blades and turbulence in a flow, and (2) obtaining the radiated sound from the lift. In this chapter, the acoustic radiation due to lift on the blades is considered, based on the Lighthill acoustic analogy approach.

The analysis of the acoustic radiation from rotating blades begins with the inhomogeneous acoustic wave equation developed by Lighthill [2], together with the boundary condition imposed by the blades. The implications of employing the Lighthill acoustic analogy approach are as follows: (1) the observation point of the acoustic radiation is far from the perturbed region so that the propagation and source terms are separable in the governing equation for wave propagation, and (2) the medium at the observation point is assumed to be at rest. The quiescent medium and the assumption that the acoustic process is isentropic simplify computing the acoustic intensity.

The Lighthill acoustic analogy approach leads to an integral equation, with Green's function, for an infinite medium where the integration is done over three spatial dimensions and one temporal dimension. Here, the time is regarded as a parameter; i.e., the so

called retarded time concept is employed. However, because of the existence of the boundary surface imposed by the blades, Green's function of the acoustic wave equation in an infinite medium connot be used without modifying the boundary condition with a Heaviside function. The modification creates new source terms such as monopole, dipole, and quadrupole sources. However, the acoustic wave equation modified by the Heaviside function yields the same Green's function as in the wave equation of an infinite medium, so that the wave equation with boundary conditions can be solved without seeking a new Green's function.

2.2. Integral Equation for Acoustic Pressure

Farassat [34] showed that the surface on a moving body can be treated as a point dipole source whose strength is equal to the total force on the virtual radiation surface, when the following relations are satisfied:

$$\tau_p >> \frac{L}{a} \quad \text{and} \quad \tau_{M_r} >> \frac{L}{a} , \tag{2.1}$$

where τ_p, τ_{M_r}, and L are the characteristic time scales of the pressure, the Mach number of the blade rotational speed, and the length scale of the virtual surface.

Thus, the acoustic wave equation to be solved for rotating blades is

$$\Box^2 = -\nabla\cdot\vec{f} , \tag{2.2}$$

where

$$\vec{f} = \sum_{m=1}^{B} \sum_{n=1}^{N} \ell_{mn}(\tau)\,\delta(\vartheta-\Omega\tau-\vartheta_m)\,\delta(Z)\,\delta(R-R_n)\frac{\Sigma R_n}{R} \tag{2.3}$$

Fig. 1 shows the configuration of the relation between the rotating dipole and the observer's point, where spherical coordinates and cylindrical coordinates are used for the observer's point and the rotating dipole, respectively.

With the aid of the fundamental solution of Eq. (2.2), i.e., Green's function of the acoustic wave equation in an infinite medium, one obtains

$$\Phi(r,\vartheta,\vartheta,t) = \frac{1}{4\pi}\int_{-\infty}^{\infty}\iiint_{\text{Vol.}} (\nabla_0\cdot\vec{f})\,\delta(\tau-t+\frac{D}{a})\frac{1}{D}R\,dR\,d\vartheta\,dZ\,d\tau \ , \tag{2.4}$$

where

$$D = (r^2 + R^2 - 2rR\sin\vartheta\cos(\vartheta-\vartheta) - 2rZ\cos\vartheta + Z^2)^{1/2} \tag{2.5}$$

$$= r - R\sin\vartheta\cos(\vartheta-\vartheta) - rZ\cos\vartheta \ . \tag{2.6}$$

The integration in Eq. (2.4) is within the stationary reference frame fixed to the center of the rotor plane. By introducing a reference frame rotating with the speed of the rotor, i.e., $\vartheta = \Omega\tau+\vartheta_m$, one obtains the following equation,

$$\Phi(r,\vartheta,\vartheta,t) = \frac{1}{4\pi}\int_{-\infty}^{\infty}\iiint_{\text{Vol.}} (\nabla_0\cdot\vec{f})\,\delta(\tau-t+\frac{D}{a})\frac{R}{D}dR\,d\vartheta\,dZ\,d\tau \ , \tag{2.7}$$

where

$$\vartheta = \Omega\tau + \vartheta_m \ . \tag{2.8}$$

Using the relation $\nabla\cdot(g\vec{f}) = g\nabla\cdot\vec{f} + \vec{f}\cdot\nabla g$, where g and f are scalar and

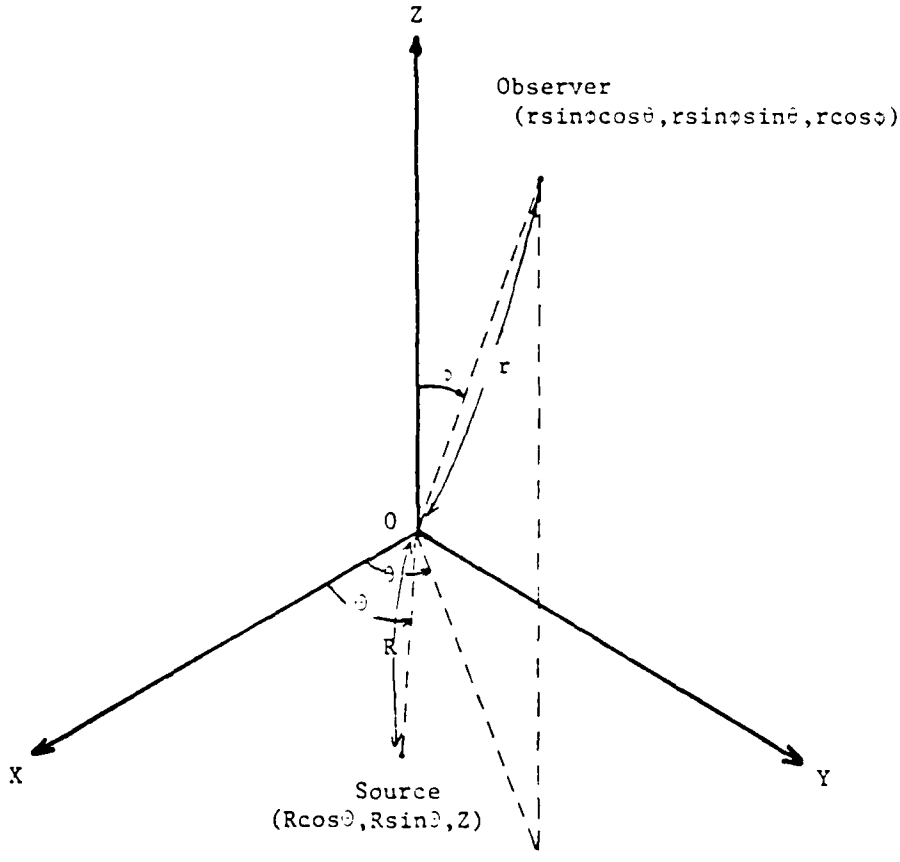

Fig. 1. Observer/Source Coordinates

vector functions, respectively, one obtains,

$$\nabla\cdot\left(\frac{\delta(\tau-t+\frac{D}{a})}{D}\vec{f}\right) = \frac{\delta(\tau-t+\frac{D}{a})}{D}\nabla\cdot\vec{f} + \vec{f}\cdot\nabla\frac{\delta(\tau-t+\frac{D}{a})}{D} \quad . \tag{2.9}$$

Utilizing Eq. (2.9) in Eq. (2.7), and using the fact that

$$\int_{\text{Vol.}} \nabla\cdot\left(\frac{\delta(\tau-t+\frac{D}{a})}{D}\vec{f}\right)dV = \int_{\text{Surface}} \frac{\delta(\tau-t+\frac{D}{a})}{D}\vec{f}\cdot\vec{n}dS = 0 \ , \tag{2.10}$$

because there always exists a surface where $\vec{f} = 0$, one obtains,

$$P(r,\theta,\phi,t) = -\frac{1}{4\pi}\int_{-\infty}^{\infty}\iiint_{\text{Vol.}} \vec{f}\cdot\nabla_o\left(\frac{\delta(\tau-t+\frac{D}{a})}{D}\right)RdRd\phi dZd\tau \ . \tag{2.11}$$

Taking the gradient of $\delta(\tau-t+D/a)/D$, then Eq. (2.11) becomes

$$P(r,\theta,\phi,t) = -\frac{1}{4\pi}\iiint_{\text{Vol.}}\int_{-\infty}^{\infty}(\vec{f}\cdot\nabla_o D)\left\{\frac{\delta'(\tau-t+\frac{D}{a})}{aD} - \frac{\delta(\tau-t+\frac{D}{a})}{D^2}\right\}\times$$

$$RdrdRd\phi dZ \ , \tag{2.12}$$

where the interchange between $d\tau$ and $RdRd\phi dZ$ is possible because the integration is within a rotating frame,

$$(\nabla_o D)_R = (R - r\sin\phi\cos(\theta-\phi))/D \ , \tag{2.13}$$

$$(\nabla_o D)_Z = (-r\cos\phi + Z)/D \ , \tag{2.14}$$

$$(\nabla_o D)_\phi = -(r\sin\phi\sin(\theta-\phi))/D \ , \tag{2.15}$$

and

$$\delta'(\tau-t+\frac{D}{a}) = \frac{d\{\delta(\tau-t+\frac{D}{a})\}}{d(\tau-t+\frac{D}{a})} \quad . \tag{2.16}$$

Eq. (2.12) is a general expression for acoustic pressure due to a distributed force, and it includes the pressure in the near and far fields. In the following section, the term for the far field pressure is extracted from Eq. (2.12).

2.3. Far Field Acoustic Pressure

Utilizing Eq. (2.3) in Eq. (2.12), and integrating with respect to dR, dZ, and dϑ,

$$p(r,\phi,t) = -\frac{1}{4\pi}\int_{-\infty}^{\infty}\sum_{m=1}^{B}\sum_{n=1}^{N}(\vec{\ell}_{mn}\cdot\nabla_o D_{mn})\Delta R_n\left\{\frac{\delta'(\tau-t+\frac{D_{mn}}{a})}{aD_{mn}} - \frac{\delta(\tau-t+\frac{D_{mn}}{a})}{D_{mn}^2}\right\}d\tau \quad , \tag{2.17}$$

where

$$D_{mn} = r - R_n \sin\phi \cos(\Omega\tau+\vartheta_m) \quad , \tag{2.18}$$

$$(\nabla_o D_{mn}) = \frac{r \sin\phi \sin(\Omega\tau+\vartheta_m)}{D_{mn}} \quad , \tag{2.19}$$

$$(\nabla_o D_{mn})_Z = -\frac{r\cos\phi}{D_{mn}} \quad , \tag{2.20}$$

and

$$(\nabla_o D_{mn})_R = \frac{R_n - r\sin\phi\cos(\Omega\tau+\vartheta_m)}{D_{mn}} \quad . \tag{2.21}$$

In the above equation, $\theta = 0$ is assumed, because the transient pressure is not considered here, as seen from the integration range of τ in Eq. (2.17). Now, integrating Eq. (2.17) with respect to τ

and imposing the condition for the acoustic far field, $2\pi r >>$ wavelength (Appendix I), then one obtains

$$P(r,\vartheta,t) = \frac{1}{4\pi} \sum_{m=1}^{B} \sum_{n=1}^{N} \left\{ \frac{\Delta R_n}{\left(1+\frac{1}{a}\frac{\partial D_{mn}}{\partial \tau}\right)} \frac{\partial}{\partial \tau} \left\{ \frac{\vec{\ell}_{mn} \cdot \nabla D_{mn}}{a\left(1+\frac{1}{a}\frac{\partial D_{mn}}{\partial \tau}\right)} \right\} \right\} . \quad (2.22)$$

Utilizing Eq. (2.18) in Eq. (2.22), one obtains

$$P(r,\vartheta,t) = \frac{1}{4\pi a r} \sum_{m=1}^{B} \sum_{n=1}^{N} \left\{ \frac{\Delta R_n}{1 + \frac{R_n \Omega}{a} \sin\vartheta \sin(\Omega\tau+\vartheta_m)} \times \right.$$

$$\left\{ \frac{\partial \ell_{mn}^{\vartheta}}{\partial \tau} \sin\vartheta \sin(\Omega\tau+\vartheta_m) - \frac{\partial \ell_{mn}^{Z}}{\partial \tau} \cos\vartheta + \ell_{mn}^{\vartheta} \Omega \sin\vartheta \times \right.$$

$$\left\{ \cos(\Omega\tau+\vartheta_m) - \frac{2}{r} R_n \sin\vartheta \right.$$

$$\left. - \frac{R_n \Omega \sin\vartheta \cos(\Omega\tau+\vartheta_m) \sin(\Omega\tau+\vartheta_m)}{a\left(1 + \frac{R_n \Omega}{a} \sin\vartheta \sin(\Omega\tau+\vartheta_m)\right)} \right\}$$

$$+ \ell_{mn}^{Z} R_n \Omega \cos\vartheta \sin\vartheta \left\{ \frac{\sin(\Omega\tau+\vartheta_m)}{r} \right.$$

$$\left. \left. + \frac{\Omega \cos(\Omega\tau+\vartheta_m)}{a\left(1 + \frac{R_n \Omega}{a} \sin\vartheta \sin(\Omega\tau+\vartheta_m)\right)} \right\} \right\} , \quad (2.23)$$

where ℓ_{mn}^{ϑ} and ℓ_{mn}^{Z} are the ϑ and Z component of $\vec{\ell}_{mn}(\tau)$, and $\ell_{mn}^{R} = 0$ is assumed on a blade.

Furthermore, imposing the condition for the geometric far field, $r >> R_n$ for all $n = 1,2,\ldots,N$, and because the time history of the pressure is not considered in the present study, one can neglect the terms with R_n/r in Eq. (2.23), yielding

$$p(r,\phi,t) = \sum_{m=1}^{B}\sum_{n=1}^{N}\left\{\frac{\Delta R_n}{4\pi a r\left(1+\frac{R_n\Omega}{a}\sin\phi\,\sin(\Omega\tau+\phi_m)\right)}\times\right.$$

$$\left\{\frac{\partial \ell_{mn}^{\Theta}}{\partial\tau}\sin\phi\,\sin(\Omega\tau+\phi_m) - \frac{\partial \ell_{mn}^{Z}}{\partial\tau}\cos\phi\right.$$

$$+ \ell_{mn}^{\Theta}\Omega\,\sin\phi\,\cos(\Omega\tau+\phi_m)\,\frac{1}{1+\frac{R_n\Omega}{a}\sin\phi\,\sin(\Omega\tau+\phi_m)}$$

$$\left.\left. + \ell_{mn}^{Z}\Omega\,\cos\phi\,\frac{\frac{R_n\Omega}{a}\sin\phi\,\cos(\Omega\tau+\phi_m)}{1+\frac{R_n\Omega}{a}\sin\phi\,\sin(\Omega\tau+\phi_m)}\right\}\right\}, \quad (2.24)$$

where

$$\tau = t - D_{mn}/a\ .$$

Introducing $\ell_{mn}^{\Theta}(\tau) = -\ell_{mn}(\tau)\sin\beta_{mn}$ and $\ell_{mn}^{Z}(\tau) = \ell_{mn}(\tau)\cos\beta_{mn}$, where $\vec{\ell}_{mn}(\tau)$ is assumed to be normal to the chord line of a thin airfoil, and $\vec{\ell}_{mn}(\tau)$ is obtained by Sears' function (see Fig. 2), Eq. (2.24) becomes,

$$p(r,\phi,t) = \frac{1}{4\pi a r}\left\{\sum_{m=1}^{B}\sum_{n=1}^{N}\frac{\Delta R_n}{\left(1+\frac{R_n\Omega}{a}\sin\phi\,\sin(\Omega\tau+\phi_m)\right)^2}\times\right.$$

$$\left\{-\frac{\partial \ell_{mn}}{\partial\tau}\sin\beta_{mn}\sin\phi\,\sin(\Omega\tau+\phi_m) - \frac{\partial \ell_{mn}}{\partial\tau}\cos\beta_{mn}\cos\phi\right.$$

$$- \ell_{mn}\Omega\,\sin\beta_{mn}\sin\phi\,\frac{\cos(\Omega\tau+\phi_m)}{1+\frac{R_n\Omega}{a}\sin\phi\,\sin(\Omega\tau+\phi_m)}$$

$$\left.\left. + \ell_{mn}\Omega\,\cos\beta_{mn}\cos\phi\,\sin\phi\times\frac{\frac{R_n\Omega}{a}\cos(\Omega\tau+\phi_m)}{1+\frac{R_n\Omega}{a}\sin\phi\,\sin(\Omega\tau+\phi_m)}\right\}\right\}. \quad (2.25)$$

Eq. (2.25) is an extension of the result of Lowson [7] and

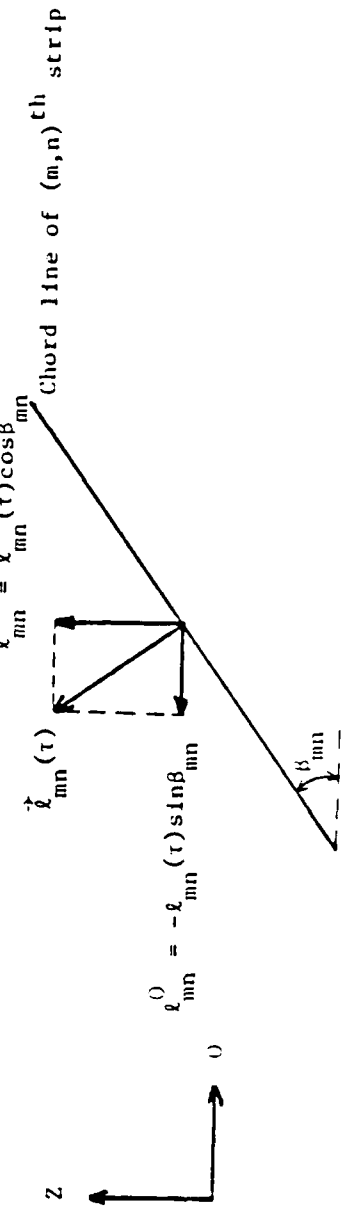

Fig. 2. Lift Vector Components at $(m,n)^{th}$ Strip

Morfey, et al. [14] which deals with the acoustic radiation from a moving point force. As will be shown below, this relates the acoustic intensity spectral density function at the observation point x with the power spectral density function of the turbulence experienced by rotating blades calculated by an aero/hydrodynamic function.

As shown in Eq. (2.25), the variation of the distance between the observer and the blade on a time axis causes a phase modulation in $\ell_{mn}(\tau)$ because $\tau = t - D_{mn}/a$. Furthermore, the variation of the Mach number of the blade velocity in the direction of the observer, i.e., $(R_n\Omega/a)\sin\phi\sin(\Omega\tau+\phi_m)$, behaves as an amplitude modulating signal of $\ell_{mn}(\tau)$ and $\partial\ell_{mn}(\tau)/\partial\tau$.

The Fourier coefficients of the modulation terms are derived in Appendix II. The following is the final result taken from Appendix II:

$$\frac{\cos(\Omega\tau+\phi_m)}{\left(1+\frac{R_n\Omega}{a}\sin\phi\sin(\Omega\tau+\phi_m)\right)^3} = \sum_{p=-\infty}^{\infty} \frac{-jp}{\frac{R_n\Omega}{a}\sin\phi}\left(\frac{|p|R_n\Omega\sin\phi}{2a}\right)^{|p|} \times \frac{e^{jp(\Omega\tau+\phi_m+\frac{\pi}{2})}}{\Gamma(|p|+1)}, \tag{2.26}$$

$$\frac{1}{\left(1+\frac{R_n\Omega}{a}\sin\phi\sin(\Omega\tau+\phi_m)\right)^2} = \sum_{p=-\infty}^{\infty}\sum_{q=-\infty}^{\infty}\left(\frac{|p|R_n\Omega\sin\phi}{2a}\right)^{|p|} \times \left(\frac{|q|R_n\Omega\sin\phi}{2a}\right)^{|q|}\frac{e^{j(p+q)(\Omega\tau+\phi_m+\frac{\pi}{2})}}{\Gamma(|p|+1)\Gamma(|q|+1)}, \tag{2.27}$$

$$\frac{\sin(\Omega\tau+\phi_m)}{\left(1+\frac{R_n\Omega}{a}\sin\phi\sin(\Omega\tau+\phi_m)\right)^2} = \sum_{p=-\infty}^{\infty}\sum_{q=-\infty}^{\infty}\frac{j_{2p}-1}{\frac{R_n\Omega}{a}\sin\phi} \times \left(\frac{|p|R_n\Omega\sin\phi}{2a}\right)^{|p|}\left(\frac{|q|R_n\Omega\sin\phi}{2a}\right)^{|q|}\frac{e^{j(p+q)(\Omega\tau+\phi_m+\frac{\pi}{2})}}{\Gamma(|p|+1)\Gamma(|q|+1)}, \tag{2.28}$$

where the approximation is made for $J_p(z) \approx (1/p!)(z/2)^p$ in Ref. [28]. Hence, the higher order terms can be neglected for small $(R_n\Omega/a)\sin\phi$.

2.4. Acoustic Intensity

One can rewrite Eq. (2.25) as follows:

$$P(r,\phi,t) = \frac{1}{4\pi a r}\sum_{m=1}^{B}\sum_{n=1}^{N}\sum_{p=-\infty}^{\infty}\left(e_{mn}^{(p)}\frac{\partial \ell_{mn}}{\partial \tau} - j\Omega f_{mn}^{(p)}\ell_{mn}\right)e^{jp(\Omega t+\phi_m+\frac{\pi}{2})}, \tag{2.29}$$

where

$$e_{mn}^{(p)} = -b_n^{(p)'}\sin\phi\,\sin\beta_{mn} - a_n^{(p)'}\cos\phi\,\cos\beta_{mn}\,, \tag{2.30}$$

$$f_{mn}^{(p)} = \sin\phi(\cos\phi\,\cos\beta_{mn} - \sin\beta_{mn})c_n^{(p)'}\,, \tag{2.31}$$

$$c_n^{(p)'} = \frac{p}{\frac{R_n\Omega}{a}\sin\phi}\left(\frac{|p|\Omega R_n\sin\phi}{2a}\right)^{|p|}\frac{1}{\Gamma(p+1)}\,, \tag{2.32}$$

$$a_n^{(p)'} = \sum_{s=-\infty}^{\infty}\sum_{k=-\infty}^{\infty}\left(\frac{|s|R_n\Omega\sin\phi}{2a}\right)^{|s|}\left(\frac{|k|R_n\Omega\sin\phi}{2a}\right)^{|k|}\times$$

$$\frac{1}{\Gamma(|s|+1)\Gamma(|k|+1)}\,,\qquad p = s + k\,, \tag{2.33}$$

and

$$b_n^{(p)'} = \sum_{s=-\infty}^{\infty}\sum_{k=-\infty}^{\infty}\frac{\delta_{2s}-1}{\frac{R_n\Omega}{a}\sin\phi}\left(\frac{|s|R_n\Omega\sin\phi}{2a}\right)^{|s|}\left(\frac{|k|R_n\Omega\sin\phi}{2a}\right)^{|k|}\times$$

$$\frac{1}{\Gamma(|s|+1)\Gamma(|k|+1)}\,,\qquad p = s + k\,. \tag{2.34}$$

Utilizing the following definition of the autocorrelation function of $P(r,\phi,t)$,

$$R_{PP}(r,\phi,t,\tau) = E\{P^*(r,\phi,t)P(r,\phi,t+\tau)\}\,, \tag{2.35}$$

one obtains

$$\mathcal{R}(r,\phi,t,\alpha) = \frac{1}{16\pi^2 a^2 r^2} \sum_{m=1}^{B} \sum_{n=1}^{N} \sum_{k=1}^{B} \sum_{\ell=1}^{N} \sum_{p=-\infty}^{\infty} \sum_{q=-\infty}^{\infty} \mathcal{R}_{mnk\ell}^{(p,q)}(\tau,\alpha) \times e^{j(q-p)(\Omega t+\frac{\pi}{2})+j(q\phi_k-p\phi_m)+jq\Omega\alpha} , \tag{2.36}$$

where

$$\mathcal{R}_{mnk\ell}^{(p,q)}(\tau,\alpha) = E\left\{\left(e_{mn}^{(p)}\frac{\partial \lambda_{mn}(\tau)}{\partial \tau} - j\Omega f_{mn}^{(p)}\lambda_{mn}(\tau)\right) \times \left(e_{k\ell}^{(q)}\frac{\partial \lambda_{mn}(\tau+\alpha)}{\partial \tau} - j\Omega f_{mn}^{(q)}\lambda_{mn}(\tau+\alpha)\right)\right\} . \tag{2.37}$$

The instantaneous acoustic intensity is given by the following relation:

$$\vec{I}(r,\phi,\theta,t) = \frac{1}{2}\mathrm{Re}\left\{\mathcal{P}(r,\phi,\theta,t)\vec{u}^{*}(r,\phi,\theta,t)\right\} , \tag{2.38}$$

where the acoustic particle velocity $\vec{u}(r,\phi,\theta,t)$ is given by the gradient of $\mathcal{P}(r,\phi,t)$ as follows:

$$\vec{u}(r,\phi,\theta,t) = \left(\frac{\partial \mathcal{P}}{\partial r}\vec{i}_r + \frac{\partial \mathcal{P}}{r\partial\phi}\vec{i}_\phi + \frac{\partial \mathcal{P}}{r\partial\theta}\vec{i}_\theta\right)\frac{1}{j\omega\rho} , \tag{2.39}$$

As r increases, $\vec{u}(r,\phi,\theta,t)$ is dominated by u_r which is the r-component of $\vec{u}$. Thus, Eq. (2.39) becomes

$$\vec{u}(r,\phi,\theta,t) = \frac{\partial \mathcal{P}}{j\omega\rho\partial r}\vec{i}_r . \tag{2.40}$$

Hence, the acoustic intensity at a large distance r is given by

$$\vec{I}(r,\phi,\theta,t) = I_r(r,\phi,\theta,t) = \frac{1}{2}\,\mathrm{Re}\left\{\frac{\hat{p}\,\tilde{p}^*}{\rho a}\right\} . \qquad (2.41)$$

Now, taking the expectation of the above intensity, one obtains

$$E\{I_r(r,\phi,\theta,t)\} = \frac{1}{2}\,\mathrm{Re}\left\{\frac{1}{\rho a}\,E\{\tilde{p}(r,\phi,\theta,t)\,\tilde{p}^*(r,\phi,\theta,t)\}\right\} . \qquad (2.42)$$

Since the pressure in Eq. (2.25) is real, Eq. (2.42) becomes

$$E\{I_r(r,\phi,\theta,t)\} = \frac{1}{2\rho a}\,E\{\tilde{p}^2(r,\phi,\theta,t)\} . \qquad (2.43)$$

Eq. (2.43) is equivalent to $\mathcal{R}_{pp}(r,\phi,t,\alpha)/\rho a$ when $\alpha = 0$. Consider the following pair of Fourier integrals:

$$S_{pp}(r,\phi,t,\omega) = \int_{-\infty}^{\infty} \mathcal{R}_{pp}(r,\phi,t,\omega)\,\frac{e^{-j\omega\alpha}}{\rho a}\,d\alpha \qquad (2.44)$$

and

$$\mathcal{R}_{pp}(r,\phi,t,\omega) = \frac{\rho a}{2\pi}\int_{-\infty}^{\infty} S_{pp}(r,\phi,t,\omega)e^{j\omega\alpha}d\alpha . \qquad (2.45)$$

Thus, from Eq. (2.36), one obtains

$$E\{I_r(r,\phi,t)\} = \frac{1}{4\pi}\int_{-\infty}^{\infty} S_{pp}(r,\phi,t,\omega)d\omega . \qquad (2.46)$$

accordingly, $S_{pp}(r,\phi,t,\omega)$ can be regarded as an instantaneous intensity spectral density function.

Hence, by taking the α-Fourier transform of Eq. (2.36), one obtains the following instantaneous acoustic intensity spectral density function:

$$S_{\phi\phi}(r,\vartheta,t,\omega) = \frac{1}{32\pi^2 a^3 r^2} \sum_{m=1}^{B} \sum_{n=1}^{N} \sum_{k=1}^{B} \sum_{\ell=1}^{N} \sum_{p=-\infty}^{\infty} \sum_{q=-\infty}^{\infty}$$

$$S^{(p,q)}_{mnk\ell}(\tau,\omega-q\Omega) e^{j(q-p)(\Omega t+\frac{\pi}{2})+j(q\vartheta_k-p\vartheta_m)} , \tag{2.47}$$

where

$$S^{(p,q)}_{mnk\ell}(\tau,\omega) = \int_{-\infty}^{\infty} \mathcal{R}^{(p,q)}_{mnk\ell}(\tau,\alpha) e^{-j\omega\alpha} \, d\alpha . \tag{2.48}$$

When $\mathcal{R}^{(p,q)}_{mnk\ell}(\tau,\alpha)$ is stationary, Eq. (2.47) becomes,

$$S_{\phi\phi}(r,\vartheta,t,\omega) = \frac{1}{32\pi^2 a^3 r^2} \sum_{m=1}^{B} \sum_{n=1}^{N} \sum_{k=1}^{B} \sum_{\ell=1}^{N} \sum_{p=-\infty}^{\infty} \sum_{q=-\infty}^{\infty}$$

$$S^{(p,q)}_{mnk\ell}(\omega-q\Omega) e^{j(q-p)(\Omega t+\frac{\pi}{2})+j(q\vartheta_k-p\vartheta_m)} . \tag{2.49}$$

Assuming $S_{\phi\phi}(r,\vartheta,t,\omega)$ is continuous and finite with respect to t, and taking a time average of Eq. (2.49) over $2\pi/\Omega$, one obtains

$$\langle S_{\phi\phi}(r,\vartheta,t,\omega)\rangle = \frac{1}{32\pi^2 a^3 r^2} \sum_{m=1}^{B} \sum_{n=1}^{N} \sum_{k=1}^{B} \sum_{\ell=1}^{N} \sum_{p=-\infty}^{\infty}$$

$$S^{(p,p)}_{mnk\ell}(\omega-p\Omega) e^{jp(\vartheta_k-\vartheta_m)} . \tag{2.50}$$

CHAPTER III

BLADE RESPONSE TO FLOW FLUCTUATION

3.1. Introduction

In Chapter II, the acoustic intensity spectral density function was derived under the conditions of compactness, i.e., the virtual source size of the rotating blades is equivalent to the physical size of the blades, and the variation of the radiation time over the blade is very small compared with the time scale of the surface pressure of the blade so that the instantaneous radiations from various parts of the blade reach the observer simultaneously. The acoustic intensity spectral density function involves the computation of the power spectrum of the lift on a blade. The present chapter considers the derivation of the impulse response function of a blade based on a two-dimensional, thin airfoil theory, and the power spectral density function of the lift by employing the correlation function of the flow fluctuations.

With the aid of the result by Jackson, et al. [24], the three-dimensional interaction between blades and flow fluctuations can be approximated by a two-dimensional strip theory using Sears' function. The lift on each strip is obtained in order to get the impulse response function of each strip. The two-dimensional strip approach imposes the restriction that the acoustic radiation due to parallel gusts (the spanwise wavenumber is zero) is dominant, as investigated

by Amiet [27]. Utilization of Sears' function imposes the restriction that the mean angle of attack is so small that the effect of the flow fluctuation parallel to the chord line of an airfoil can be neglected as a second order effect. Hence, our concern is with the response of a thin airfoil with zero mean angle of attack to an upwash velocity fluctuation, where the airfoil is assumed to be lightly loaded. Furthermore, since it is assumed that the frozen flow fluctuation pattern is convected, there is a one-to-one correspondence between frequency and wavenumber. In addition, the blade-to-blade interaction is not included in the impulse response function of a blade.

3.2. Transfer Function of Blade

In general, a flow velocity fluctuation with convection velocity U_1 can be expressed by the following, four-dimensional, Fourier transform pair:

$$\vec{V}(\vec{y},\tau) = \frac{1}{(2\pi)^4} \iiiint_{-\infty}^{\infty} \vec{A}(k_1,k_2,k_3,\omega) e^{j\{\vec{k}\cdot\vec{y}+(k_1U_1+\omega)\tau\}} d\omega dk_1 dk_2 dk_3 , \tag{3.1}$$

and

$$\vec{A}(k_1,k_2,k_3,\omega) = \iiiint_{-\infty}^{\infty} \vec{V}(\vec{y},\tau) e^{-j\{\vec{k}\cdot\vec{y}+(k_1U_1+\omega)\tau\}} dt dy_1 dy_2 dy_3 . \tag{3.2}$$

When the flow has a property such that $\omega << k_1U_1$ in Eq. (3.1), Eq. (3.1) becomes

$$\vec{V}(\vec{y},\tau) = \frac{1}{(2\pi)^4} \iiiint_{-\infty}^{\infty} \vec{A}(k_1,k_2,k_3,\omega) e^{j(\vec{k}\cdot\vec{y}+k_1U_1\tau)} d\omega dk_1 dk_2 dk_3 . \tag{3.3}$$

Since $\int_{-\infty}^{\infty} \vec{A}(k_1,k_2,k_3,\omega)d\omega = \vec{A}(k_1,k_2,k_3,\tau)$, when $\tau = 0$, Eq. (3.3) becomes

$$\vec{V}(y,\tau) = \frac{1}{(2\pi)^3} \iiint_{-\infty}^{\infty} \vec{A}(k_1,k_2,k_3,\tau=0)e^{j(\vec{k}\cdot\vec{y}+k_1U_1\tau)}dk_1dk_2dk_3 , \tag{3.4}$$

where $\vec{A}(k_1,k_2,k_3,\tau) = \frac{1}{2\pi}\int_{-\infty}^{\infty} \vec{A}(k_1,k_2,k_3,\omega)e^{j\omega\tau}d\omega$. Hence, $k_1U_1 >> \omega$ is equivalent to a frozen velocity fluctuation pattern, since $\vec{A}(k_1,k_2,k_3,\tau=0)$ is the wavenumber spectrum of the velocity fluctuation at an initial time $\tau=0$. In other words, the frozen velocity fluctuation pattern assumption is valid when the typical time scale of the fluctuation with no convection is much larger than that of the frozen fluctuation with convection.

Due to the frozen fluctuation pattern assumption, the Fourier component of the temporal variation, i.e., $e^{jk_1U_1\tau}$, can be related to that of a spatial variation, i.e., $e^{j\vec{k}\cdot\vec{y}}$, through k_1. Thus, a one-to-one correspondence exists between the frequency and wavenumber domain, i.e., k_1U_1 and k_1.

In addition, the above restriction, $\omega << k_1U_1$, can be relaxed because in the computation of the lift on a blade it needs only be assumed that the temporal variation is negligible during the convection time for the fluctuation to pass through the blade.

Assuming linearized, small perturbation analysis of the thin airfoil response to a frozen velocity fluctuation pattern, with a convection velocity U_1 in the y_1 direction, as shown in Fig. 3, the response can be expressed by the sum of the response to each Fourier component $A(k_1,k_2,k_3)e^{j(\vec{k}\cdot\vec{y}+k_1U_1\tau)}$, where $A(k_1,k_2,k_3)$ implies

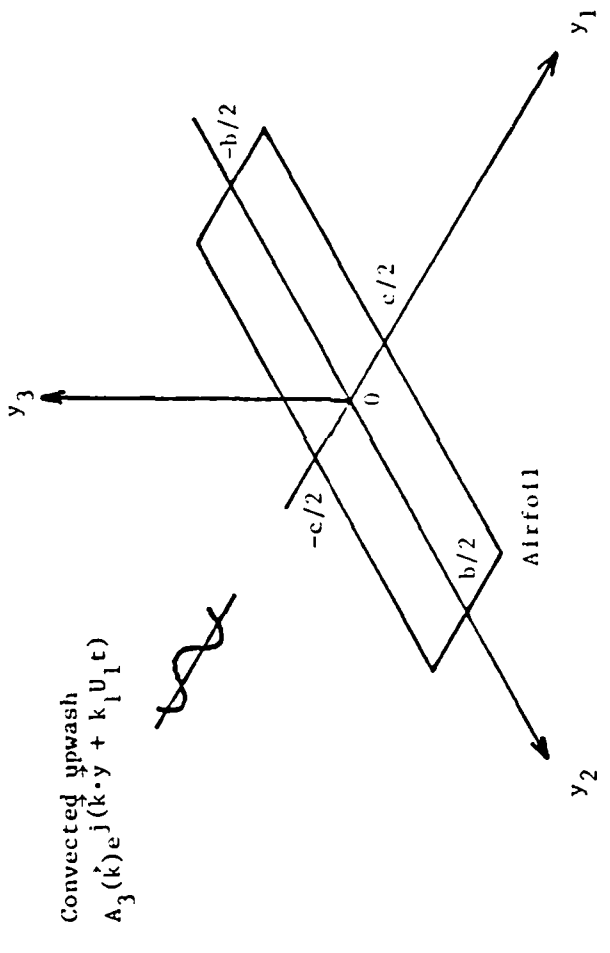

Fig. 3. Finite Span Thin Airfoil

$A(k_1,k_2,k_3,\tau = 0)$. The lift on a blade with a spanwise length b and a chordwise length c can be given by the following integration,

$$\ell_3(\tau) = \int\int\int_{-\infty}^{\infty} \int_{-c/2}^{c/2} \int_{-b/2}^{b/2} \int_{-o}^{+o} G_{3j}(\vec{k},\vec{y}) A_j(\vec{k}) e^{j(\vec{k}\cdot\vec{y}+k_1U_1\tau)} \delta(y_3) d\vec{y} d\vec{k} , \tag{3.5}$$

where $G_{3j}(\vec{k},\vec{y})$ is an aero/hydrodynamic function in tensor notation.

Neglecting the lift due to the velocity fluctuations parallel to the blade surface, because of their second order effect, and assuming incompressible flow so that $\vec{k}$ and $\vec{A}$ are orthogonal each other, one obtains

$$\ell_3(\tau) = \int\int\int_{-\infty}^{\infty} \int_{-c/2}^{c/2} \int_{-b/2}^{b/2} \int_{-o}^{+o} G_{33}(\vec{k},\vec{y}) A_3(\vec{k}) e^{j(\vec{k}\cdot\vec{y}+k_1U_1\tau)} \delta(y_3) d\vec{y} d\vec{k} . \tag{3.6}$$

The integration of Eq. (3.6) over y_3 yields

$$\ell_3(\tau) = \int\int\int_{-\infty}^{\infty} \int_{-c/2}^{c/2} \int_{-b/2}^{b/2} G_{33}(\vec{k},y_1,y_2) A_3(\vec{k}) \times e^{j(k_1y_1+k_2y_2+k_1U_1\tau)} dy_1 dy_2 d\vec{k} . \tag{3.7}$$

By assuming $G_{33}(k_1,k_2,k_3,y_1,y_2)$ to be constant over the blade span, and not considering edge effect (the tip of the airfoil), Eq. (3.7) becomes

$$\ell_3(\tau) = \int\int\int_{-\infty}^{\infty} \int_{-c/2}^{c/2} \int_{-b/2}^{b/2} G_{33}(\vec{k},y_2) A_3(\vec{k}) \times e^{j(k_1y_1+k_2y_2+k_1U_1\tau)} dy_1 dy_2 d\vec{k} . \tag{3.8}$$

Integrating the above equation over the blade span from -b/2 to +b/2, one obtains

$$\ell_3(\tau) = \int\int\int_{-\infty}^{\infty} G_{33}(\vec{k},y_1)A_3(\vec{k})2b\ \mathrm{sinc}(k_2b)e^{j(k_1y_1+k_1U_1\tau)}dy_1d\vec{k} \ . \tag{3.9}$$

If k_2b is very small so that $\mathrm{sinc}(k_2b)$ becomes approximately 1 or, equivalently, the typical length scale of the flow fluctuation is much longer than the blade span length, then integrating Eq. (3.8) with respect to k_2 yields

$$\ell_3(\tau) = \int\int_{-\infty}^{\infty}\int_{-c/2}^{c/2} G_{33}(k_1,k_3,y_1)A_3(k_1,k_2=0,k_3) \times$$

$$2be^{j(k_1y_1+k_1U_1\tau)}dy_1dk_1dk_3 \ . \tag{3.10}$$

Since $\vec{k}$ and $\vec{A}$ are orthogonal, and the airfoil is very thin in the y_3 direction, $G_{33}(k_1,k_3,y_1)$ is insensitive to k_3. Thus, integrating Eq. (3.10) with respect to y_1, one obtains

$$\ell_3(\tau) = 2bH(k_1)\int_{-\infty}^{\infty} A_3(k_1,k_3)e^{jk_1U_1\tau}\,dk_3 \ , \tag{3.11}$$

where

$$H(k_1) = \int_{-c/2}^{c/2} G_{33}(k_1,y_1)e^{jk_1y_1}\,dy_1 \ .$$

Eq. (3.11) shows that $H(k_1)$ can be replaced with Sears' function for a two-dimensional thin airfoil. The function is given by

$$H(k_1) = \pi\rho U_1 c \frac{J_0(\frac{k_1 c}{2})H_1^{(1)}(\frac{k_1 c}{2}) - H_0^{(1)}(\frac{k_1 c}{2})J_1(\frac{k_1 c}{2})}{H_1^{(1)}(\frac{k_1 c}{2}) - jH_0^{(1)}(\frac{k_1 c}{2})} \quad . \qquad (3.12)$$

Its approximate form is

$$H(k_1) \approx \pi\rho U_1 c \frac{e^{-j\frac{k_1 c}{2}(1 - \frac{\pi^2}{2(1+\pi k_1 c)})}}{\sqrt{1 + \pi k_1 c}} \quad , \quad k_1 \geq 0 \ , \qquad (3.13)$$

where this approximation is done, not by taking the limitation of Eq. (3.12) as k_1 increases or decreases, but rather by observing that Eq. (3.12) can be approximated to within a few percent over most of its range. This approximation of the amplitude was done by Liepmann [35], and approximation of phase was done by Giesing, et al. [36].

The integration with respect to k_3 in Eq. (3.11) yields the contribution due to the upwash at $y_3 = 0$, so that $A_3(k_1)$ can be obtained by measuring the upwash of the airfoil at $y_3 = 0$, where $A_3(k_1) = \int_{-\infty}^{\infty} A_3(k_1,k_3)e^{jk_3 y_3}\, dk_3$ at $y_3 = 0$. By using the notation $A_3(k_1)$, Eq. (3.11) becomes

$$\ell_3(\tau) = 2bH(k_1)A_3(k_1)e^{jk_1U_1\tau} \ . \qquad (3.14)$$

In the above equation, $H(k_1)$ can be regarded as a transfer function for the response of a thin airfoil whose input is $A_3(k_1)e^{jk_1U_1\tau}$. Furthermore, since k_1U_1 can be regarded as an angular frequency, $H(k_1)$ and $A_3(k_1)e^{jk_1U_1\tau}$ can be written as $H(\omega/U_1)$ and $A_3(\omega/U_1)e^{j\omega\tau}$, respectively, where $\omega = k_1U_1$. The implication of Eq. (3.14) is that there is a one-to-one correspondence between a wavenumber and an

angular frequency, that the airfoil can be treated in time and frequency domains instead of space and wavenumber domains, and that Sears' function can be regarded as the τ-Fourier transform of the impulse response function of the airfoil.

Accordingly, Eq. (3.14) yields the following convolution integral,

$$\ell_3(\tau) = \int_{-\infty}^{\infty} h(\tau-\alpha)u(\alpha)d\alpha \cdot 2b \ , \tag{3.15}$$

where $u(\alpha)$ is the upwash measured on a time axis.

Finally, since $\ell_3(\tau)$ is obtained by integration over the entire airfoil or the strip of the airfoil so that the airfoil or strip can be replaced with a dipole, the upwash on the integration area has to be well correlated so that the dipole can represent the lift on the integration area. As an important result, since the lift is obtained in a time domain and in a frequency domain, Eq. (3.14) becomes insensitive to the geometrical orientation and/or position of the airfoil explicitly, although the upwash includes the geometrical information implicitly.

3.3. Correlation Function of Lift and its Time Derivative

Adopting the model discussed in Section 3.2., one can obtain the following lift at the n^{th} strip of the m^{th} blade,

$$\ell_{mn}(\tau) = \int_{-\infty}^{\infty} h_{mn}(\tau-\sigma)u_{mn}(\sigma)d\sigma \cdot 2R_n \ , \tag{3.16}$$

where Eq. (3.15) is utilized, and $u_{mn}(\tau)$ is the upwash at the n^{th}

strip of the m^{th} blade. Hence, the correlation function between $\ell_{mn}(\tau)$ and $\ell_{k\ell}(\tau)$, where k and ℓ denote the k^{th} blade and ℓ^{th} strip, respectively, is given by

$$\mathcal{R}^{\ell\ell}_{mnk\ell}(\tau,\alpha) = E\{\ell^{*}_{mn}(\tau)\ell_{k\ell}(\tau+\alpha)\} \ . \tag{3.17}$$

Utilizing Eq. (3.11) in Eq. (3.17), one obtains

$$\mathcal{R}^{\ell\ell}_{mnk\ell}(\tau,\alpha) = \int_{-\infty}^{\infty}\int h^{*}_{mn}(\eta_1)h_{k\ell}(\eta_2)\mathcal{R}^{uu}_{mnk\ell}(\tau,\alpha-\eta_2+\eta_1)d\eta_1 d\eta_2 \Delta R_n \Delta R_\ell \ . \tag{3.18}$$

By taking the α-Fourier transform of Eq. (3.18), one obtains

$$S^{\ell\ell}_{mnk\ell}(\tau,\omega) = H^{*}_{mn}(\omega)H_{k\ell}(\omega)\ S^{uu}_{mnk\ell}(\tau,\omega)\Delta R_n \Delta R_\ell \ . \tag{3.19}$$

The correlation function and the spectrum of $\ell_{mn}(\tau)$ and $\ell_{k\ell}(\tau)$ as well as those of $\partial\ell_{mn}(\tau)/\partial\tau$ and $\partial\ell_{k\ell}(\tau)/\partial\tau$ are needed to obtain the autocorrelation function of the acoustic pressure at the observer point. By taking the time derivative of Eq. (3.16), one obtains

$$\frac{\partial\ell_{mn}(\tau)}{\partial\tau} = \int_{-\infty}^{\infty}\frac{\partial}{\partial\tau}h_{mn}(\tau-\eta)u_{mn}(\tau)d\eta\cdot\Delta R_n \ . \tag{3.20}$$

Eq. (3.20) shows that the time derivative of $\ell_{mn}(\tau)$ can be regarded as the output of the system whose impulse response function is $\partial h_{mn}(\tau)/\partial\tau$. Therefore, one obtains the following by the same method as used in obtaining Eq. (3.19):

$$S^{\ell\ell'}_{mnk\ell}(\tau,\omega) = H^{*}_{mn}(\omega)j\omega H_{k\ell}(\omega)S^{uu}_{mnk\ell}(\tau,\omega)\Delta R_n \Delta R_\ell \ , \tag{3.21}$$

$$S^{\ell'\ell}_{mnk\ell}(\tau,\omega) = -j\omega H^{*}_{mn}(\omega)H_{k\ell}(\omega)S^{uu}_{mnk\ell}(\tau,\omega)\Delta R_n \Delta R_\ell \ , \tag{3.22}$$

and

$$S^{\ell'\ell'}_{mnk\ell}(\tau,\omega) = \omega^2 H^{*}_{mn}(\omega)H_{k\ell}(\omega)S^{uu}_{mnk\ell}(\tau,\omega)\Delta R_n \Delta R_\ell \ , \tag{3.23}$$

where ℓ' denotes the time derivative of the lift.

CHAPTER IV

POWER SPECTRUM OF TURBULENCE INTO ROTOR

4.1. Introduction

As shown in Chapter II and III, the power spectrum of the inflow to a rotor is necessary in order to obtain the acoustic intensity spectral density function of the noise radiation from the rotor. The present chapter deals with the power spectrum density function for the upwash at rotating blades with and without inlet struts.

For turbulent flows with no struts, two cases are to be considered: (1) the turbulence is homogeneous, isotropic, and frozen, and (2) the turbulence in (1) is elongated on its course to the rotor plane. The second case is pursued to obtain results for practical situations where the eddy to a rotor is elongated, i.e., anisotropic.

For turbulent flows with struts, it is assumed that: (1) the turbulence in the non-disturbed inflow and wakes behind the inlet struts can be treated as in the case with no struts, (2) the wake turbulence is statistically independent of the non-disturbed inflow turbulence, (3) the turbulence in each wake is statistically independent of that in other wakes, (4) the random variables, such as the center position and width of each wake, are governed by uniform distribution functions where these random variables are statistically independent of each other, and (5) no overlap occurs among wakes.

Furthermore, in the situation with inlet struts, the mean flow

velocity defect behind vanes and the stator-rotor interaction due to potential fields, such as were investigated by Kemp, et al. [37], can be regarded as a steady non-uniform flow. A deterministic function is introduced in order to take this into account.

4.2. Isotropic Turbulence with No Struts

In statistically homogeneous and stationary turbulence, the correlation function of the turbulence velocities, $u_i(\vec{\rho}_1,t_1)$ and $u_j(\vec{\rho}_2,t_2)$ where i,j = 1, 2, 3, is given by

$$E\{u_i^*(\vec{\rho}_1,t_1)u_j(\vec{\rho}_2,t_2)\} = \mathcal{R}_{12}^{u_iu_j}(\vec{\rho},\alpha) \ , \tag{4.1}$$

where $\vec{\rho} = \vec{\rho}_1 - \vec{\rho}_2$ and $\alpha = t_1 - t_2$. Furthermore, by assuming frozen, isotropic turbulence, Eq. (4.1) becomes

$$E\{u_i^*(\vec{\rho}_1,t_1)u_j(\vec{\rho}_2,t_2)\} = \mathcal{R}_{12}^{u_iu_j}(|\vec{\rho}|) \ . \tag{4.2}$$

Under the above assumptions, i.e., that turbulence is homogeneous, frozen, and isotropic, von Karman, et al. [38] derived the following correlation function:

$$\mathcal{R}_{12}^{u_iu_j}(|\vec{\rho}|) = \overline{u^2}\left\{\frac{f(|\vec{\rho}|) - g(|\vec{\rho}|)}{|\vec{\rho}|^2}\rho_i\rho_j + g(|\vec{\rho}|)\delta_{ij}\right\} \ ,$$

$$i,j = 1,2,3 \ , \tag{4.3}$$

where $f(|\vec{\rho}|)$ is a longitudinal correlation coefficient function defined by

$$f(|\vec{\rho}|) = \frac{E\{u^*_{\rho_1} u_{\rho_2}\}}{\overline{u^2}} \quad , \tag{4.4}$$

$g(|\vec{\rho}|)$ is a transverse correlation coefficient function defined by

$$g(|\vec{\rho}|) = \frac{E\{u^*_{t_1} u_{t_2}\}}{\overline{u^2}} \quad , \tag{4.5}$$

and $\overline{u^2}$ is the mean square value of three components of the velocity, u_1, u_2, and u_3, such that

$$\overline{u^2} = \overline{u_1^2} = \overline{u_2^2} = \overline{u_3^2} \tag{4.6}$$

throughout the homogeneous and isotropic velocity field.

Furthermore, in an incompressible fluid medium the two correlation coefficients, $g(|\vec{\rho}|)$ and $f(|\vec{\rho}|)$, have the following relation as shown in Ref. [39]:

$$g(|\vec{\rho}|) = f(|\vec{\rho}|) + \frac{|\vec{\rho}|}{2} \frac{\partial f(|\vec{\rho}|)}{\partial |\vec{\rho}|} \quad . \tag{4.7}$$

Now consider the correlation function of the upwash at rotating blade under the following assumptions: (1) an incompressible fluid medium, (2) frozen turbulence pattern convected with an axial flow velocity U_3, and (3) homogeneous and isotropic turbulence, see Fig. 4. Under these assumptions, Lane [33] derived the correlation function of the upwash at rotating blades provided that the longitudinal correlation coefficient $f(|\vec{\rho}|)$ is assumed to be

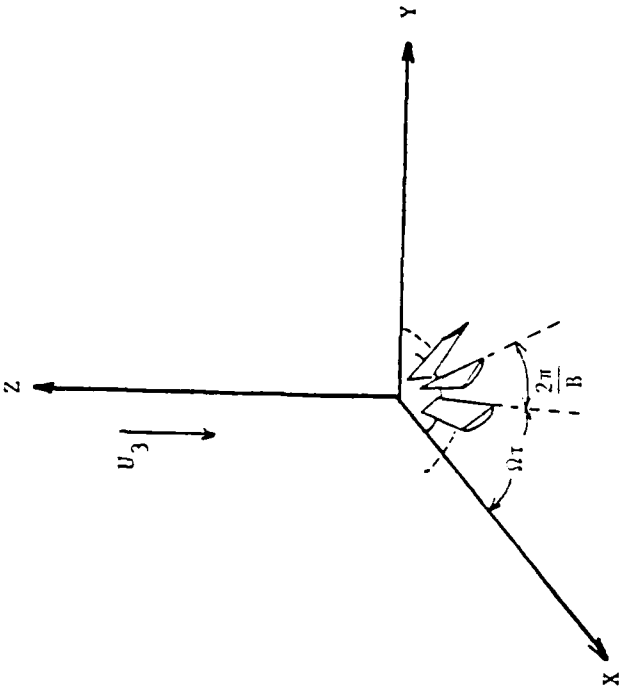

Fig. 4. Rotor in Cylindrical Coordinates

$$f(|\vec{\rho}|) = \exp\left(-\frac{|\vec{\rho}|}{\Lambda_i}\right) , \tag{4.8}$$

and utilizing Eq. (4.3) and Eq. (4.7).

The upwash correlation function derived by Lane [33] is as follows:

$$\mathcal{R}^{uu}_{mnk\ell}(\alpha) = \overline{u^2}\left\{E(\alpha)\left(1 - \frac{\rho(\alpha)}{2\Lambda_i}\right) + \frac{F(\alpha)}{2\rho(\alpha)\Lambda_i}\right\}\exp\left(-\frac{|\vec{\rho}|}{\Lambda_i}\right) , \tag{4.9}$$

where

$$E(\alpha) = \cos^2\beta + \cos\left(\Omega\alpha + \frac{2\pi(k-m)}{B}\right)\sin^2\beta , \tag{4.10}$$

$$F(\alpha) = (U_3\alpha)^2\cos^2\beta + R_{mn}R_{k\ell}\sin^2\beta\,\sin^2\left(\Omega\alpha + \frac{2\pi(k-m)}{B}\right) , \tag{4.11}$$

and

$$\rho^2(\alpha) = (U_3\alpha)^2 + R_{mn}^2 + R_{k\ell}^2 - 2R_{mn}R_{k\ell}\cos\left(\Omega\alpha + \frac{2\pi(k-m)}{B}\right) . \tag{4.12}$$

The stagger angle β_{mn} is approximated by a constant, β, for all m and n. In other words, the variation of the blade twist is assumed to be small.

Eq. (4.9) can be written in terms of non-dimensional variables, so that

$$\mathcal{R}^{uu}_{mnk\ell}(\alpha) = \overline{u^2}\left\{E(\alpha)\left(1 - \frac{\rho_1(\alpha)}{2}\right) + \frac{F_1(\alpha)}{2\rho_1(\alpha)}\right\}\exp\left(-\rho_1(\alpha)\right), \tag{4.13}$$

where

$$\rho_1^2(\alpha) = \left(\frac{U_3\alpha}{\Lambda_i}\right)^2 + \left(\frac{R_{mn}}{\Lambda_i}\right)^2 + \left(\frac{R_{k\ell}}{\Lambda_i}\right)^2 - 2\frac{R_{mn}R_{k\ell}}{\Lambda_i^2}\cdot \cos\left(\Omega\alpha + \frac{2\pi(k-m)}{B}\right) , \tag{4.14}$$

and

$$F_1(\alpha) = \left(\frac{U_3\alpha}{\Lambda_i}\right)^2\cos^2\beta + \frac{R_{mn}R_{k\ell}}{\Lambda_i^2}\sin^2\beta\,\sin^2\left(\Omega\alpha + \frac{2\pi(k-m)}{B}\right) . \tag{4.15}$$

Now consider the case that $R_{mn} = R_{k\ell} = R$ for all m, n, k, and ℓ. Eq. (4.13), Eq. (4.14), and Eq. (4.15) change as follows:

$$\mathcal{R}^{uu}_{mk}(\alpha) = \overline{u^2}\{E(\alpha)(1 - \frac{\rho_1(\alpha)}{2}) + \frac{F_1(\alpha)}{2\rho_1(\alpha)}\}e^{-\rho_1(\alpha)} , \tag{4.16}$$

where

$$\rho_1^2(\alpha) = \left(\frac{U_3\alpha}{\Lambda_i}\right)^2 + 2\left(\frac{R}{\Lambda_i}\right)^2\{1 - \cos(\Omega\alpha + \frac{2\pi(k-m)}{B})\} , \tag{4.17}$$

and

$$F_1(\alpha) = \left(\frac{U_3\alpha}{\Lambda_i}\right)^2\cos^2\beta + \left(\frac{R}{\Lambda_i}\right)^2\sin^2\beta\,\sin^2(\Omega\alpha + \frac{2\pi(k-m)}{B}) . \tag{4.18}$$

4.3. Non-isotropic Turbulence with No Struts

It was shown by Ribner, et al. [40], based on the continuity and conservation of angular momentum of fluid elements, how a contracting flow changes the incoming turbulence spectrum and its intensity and length scales. This type of contracting stream occurs in the flow into a stationary rotor. However, in attempting to apply this result, the spectrum obtained in a wavenumber domain is very difficult to convert to one in a frequency domain. This difficulty arises because of the rotation of the blades and because the frequency is a function of the angle between the wavenumber vector and the blade stagger angle orientation.

Furthermore, Chandrasekhar [41] showed that the general form of the velocity correlation tensor in an axisymmetric turbulence can be expressed by two arbitrary scalar functions. However, the task of obtaining the arbitrary scalar functions constituting the correlation tensor is difficult due to the fact that the power spectral density

function of the correlation function must satisfy the non-negative condition. For example, as pointed out by Kerschen, et al. [42], the restrictive condition is not satisfied even by selecting a one-dimensional correlation function, such as an exponential function.

Since the treatment of the isotropic turbulence has been done kinematically and geometrically in Section 4.2., that treatment is extended, according to Ribner, et al. [40], to the turbulence ingested by a rotor. The inflow turbulence scale is assumed to be modified in the following manner:

$$\mathcal{R}_{ij}(x_1,x_2,x_3) = \mathcal{R}^{in}_{ij}(\gamma x_1,\gamma x_2,\delta x_3) \quad , \tag{4.19}$$

where the superscript "in", δ, and γ denotes the inflow isotropic turbulence, the turbulence elongation rate, and the turbulence contraction rate, respectively. The above assumption asserts that the statistics governing the inflow turbulence are not changed through the flow contraction but that the shape of the domain of the statistics is distorted. In other words, the isocorrelation contours are distorted through the flow contraction.

The correlation function of the upwash between two points (m,n) and (k,ℓ) in a contracted flow field is given by

$$\mathcal{R}^{uu}_{mnk\ell}(\alpha) = \overline{(u^{in})^2}\left\{E_2(\alpha)\left(1 - \frac{\sigma_2(\alpha)}{2}\right) + \frac{F_2(\alpha)}{2\sigma_2(\alpha)}\right\}e^{-\sigma_2(\alpha)} \quad , \tag{4.20}$$

where

$$F_2(\alpha) = \left\{\frac{U_3\alpha_1}{\delta\Lambda_1}\right\}^2\cos^2\beta + \frac{R_{mn}R_{k\ell}}{\gamma^2\Lambda_1^2}\sin^2\beta\,\sin^2\left(\Omega\alpha + \frac{2\pi(k-m)}{B}\right) \quad , \tag{4.21}$$

$$E_2(\alpha) = \cos^2\beta + \cos\left(\Omega\alpha + \frac{2\pi(k-m)}{B}\right)\sin^2\beta \quad , \tag{4.22}$$

and

$$\rho_2^2(\alpha) = \left(\frac{U_3\alpha}{\delta\lambda_i}\right)^2 + \left(\frac{R_{mn}}{\gamma\lambda_i}\right)^2 + \left(\frac{R_{k\ell}}{\gamma\lambda_i}\right)^2 - 2\frac{R_{mn}R_{k\ell}}{\gamma^2\lambda_i^2}\cos(\Omega\alpha + \frac{2\pi(k-m)}{B}) \quad . \tag{4.23}$$

When $R_{mn} = R_k = R$ for all m, n, k, and ℓ, the above equations become

$$\mathcal{R}^{uu}_{mnk\ell}(\alpha) = \overline{(u^{in})^2}\left\{E_2(\alpha)(1 - \frac{\rho_2(\alpha)}{2}) + \frac{F_2(\alpha)}{2\rho_2(\alpha)}\right\}e^{-\rho_2(\alpha)} \quad , \tag{4.24}$$

where

$$F_2(\alpha) = \left(\frac{U_3\alpha}{\delta\lambda_i}\right)^2\cos^2\beta + \left(\frac{R}{\gamma\lambda_i}\right)^2\sin^2\beta\sin^2(\Omega\alpha + \frac{2\pi(k-m)}{B}) \quad , \tag{4.25}$$

$$E_2(\alpha) = \cos^2\beta + \cos(\Omega\alpha + \frac{2\pi(k-m)}{B})\sin^2\beta \quad , \tag{4.26}$$

and

$$\rho_2^2(\alpha) = \left(\frac{U_3\alpha}{\delta\lambda_i}\right)^2 + 2\left(\frac{R}{\gamma\lambda_i}\right)^2\{1 - \cos(\Omega\alpha + \frac{2\pi(k-m)}{B})\} \quad . \tag{4.27}$$

4.4. Power Spectrum of Upwash with Struts

The upwash to blades operating downstream of a set of struts is assumed to be expressed by the following equation:

$$u_{mn}(\tau) = \{1 - \sum_{p=-\infty}^{\infty}\sum_{q=0}^{S-1}\mathrm{Rect}\left(\frac{\tau - \frac{2\pi p}{\Omega} - \frac{2\pi q}{\Omega S} + \frac{2\pi m}{\Omega B} - t_{pqm}}{w_{pqm}}\right)\}u^i_{mn}(\tau)$$

$$+ \sum_{p=-\infty}^{\infty}\sum_{q=0}^{S-1}\mathrm{Rect}\left(\frac{\tau - \frac{2\pi p}{\Omega} - \frac{2\pi q}{\Omega S} + \frac{2\pi m}{\Omega B} - t_{pqm}}{w_{pqm}}\right)u^q_{mn}(\tau)$$

$$+ M_{mn}(\tau) \quad , \tag{4.28}$$

where u^i_{mn} and u^q_{mn} are the turbulent velocities of the inflow and the

wake, respectively, and it is assumed that: (1) no wake is overlapped with another, (2) the function Rect(τ) is given by

$$\text{Rect}(\tau) = \begin{cases} 1 & |\tau| \leq 1 \\ 0 & \text{otherwise} , \end{cases} \tag{4.29}$$

and t_{qpm} and w_{qpm} are random variables for the position and width of the Rect(τ) function whose probability density functions are given by the following:

$$p_r(t_{qpm}) = \begin{cases} \frac{1}{2\Delta} & |t_{qpm}| \leq \Delta \\ 0 & \text{otherwise} , \end{cases} \tag{4.30}$$

and

$$p_r(w_{qpm}) = \begin{cases} \frac{1}{\Delta_2 - \Delta_1} & \Delta_1 \leq w_{qpm} \leq \Delta_2 \\ 0 & \text{otherwise} , \end{cases} \tag{4.31}$$

where Δ, Δ_1, and Δ_2 are determined so that no overlap among wakes occurs, (3) the function $u^q_{mn}(\tau)$ is the turbulent velocity in the wake of the q^{th} inlet strut interacting with the n^{th} segment of the m^{th} rotating blade, (4) $E\{u^i_{mn}(\tau)\} = E\{u^q_{k\ell}(\tau)\} = 0$ for all m, n, k, ℓ, and q, (5) $u^q_{mn}(\tau)$'s for q = 0,.....,S-1 are statistically independent of each other, (6) the correlation function of $u^i_{mn}(\tau)$ and $u^i_{k\ell}(\tau)$ is given by Eq. (4.20), (7) the correlation function of $u^q_{mn}(\tau)$ and $u^q_{k\ell}(\tau)$ is given by

$$\mathcal{R}^{qq}_{mnk\ell}(\alpha) = e^{-\sigma_2(\alpha)}\{\Xi_2(\alpha)(1 - \frac{\sigma_2(\alpha)}{2}) + \frac{F_2(\alpha)}{2\sigma_2(\alpha)}\}\overline{(u^q)^2} , \tag{4.32}$$

where

$$F_2(\alpha) = \left(\frac{U_{3\alpha}}{\delta_w \Lambda_w}\right)^2 \cos^2\beta + \frac{R_{mn}R_{k\ell}}{\gamma_w^2\Lambda_w^2} \sin^2\beta \sin^2(\Omega\alpha + \frac{2\pi(k-m)}{B}) \ , \tag{4.33}$$

$$E_2(\alpha) = \cos^2\beta + \cos(\Omega\alpha + \frac{2\pi(k-m)}{B})\sin^2\beta \ , \tag{4.34}$$

and

$$\rho_2^2(\alpha) = \left(\frac{U_{3\alpha}}{\delta_w \Lambda_w}\right)^2 + \left(\frac{R_{mn}}{\gamma_w \Lambda_w}\right)^2 + \left(\frac{R_{k\ell}}{\gamma_w \Lambda_w}\right)^2 - 2\frac{R_{mn}R_{k\ell}}{\gamma_w^2\Lambda_w^2}\cos(\Omega\alpha + \frac{2\pi(k-m)}{B}) \ , \tag{4.35}$$

(8) the function $M_{mn}(\tau)$ is a deterministic function due to the steady circulation and mean velocity defect of the upstream strut, and

(9) the variables t_{qpm} and w_{qpm} are statistically independent for all q, p, and m.

Now consider the correlation function of the upwash which is given as

$$\begin{aligned} \mathcal{R}^{uu}_{mnk\ell}(\tau,\alpha) = \Big\{1 - \sum_{p=-\infty}^{\infty}\sum_{q=0}^{S-1}\big(E\{\text{Rect 1}\}+E\{\text{Rect 2}\}\big)\Big\}\mathcal{R}^{ii}_{mnk\ell}(\alpha) \\ + \sum_{p_1=-\infty}^{\infty}\sum_{q_1=0}^{S-1}\sum_{p_2=-\infty}^{\infty}\sum_{q_2=0}^{S-1} E\{\text{Rect 1}\}E\{\text{Rect 2}\} \times \\ \Big(\mathcal{R}^{ii}_{mnk\ell}(\alpha) + \mathcal{R}^{q_1q_2}_{mnk\ell}(\alpha)\delta_{q_1q_2}\Big) + E\{M^*_{mn}(\tau)M_{k\ell}(\tau+\alpha)\} \ , \end{aligned} \tag{4.36}$$

where

$$\text{Rect 1} = \text{Rect}^*\left(\frac{\tau - \frac{2-p_1}{\Omega} - \frac{2-q_1}{\Omega S} + \frac{2-m}{B\Omega} + t_{qp_1m}}{w_{q_1p_1m}}\right) \ , \tag{4.37}$$

and

$$\text{Rect 2} = \text{Rect}\left(\frac{\tau - \frac{2-p_2}{\Omega} - \frac{2-q_2}{\Omega S} + \frac{2-k}{B\Omega} + t_{p_2q_2k}}{w_{p_2q_2k}}\right) \ . \tag{4.38}$$

By taking the expectation of Eq. (4.36), one obtains

$$\mathcal{R}^{uu}_{mnk\ell}(\tau,\alpha) = \Big\{1 - \sum_{p=-\infty}^{\infty}\sum_{q=0}^{S-1}\Big(g_n^*\Big(\tau - \frac{2\pi p}{\Omega} - \frac{2\pi q}{\Omega S} + \frac{2\pi m}{B\Omega}\Big)$$

$$+ g_\ell\Big(\tau + \alpha - \frac{2\pi p}{\Omega} - \frac{2\pi q}{\Omega S} + \frac{2\pi k}{B\Omega}\Big)\Big)$$

$$+ \sum_{p_1=-\infty}^{\infty}\sum_{q_1=0}^{S-1}\sum_{p_2=-\infty}^{\infty}\sum_{q_2=0}^{S-1} g_n^*\Big(\tau - \frac{2\pi p_1}{\Omega} - \frac{2\pi q_1}{\Omega S} + \frac{2\pi m}{B\Omega}\Big) \times$$

$$g_\ell\Big(\tau + \alpha - \frac{2\pi p_2}{\Omega} - \frac{2\pi q_2}{\Omega S} + \frac{2\pi k}{B\Omega}\Big)\Big\}\,\mathcal{R}^{ii}_{mnk\ell}(\alpha)$$

$$+ \sum_{q=0}^{S-1}\mathcal{R}^{qq}_{mnk\ell}(\alpha)\sum_{p_1=-\infty}^{\infty}\sum_{p_2=-\infty}^{\infty}$$

$$g_n^*\Big(\tau - \frac{2\pi p_1}{\Omega} - \frac{2\pi q}{\Omega S} + \frac{2\pi m}{B\Omega}\Big) \times$$

$$g_\ell\Big(\tau + \alpha - \frac{2\pi p_2}{\Omega} - \frac{2\pi q}{\Omega S} + \frac{2\pi k}{B\Omega}\Big)$$

$$+ M^*_{mn}(\tau)M_{k\ell}(\tau+\alpha)\ , \qquad (4.39)$$

where

$$g_n(\tau) = \begin{cases} 0 & |\tau| \geq \Delta_2+\Delta \\ \dfrac{1}{4\Delta(\Delta_2-\Delta_1)}(\Delta_2 - |\tau| + \Delta)^2 & \Delta_2+\Delta \geq |\tau| \geq \Delta_2-\Delta \\ \dfrac{1}{\Delta_2-\Delta_1}\Big\{2\Delta - \dfrac{1}{2}\Big(1 - \dfrac{1}{2\Delta}(\Delta_2 - |\tau| - \Delta)\Big)\{|\tau| + 3\Delta - \Delta_2\}\Big\} & \Delta_2-\Delta \geq |\tau| \geq \Delta_2-3\Delta \\ 1 & |\tau| \leq \Delta_2-3\Delta\ . \end{cases}$$

(4.40)

Expanding the functions $g_n(\tau)$ and $M_{mn}(\tau)$ in a Fourier series, Eq. (4.39) becomes

$$\mathcal{R}^{uu}_{mnk}(\tau,\alpha) = \Bigg\{1 - \sum_{p=-\infty}^{\infty} a_n^{(p)*} e^{-j\left(\frac{2\pi mpS}{B} + pS\Omega\tau\right)}$$

$$- a_\ell^{(p)} e^{j\left(\frac{2\pi mpS}{B} + pS\Omega(\tau+\alpha)\right)}$$

$$+ \sum_{p_1=-\infty}^{\infty} \sum_{p_2=-\infty}^{\infty} a_n^{(p_1)*} a_\ell^{(p_2)} \times$$

$$e^{j\left(\frac{2\pi S}{B}(kp_2-mp_1)+S\Omega(p_2-p_1)\tau+p_2S\Omega\alpha\right)} \mathcal{R}^{ii}_{mnk\ell}(\tau)$$

$$+ \sum_{q=0}^{S-1} \mathcal{R}^{qq}_{mnk\ell}(\alpha) \sum_{p_1=-\infty}^{\infty} \sum_{p_2=-\infty}^{\infty} c_n^{(p_1)*} c_\ell^{(p_2)} \times$$

$$e^{j\left(\frac{2\pi q}{S}(q_1-q_2)+\frac{2\pi}{B}(kp_2-mp_1)+\Omega(p_2-p_1)\tau+p_2\Omega\alpha\right)}$$

$$+ \sum_{s_1=-\infty}^{\infty} \sum_{s_2=-\infty}^{\infty} b_n^{(s_1)*} b_\ell^{(s_2)} \times$$

$$e^{j\left(\frac{2\pi S}{B}(s_2k-s_1m)+\frac{2\pi}{B}(kp_2-mp_1)+(p_2-p_1)\Omega\tau+p_2\Omega\alpha\right)} , \tag{4.41}$$

where

$$\sum_{p=-\infty}^{\infty} \sum_{q=0}^{S-1} g_n\left(\tau - \frac{2\pi p}{\Omega} - \frac{2\pi q}{\Omega S}\right) = \sum_{p=-\infty}^{\infty} a_n^{(p)} e^{jpS\Omega\tau} , \tag{4.42}$$

$$\sum_{p=-\infty}^{\infty} g_n\left(\tau - \frac{2\pi p}{\Omega} - \frac{2\pi q}{\Omega S}\right) = \sum_{p=-\infty}^{\infty} c_n^{(p)} e^{jp\Omega\left(\tau - \frac{2\pi q}{\Omega S}\right)} , \tag{4.43}$$

and

$$M_{mn}(\tau) = \sum_{s=-\infty}^{\infty} b_n^{(s)} e^{jsS\Omega\left(\tau + \frac{2\pi m}{B\Omega}\right)} , \tag{4.44}$$

where $M_{mn}(\tau)$ is assumed to be a periodic function with a period $2\pi/S\Omega$. Now, taking the α-Fourier transform of Eq. (4.41), one obtains

$$S^{uu}_{mnk\ell}(\tau,\omega) = (1 - \sum_{p=-\infty}^{\infty} a_n^{(p)*} e^{-j\{\frac{2\pi mpS}{B} - pS\Omega\tau\}}) S^{ii}_{mnk\ell}(\omega)$$

$$- \sum_{p=-\infty}^{\infty} a_\ell^{(p)} e^{j\{\frac{2\pi kpS}{B} + pS\Omega\tau\}} S^{ii}_{mnk\ell}(\omega - pS\Omega)$$

$$+ \sum_{p_1=-\infty}^{\infty} \sum_{p_2=-\infty}^{\infty} a_n^{(p_1)*} a_\ell^{(p_2)} \times$$

$$e^{j\{\frac{2\pi S}{B}(kp_2 - mp_1) + S\Omega(p_2 - p_1)\tau\}} S^{ii}_{mnk\ell}(\omega - p_2 S\Omega)$$

$$+ S \sum_{p=-\infty}^{\infty} \sum_{q=-\infty}^{\infty} c_n^{(qS+p)*} c_\ell^{(p)} \times$$

$$e^{j\{\frac{2\pi}{B}(k-m)p - mqS + qS\Omega\tau\}} S^{ww}_{mnk\ell}(\omega - p\Omega)$$

$$+ \sum_{s_1=-\infty}^{\infty} \sum_{s_2=-\infty}^{\infty} b_n^{(s_1)*} b_\ell^{(s_2)} \times$$

$$e^{j\{\frac{2\pi S}{B}(s_2 k - s_1 m) + (s_2 - s_1)S\Omega\tau\}} \delta(\omega - s_2 S\Omega) \quad , \quad (4.45)$$

where $S^{ww}_{mnk\ell}(\omega)$ is the α-Fourier transform of $\mathcal{R}^{qq}_{mnk\ell}(\alpha)$ for all q, assuming $\mathcal{R}^{qq}_{mnk\ell}(\alpha)$ is the same for all $q = 0,1,\ldots,S-1$.

CHAPTER V

ACOUSTIC INTENSITY SPECTRUM DUE TO INTERACTION OF A ROTOR WITH TURBULENCE

5.1. Introduction

In Chapter II, the acoustic radiation intensity from rotating blades in a free space was obtained and was related to the power spectrum of the lift of rotating blades under the condition that the distributed pressure on each blade is compact. In Chapter III, the impulse response function of a blade was derived so that the lift can be obtained in a time domain and in a frequency domain. In Chapter IV, the correlation function of the upwash to the blades and its spectrum were derived.

In the present chapter, the results in Chapter II, III, and IV are combined so that the acoustical intensity spectrum can be obtained. In deriving the explicit expression for the acoustic intensity, it is shown that the retarded time difference of the lift among blades can be neglected. The condition necessary for this demonstration to be valid is more relaxed than that for the dipole domination over other radiation sources.

5.2. Retarded Time Difference

Since the results in Chapter IV were obtained at the time associated with the emission of the acoustic radiation on blades, those results cannot be substituted into the results in Chapter II

where the correlation is taken at the observation time when the radiation reaches the observer's point. In other words, the correlation function for the blade lift $\mathcal{R}^{(p,q)}_{mnk\ell}(\tau,x)$ is obtained at two different times $t - D_{mn}/a$ and $t + x - D_{k\ell}/a$.

Now consider under what condition the following approximation is attainable so that the retarded time difference can be neglected in the correlation function, $\mathcal{R}^{(p,q)}_{mnk\ell}(\tau,x)$, in Eq. (2.36),

$$\ell_{mn}(t - \frac{D_{mn}}{a}) \approx \ell_{mn}(t - \frac{r}{a}) \ . \tag{5.1}$$

By Taylor series expansion, one can get the following expansion of $\ell_{mn}(t - D_{mn}/a)$,

$$\ell_{mn}(t - \frac{D_{mn}}{a}) = \ell_{mn}(t - \frac{r}{a}) + \frac{d\ell_{mn}(t - \frac{r}{a})}{dt} \cdot \left(\frac{R_{mn}\sin\phi \cos\{\Omega(t - \frac{D_{mn}}{a}) + \gamma_m\}}{a}\right) + \text{error terms} \ . \tag{5.2}$$

Hence, if it can be assumed that the typical time scale of $\ell_{mn}(\tau)$ is very large compared with R_{mn}/a or, equivalently, that the upper cutoff frequency of $\ell_{mn}(\tau)$ is much lower than a/R_{mn}, then the approximation in Eq. (5.1) is attained. This condition is relatively relaxed when compared with the one for the dipole domination over other radiation sources such as was given by Goldstein [6]:

$$\tau_m >> \frac{L}{a(1 - M_r)} \ , \tag{5.3}$$

where τ_m, L, and M_r are a characteristic time for the source fluctuations measured in the moving frame with a convected flow, a characteristic source dimension, and a Mach number of the body speed component in the direction of the observer, respectively. Further, fans with low rotational speed and small radial size are more likely to satisfy the condition for the approximation in Eq. (5.1).

Since $\lambda_{mn}(t - D_{mn}/a)$ is given by the convolution integral in Eq. (3.15), then the following equation is obtained so that the condition required for the approximation in Eq. (5.1) is imposed on either $h_{mn}(\tau)$ or $u_{mn}(\tau)$.

$$\int_{-\infty}^{\infty} h_{mn}(\tau-\eta)u_{mn}(\eta)d\eta = \int_{-\infty}^{\infty} h_{mn}(\eta)u_{mn}(\tau-\eta)d\eta \ . \tag{5.4}$$

Thus, one can obtain the condition for the approximation to be imposed on $h_{mn}(\tau)$ or $u_{mn}(\tau)$; i.e., the typical time scale of $h_{mn}(\tau)$ or $u_{mn}(\tau)$ should be much larger than $R_{mn}\sin\phi/a$ or equivalently, the upper cutoff frequency of $h_{mn}(\tau)$ and $u_{mn}(\tau)$ are derived in the same fashion as was done in Eq. (5.2). This condition is easily obtained when the observer is near the axis of the rotor, and is relaxed when compared with the condition of dipole domination, (5.3).

First, consider the condition on $u_{mn}(\tau)$, using its typical length scale L and its convection velocity $R_{mn}\Omega$, where $U_3 << R_{mn}\Omega$ is assumed. According to the condition, one obtains the following expression:

$$\frac{R_{mn}}{L} << \frac{a}{R_{mn}\Omega \sin\phi} \tag{5.5}$$

Thus, low rotational speed and/or small ratio of rotor radius and turbulence length scale are required so as to obtain the approximation. As mentioned before, the condition, (5.5) is more likely to be satisfied in water than in air. When the observer is at $\phi = 0$, the condition is automatically satisfied, i.e., there is no retarded time difference for the lift distribution on the blades.

Next, consider the condition on $h_{mn}(\tau)$. Let f_{cut} be the upper cutoff frequency of $h_{mn}(\tau)$, where f_{cut} is defined by -3 dB = 10 log $\{H_{mn}(2\pi f_{cut})/H_{mn}(0)\}$. Then, the condition to be imposed on $h_{mn}(\tau)$ is obtained as follows,

$$\frac{R_n}{2\pi c} << \frac{a}{R_{mn}\Omega \sin\varphi} . \tag{5.6}$$

(5.6) shows that low rotational speed and/or low aspect ratio rotors are most likely to satisfy the condition.

Furthermore, for the time derivative of $\ell_{mn}(\tau)$, the results for $u_{mn}(\tau)$ and $h_{mn}(\tau)$ are applicable based on the following equations:

$$\frac{\partial \ell_{mn}(\tau)}{\partial \tau} = \int_{-\infty}^{\infty} \frac{\partial h_{mn}(\eta)}{\partial \eta} u_{mn}(\tau-\eta)d\eta , \tag{5.7}$$

and

$$\frac{\partial \ell_{mn}(\tau)}{\partial \tau} = \int_{-\infty}^{\infty} h_{mn}(\tau-\eta)\frac{\partial u_{mn}(\eta)}{\partial \eta} d\eta . \tag{5.8}$$

In the present study, either one of the results (5.5) and (5.6), or both of them may be assumed to be satisfied by the rotor such that the rotor is operated at low rotational speed, the flow fluctuation length scale is large compared with the rotor radius, and the cutoff frequency satisfies (5.6). In the subsequent derivations, the

retarded time difference is neglected in the spectrum analysis for the rotor in a free space. It should be noted that this assumption is imposed only on the retarded time difference associated with the lift on a blade, while the retarded time difference associated with the distance between the rotor and the observer is included in the present study as was done in Chapter II.

5.3. Acoustic Intensity Spectrum from a Rotor Operating in Free Space

By neglecting the retarded time difference, under the assumption discussed in Section 5.2., Eq. (2.36) becomes

$$\mathcal{R}^{(p,q)}_{mnk\ell}(t - \frac{r}{a},\alpha) = e^{(p)}_{mn} e^{(q)}_{k\ell} \mathcal{Q}^{\ell'\ell'}_{mnk\ell}(t - \frac{r}{a},\alpha)$$

$$+ \alpha^2 f^{(p)}_{mn} f^{(q)}_{k\ell} \mathcal{Q}^{\ell\ell}_{mnk\ell}(t - \frac{r}{a},\alpha)$$

$$+ j\alpha\{f^{(p)}_{mn} e^{(q)}_{k\ell} \mathcal{Q}^{\ell\ell'}_{mnk\ell}(t - \frac{r}{a},\alpha)$$

$$- e^{(p)}_{mn} f^{(q)}_{k\ell} \mathcal{Q}^{\ell'\ell}_{mnk\ell}(t - \frac{r}{a},\alpha)\} \quad . \tag{5.9}$$

Then, taking the α-Fourier transform of Eq. (5.9), and using Eq. (3.19) through Eq. (3.23), one obtains

$$S^{(p,q)}_{mnk\ell}(t - \frac{r}{a},\omega) = H^{*}_{mn}(\omega) H_{k\ell}(\omega) S^{uu}_{mnk\ell}(t - \frac{r}{a},\omega) \Delta R_n \Delta R_\ell \times$$

$$\{\omega^2 e^{(p)}_{mn} e^{(q)}_{k\ell} + \omega^2 f^{(p)}_{mn} f^{(q)}_{k\ell} + \omega e^{(p)}_{mn} f^{(q)}_{k\ell}$$

$$- \omega f^{(p)}_{mn} e^{(q)}_{k\ell}\} \quad . \tag{5.10}$$

Utilizing Eq. (5.10) in Eq. (2.47), and replacing t - r/a with t, one obtains

$$S_{yy}(r,\phi,t,\omega) = \frac{1}{32\pi^2 a^3 r^2} \sum_{m=1}^{B} \sum_{n=1}^{N} \sum_{k=1}^{B} \sum_{\ell=1}^{N} \sum_{p=-\infty}^{\infty} \sum_{q=-\infty}^{\infty}$$

$$H^*_{mn}(\omega-q\Omega) H_{k\ell}(\omega-q\Omega) \Delta R_n \Delta R_\ell e^{j\frac{2\pi}{B}(kq-mp)} \times$$

$$S^{uu}_{mnk\ell}(t,\omega-q\Omega) e^{j(q-p)(\Omega t+\frac{\pi}{2})} \times$$

$$\{(\omega-q\Omega)^2 e^{(p)}_{mn} e^{(q)}_{k\ell} + \Omega^2 f^{(p)}_{mn} f^{(q)}_{k\ell}$$

$$- (\omega-q\Omega)\Omega f^{(p)}_{mn} e^{(q)}_{k\ell} + (\omega-q\Omega)\Omega e^{(p)}_{mn} f^{(q)}_{k\ell}\} . \tag{5.11}$$

Taking the time average of Eq. (5.11) over the period $2\pi/\Omega$, under the assumption that $S_{yy}(r,\phi,t,\omega)$ is continuous and finite with respect to t, introducing the typical section idea such that $H_{mn}(\omega) = H(\omega)$ for all m and n, and replacing a blade with a dipole, one obtains

$$S_{yy}(r,\phi,t,\omega) = \frac{(\Delta R_T)^2}{32\pi a^3 r^2} \sum_{p=-\infty}^{\infty} |H(\omega-p\Omega)|^2 \times$$

$$\{(\omega-p\Omega)^2 (e^{(p)}_T)^2 + (f^{(p)}_T)^2\} \times$$

$$\{\sum_{m=1}^{B} \sum_{k=1}^{B} e^{-j\frac{2}{B}p(k-m)} S^{uu}_{mk}(\omega-p\Omega)\} . \tag{5.12}$$

Before utilizing Eq. (4.13) in Eq. (5.12), let us consider the non-dimensional parameters of $S^{uu}_{mk}(\omega)$, so that functionally the power

spectrum $S_{mk}^{uu}(\omega)$ can be expressed as

$$S_{mk}^{uu}(\omega) = \frac{\overline{u^2}}{\Omega} S\left(\frac{U_3}{\Lambda\Omega}, \frac{R_m}{\Lambda_i}, \frac{R_k}{\Lambda_i}, \frac{\omega}{\Omega}\right) . \tag{5.13}$$

Now, utilizing Eq. (4.13), Eq. (5.13), and Eq. (3.13) in Eq. (5.12), and non-dimensionalizing the result, yields the following:

$$\frac{S_{yy}(r,\phi,t,\omega)}{\rho a^2 R_T} = \frac{1}{32}\left(\frac{c_T}{r}\right)^2\left(\frac{\Delta R_T}{R_T}\right)^2\left(\frac{R_T\Omega}{a}\right)^3\left(\frac{\overline{u^2}}{a^2}\right) \times \sum_{p=-\infty}^{\infty}\left\{\frac{\left(\frac{\omega-p\Omega}{\Omega}\right)^2\left(e_T^{(p)}\right)^2 + \left(f_T^{(p)}\right)^2}{\pi\left(\frac{\omega-p\Omega}{\Omega}\right)\left(\frac{c_T}{R_T}\right) + 1} \times S_B\left(\frac{U_3}{\Lambda\Omega}, \frac{R_T}{\Lambda_i}, \frac{\omega-p\Omega}{\Omega}\right)\right\} , \tag{5.14}$$

where

$$S_B\left(\frac{U_3}{\Lambda_i\Omega}, \frac{R_T}{\Lambda_i}, \frac{\omega-p\Omega}{\Omega}\right) = \frac{\Omega}{\overline{u^2}} \sum_{m=1}^{B}\sum_{k=1}^{B} e^{j\frac{2\pi}{B}p(k-m)} S_{mk}^{uu}\left(\frac{U_3}{\Lambda_i\Omega}, \frac{R_T}{\Lambda_i}, \frac{\omega-p\Omega}{\Omega}\right) , \tag{5.15}$$

and $R_T\Omega \approx \{(R_T\Omega)^2+U_3^2\}^{1/2}$ is assumed.

When taking the turbulence contraction and elongation into account, one obtains

$$\frac{S_{yy}(r,\phi,t,\omega)}{\rho a^2 R_T} = \frac{1}{32}\left(\frac{c_T}{r}\right)^2\left(\frac{\Delta R_T}{R_T}\right)^2\left(\frac{\overline{u^2}}{a^2}\right)\left(\frac{R_T\Omega}{a}\right)^3 \times \sum_{p=-\infty}^{\infty}\left\{\frac{\left(\frac{\omega-p\Omega}{\Omega}\right)^2\left(e_T^{(p)}\right)^2 + \left(f_T^{(p)}\right)^2}{1 + -\left(\frac{\omega-p\Omega}{\Omega}\right)\left(\frac{c_T}{R_T}\right)} \times S_B\left(\frac{U_3}{\Lambda_i\Omega}, \frac{R_T}{\Lambda_i}, \frac{\omega-p\Omega}{\Omega}\right)\right\} . \tag{5.16}$$

5.4. Acoustic Intensity Spectrum from Open Duct via Free Rotor Model

This model predicts the free-space radiation and hence may be regarded only as a source model. Because of this simplicity, the effect of the duct is not involved in the computation. As pointed out by Lansing [43], this model appears to overestimate greatly the radiated noise, and to have a completely different directivity pattern than his exact theory claims. However, this model can be used for diagnostic purposes on fans.

Again, neglecting the retarded time difference, as was done in Section 5.2., and utilizing Eq. (4.45) in Eq. (5.11), Eq. (5.11) becomes as follows:

$$
\begin{aligned}
S_{pp}(r,\phi,t,\omega) = \frac{1}{32\pi^2 a^3 r^2 \rho} \sum_{m=1}^{B} \sum_{n=1}^{N} \sum_{k=1}^{B} \sum_{\ell=1}^{N} \sum_{p=-\infty}^{\infty} \sum_{q=-\infty}^{\infty}
&H^{*}_{mn}(\omega-q\Omega) H_{k\ell}(\omega-q\Omega) \Delta R_n \Delta R_\ell e^{j\frac{2\pi}{B}(kq-mp)} \times \\
&\{(\omega-q\Omega)^2 e^{(p)}_{mn} e^{(q)}_{k\ell} + \Omega^2 f^{(p)}_{mn} f^{(q)}_{k\ell} \\
&\quad - (\omega-q\Omega)\Omega f^{(p)}_{mn} e^{(q)}_{k\ell} + (\omega-q\Omega)\Omega e^{(p)}_{mn} f^{(q)}_{k\ell}\} \times \\
&\Big\{\Big(1 - \sum_{s=-\infty}^{\infty} a_n^{(s)*} e^{-j(\frac{2\pi ms}{B} + s\Omega t)}\Big) S^{ii}_{mnk\ell}(\omega-q\Omega) \\
&\quad - \sum_{s=-\infty}^{\infty} a_\ell^{(s)} e^{j(\frac{2\pi ks}{B} - s\Omega t)} S^{ii}_{mnk\ell}(\omega-s\Omega-q\Omega) \\
&+ \sum_{s_1=-\infty}^{\infty} \sum_{s_2=-\infty}^{\infty} a_n^{(s_1)*} a_\ell^{(s_2)} \times
\end{aligned}
$$

$$e^{j\{\frac{2\pi S}{B}(ks_2-ms_1)+S\Omega(s_2-s_1)t\}}S^{ii}_{mnk\ell}(\omega-s_2S\Omega-q\Omega)$$

$$+ S\sum_{s_1=-\infty}^{\infty}\sum_{s_2=-\infty}^{\infty} c_n^{(s_2S+s_1)^*}c_\ell^{(s_1)} \times$$

$$e^{j\frac{2\pi}{B}\{(k-m)s_1-ms_2S\}+js_2S\Omega t} \times$$

$$S^{ww}_{mnk\ell}(\omega-s_1\Omega-q\Omega)e^{j(q-p)(\Omega t+\frac{\tau}{2})}$$

$$+\sum_{s_1=-\infty}^{\infty}\sum_{s_2=-\infty}^{\infty} b_n^{(s_1)}b_\ell^{(s_2)} \times$$

$$e^{j\frac{2\pi S}{B}(s_2k-s_1m)+j(s_2-s_1)S\Omega t}\ \delta(\omega-q\Omega-s_2S\Omega)\Big] . \tag{5.17}$$

Now, taking the time average of Eq. (5.17) over $2\pi/\Omega$, one obtains

$$\langle S_{yy}(r,\theta,t,\omega)\rangle = \frac{1}{32\pi^2a^3r^2\theta}\sum_{m=1}^{B}\sum_{n=1}^{N}\sum_{k=1}^{B}\sum_{\ell=1}^{N}\sum_{q=-\infty}^{\infty}$$

$$H^*_{mn}(\omega-q\Omega)H_{k\ell}(\omega-q\Omega)\Delta R_n\Delta R_\ell e^{j\frac{2\pi}{B}(k-m)q} \times$$

$$\{(\omega-q\Omega)^2e_n^{(q)}e_\ell^{(q)} + \Omega^2f_n^{(q)}f_\ell^{(q)}$$

$$- (\omega-q\Omega)\Omega f_n^{(q)}f_\ell^{(q)} + (\omega-q\Omega)\Omega e_n^{(q)}f_\ell^{(q)}\} \times$$

$$\Big[\{1-a_n^{(0)}-a_\ell^{(0)^*}\}S^{ii}_{mnk\ell}(\omega-q\Omega)$$

$$+\sum_{s=-\infty}^{\infty} a_n^{(s)^*}a_\ell^{(s)}e^{j\frac{2-S}{B}(k-m)s}S^{ii}_{mnk\ell}(\omega-sS\Omega-q\Omega)$$

$$+ S \sum_{s=-\infty}^{\infty} c_n^{(s)*} c_\ell^{(s)} e^{j\frac{2\pi}{B}(k-m)s} S_{mnk\ell}^{ii}(\omega - s\Omega - q\Omega)$$

$$+ \sum_{s=-\infty}^{\infty} b_n^{(s)*} b_\ell^{(s)} e^{j\frac{2\pi S}{B}(k-m)s} \delta(\omega - q\Omega - sS\Omega) \Bigg] , \tag{5.18}$$

where it is assumed that the terms $e_n^{(p)}$, $e_\ell^{(q)}$, $f_n^{(p)}$, $f_\ell^{(q)}$ for $(q - p) > S$ are negligible, and that $S_{\phi\phi}(r,\phi,t,\omega)$ is finite and continuous with respect to t. In fact, as $(R_n\Omega\sin\phi)/a$ decreases the above assumption becomes more accurate. (See Eq. (2.30) and Eq. (2.31).)

Now representing a blade by a dipole, and introducing the typical section idea for the impulse reseponse function of the blade, one obtains

$$\langle S_{pp}(r,\phi,t,\omega)\rangle = \frac{1}{32\pi^2 a^3 r^2 \rho} \sum_{m=1}^{B} \sum_{k=1}^{B} \sum_{q=-\infty}^{\infty} |H(\omega - q\Omega)|^2 \Delta R_T^2 \times$$

$$e^{j\frac{2\pi}{B}(k-m)q} \{(\omega - q\Omega)^2 (e_T^{(q)})^2 + \Omega^2 (f_T^{(q)})^2\} \times$$

$$\Bigg[(1 - a_T^{(0)} - a_T^{(0)*}) S_{mk}^{ii}(\omega - q\Omega)$$

$$+ \sum_{s=-\infty}^{\infty} |a_T^{(s)}|^2 e^{j\frac{2\pi S}{B}(k-m)s} S_{mk}^{ii}(\omega - sS\Omega - q\Omega)$$

$$+ \sum_{s=-\infty}^{\infty} |b_T^{(s)}|^2 e^{j\frac{2\pi S}{B}(k-m)s} \delta(\omega - q\Omega - sS\Omega)$$

$$+ S \sum_{s=-\infty}^{\infty} |c_T^{(s)}|^2 e^{j\frac{2\pi}{B}(k-m)s} S_{mk}^{ww}(\omega - s\Omega - q\Omega) \Bigg] . \tag{5.19}$$

Utilizing Eq. (5.15) in Eq. (5.19), and non-dimensionalizing the result, one obtains

$$\frac{S_{pp}(r,\vartheta,t,\omega)}{\rho a^2 R_T} = \frac{1}{32}\left(\frac{c_T}{r}\right)^2\left(\frac{\Delta R_T}{R_T}\right)^2\left(\frac{\overline{(u^i)^2}}{a^2}\right)\left(\frac{R_T\Omega}{a}\right)^3 \times$$

$$\sum_{q=-\infty}^{\infty} \frac{\left(\frac{\omega-q\Omega}{\Omega}\right)^2 (e_T^{(q)})^2 + (f_T^{(q)})^2}{1+\tau\left(\frac{\omega-q\Omega}{\Omega}\right)\left(\frac{c_T}{R_T}\right)} \times$$

$$\left\{(1-a_T^{(0)}-a_T^{(0)^*})S_B\left(\frac{U_3}{\delta_i\lambda_i\Omega}, \frac{R_T}{\gamma_i\lambda_i}, \frac{\omega-q\Omega}{\Omega}\right)\right.$$

$$+ \sum_{s=-\infty}^{\infty} |a_T^{(s)}|^2 S_B\left(\frac{U_3}{\delta_i\lambda_i\Omega}, \frac{R_T}{\gamma_i\lambda_i}, \frac{\omega-s\Omega-q\Omega}{\Omega}\right)$$

$$+ \frac{\overline{(u^w)^2}}{\overline{(u^i)^2}} S \sum_{s=-\infty}^{\infty} |c_T^{(s)}|^2 S_B\left(\frac{U_3^w}{\lambda_w\Omega}, \frac{R_T}{\lambda_w}, \frac{\omega-s\Omega-q\Omega}{\Omega}\right)$$

$$\left. + \frac{B^2\Omega}{\overline{(u^i)^2}} \sum_{\substack{s=-\infty \\ (sB/S)=\text{integer}}}^{\infty} |b_T^{(s)}|^2 \delta(\omega-q\Omega-sB\Omega)\right\} . \qquad (5.21)$$

When there is no strut, setting $a^{(s)} = b^{(s)} = 0$ for all s, in Eq. (5.20) and Eq. (5.21), yields an equation equivalent to Eq. (5.14) and Eq. (5.16), respectively.

When the observer is at $\vartheta = 0$, then Eq. (5.21) becomes

$$\frac{S_{pp}(r,\vartheta,t,\omega)}{\rho a^2 R_T} = \frac{1}{32}\left(\frac{R_T}{r}\right)^2\left(\frac{\Delta R_T}{R_T}\right)^2\left(\frac{c_T}{R_T}\right)^2\left(\frac{\overline{(u^i)^2}}{a^2}\right)\left(\frac{R_T\Omega}{a}\right)^3 \frac{\left(\frac{\omega}{\Omega}\right)^2}{1+\tau\frac{\omega}{\Omega}\frac{c_T}{R_T}} \times$$

$$\left\{(1-a_T^{(0)}-a_T^{(0)^*})S_B\left(\frac{U_3}{\delta_i\lambda_i\Omega}, \frac{R_T}{\gamma_i\lambda_i}, \frac{\omega}{\Omega}\right)\right.$$

$$+ \sum_{s=-\infty}^{\infty} |a_T^{(s)}|^2 S_B\left(\frac{U_3}{\delta_i\lambda_i\Omega}, \frac{R_T}{\gamma_i\lambda_i}, \frac{\omega-s\Omega}{\Omega}\right)$$

$$+\frac{\overline{(u^w)^2}}{\overline{(u^i)^2}}S\sum_{s=-\infty}^{\infty}|c_T^{(s)}|^2 S_B\left(\frac{U_3^w}{\Lambda_w\Omega},\ \frac{R_T}{\Lambda_w},\ \frac{\omega-s\Omega}{\Omega}\right)$$

$$+\frac{B^2\Omega}{\overline{(u^i)^2}}\sum_{\substack{s=-\infty \\ (sB/S)=\text{integer}}}^{\infty}|b_T^{(s)}|^2\delta(\omega-sB\Omega)\Big\}\ . \qquad (5.22)$$

CHAPTER VI

NUMERICAL RESULTS

6.1. Introduction

In Chapter V, the time averaged intensity function of the acoustic radiation from rotating blades was derived by replacing blades with rotating dipoles. This derivation was done under the following turbulent inflow conditions: turbulent ingestion with no inlet strut wakes, inflow turbulence elongation and contraction with no inlet strut wakes, and turbulent ingestion with inlet strut wakes.

For the present derivation, a blade was assumed to be acoustically compact. A rotating dipole model was pursued so that the effect of the dipole rotation can be accounted for explicitly. Sears' function was regarded as an impulse response function of a blade, so that the analysis was done in time and frequency domains. There was no blade-to-blade interaction to be included, such as that developed by Kemp, et al. [1]. Further, the dipole source was assumed to be predominant over other radiation sources, so that the retarded time difference among the lift of blades can be neglected. It was assumed that the inlet struts do not affect the sound propagation and that the distance from the rotor to the duct exit is much shorter than the sound wavelength so that duct effects on propagation are negligible. Finally, the turbulence was assumed to be frozen, homogeneous, and isotropic.

In this chapter, computations are done for the results in Chapter V such as Eq. (5.16) and Eq. (5.22) by changing the number of struts and rotor blades, the spacing between struts and a rotor, the observation angle, and non-dimensional parameters such as $U_3/\Lambda_i\Omega$ and R_T/Λ_i. In particular, the variation of these non-dimensional parameters is made around an axial flow velocity of U_3 = 30 m/sec, a rotor radius of R_T = 0.30 m, a rotor rotational speed of Ω = 220 rad/sec, an inflow turbulence length scale Λ_i = 0.15 m and 0.017 m, and a wake turbulence length scale Λ_w = 0.0068 m.

6.2. Numerical Results

Figs. 5, 6, and 7 show the non-dimensionalized $\langle S_{pp}(r,\phi,t,\omega)\rangle$ dependent on the non-dimensional parameters, $U_3/\Lambda_i\Omega$ and R_T/Λ_i. These figures show that as $U_3/\Lambda_i\Omega$ decreases, the level of the blade-passing frequency and its multiples increases, and as R_T/Λ_i increases those levels also increase. Further, as R_T/Λ_i increases, the overall level increases.

Hence, it is clear that the kinematic relation R_T/Λ_i cannot explain fully the spectrum profile without the dynamic relation $U_3/\Lambda_i\Omega$. The effect of $U_3/\Lambda_i\Omega$ on the spectrum is the same as that obtained by Homicz [8]. However, the effect of R_T/Λ_i on the spectrum for constant $U_3/\Lambda_i\Omega$ is the opposite of that claimed by Mani [15]. This is probably due to the fact that Mani did not consider the variation of $U_3/\Lambda_i\Omega$ when he varied R_T/Λ_i as a parameter. Further investigation of this matter is necessary.

Further, as the rotational speed increases, the bandwidth and the level at the blade-passing frequency and its multiples are

increased, and as the axial flow velocity increases, the blade-passing frequency and its multiples appear clearly. The above phenomena can be observed through the variation of $U_3/\Lambda_i\Omega$ in Figs. 5, 6, and 7.

Fig. 8 shows that as B increases, the bandwidth of the peak at the blade-passing frequency and its multiples increases. In this example, as B is increased from 3 to 9, the width at the blade-passing frequency has approximately triples. In this figure, the horizontal axis is $\omega/B\Omega$. This tendency is mentioned also by Homicz [8].

Figs. 9, 10, and 11 show the observer angle dependence of the non-dimensionalized $\langle S_{pp}(r,\vartheta,t,\omega)\rangle$. Fig. 10 shows that the domination of the blade-passing frequency is reduced as the observer angle increases. The extra wiggles in Fig. 10 are due to the dipole rotation. This shows that the disk model of a rotor is not sufficient even when the rotor radius is about 0.3 and its rotational speed Mach number is about 0.2.

In the computations in Figs. 9 through 11, the summation in Eq. (5.16) is done for the first five terms after observing that the computed result from the first seven terms is not different from that using the first five terms.

Fig. 12 shows the influence of the kinematic contraction and elongation of the inflow turbulence on the noise spectrum. The elongation and contraction produce a large effect on the spectrum as reported by Hanson [16]; although Hanson's elongation and contraction are done by the statistics of the eddies chopped by rotating blades. As shown in Fig. 12, the elongation and contraction rates, 2.0 and 0.5, respectively, create peaks at the blade-passing frequency and its multiples even if there is no high level of peak with no contraction

and elongation.

Figs. 13, 14, 15, and 16 show the non-dimensionalized $\langle S_{pp}(r,\phi,t,\omega)\rangle$ for the rotor operating in strut wakes. In this example, there is no clear influence of the wake turbulence on the spectrum profile. However, the effect of the mean flow deficit due to the inlet struts is pronounced unless the number of struts and rotor blades are chosen such that the least common multiple of B and S times Ω is in the cutoff range of Sears' function.

In Figs. 14 through 16, the wake position function Rect(t) is assumed to be deterministic, as shown in Fig. 17. The assumed mean flow deficit profile behind the struts is shown in Fig. 18. The wake turbulence convection velocity U_3^w is set to be $U_3 - u_c/2$, and the turbulence intensity variation according to the distance from the trailing edge of the upstream strut is given by $\overline{((u^w)^2)}^{1/2}/U_3 = 0.08(2x/c + 0.05)^{-0.35}$, where x is the coordinate along the airfoil measured from the trailing edge, and c is the length of the airfoil, see Ref. [44]. In the computation shown in Figs. 14 through 16, no consideration is made of the wake turbulence length scale variation with changes in rotor-strut spacing d. In fact, the length scales, Λ_i and Λ_w, are too small to represent a blade with a dipole; indeed, the dipole domination may not even be attained.

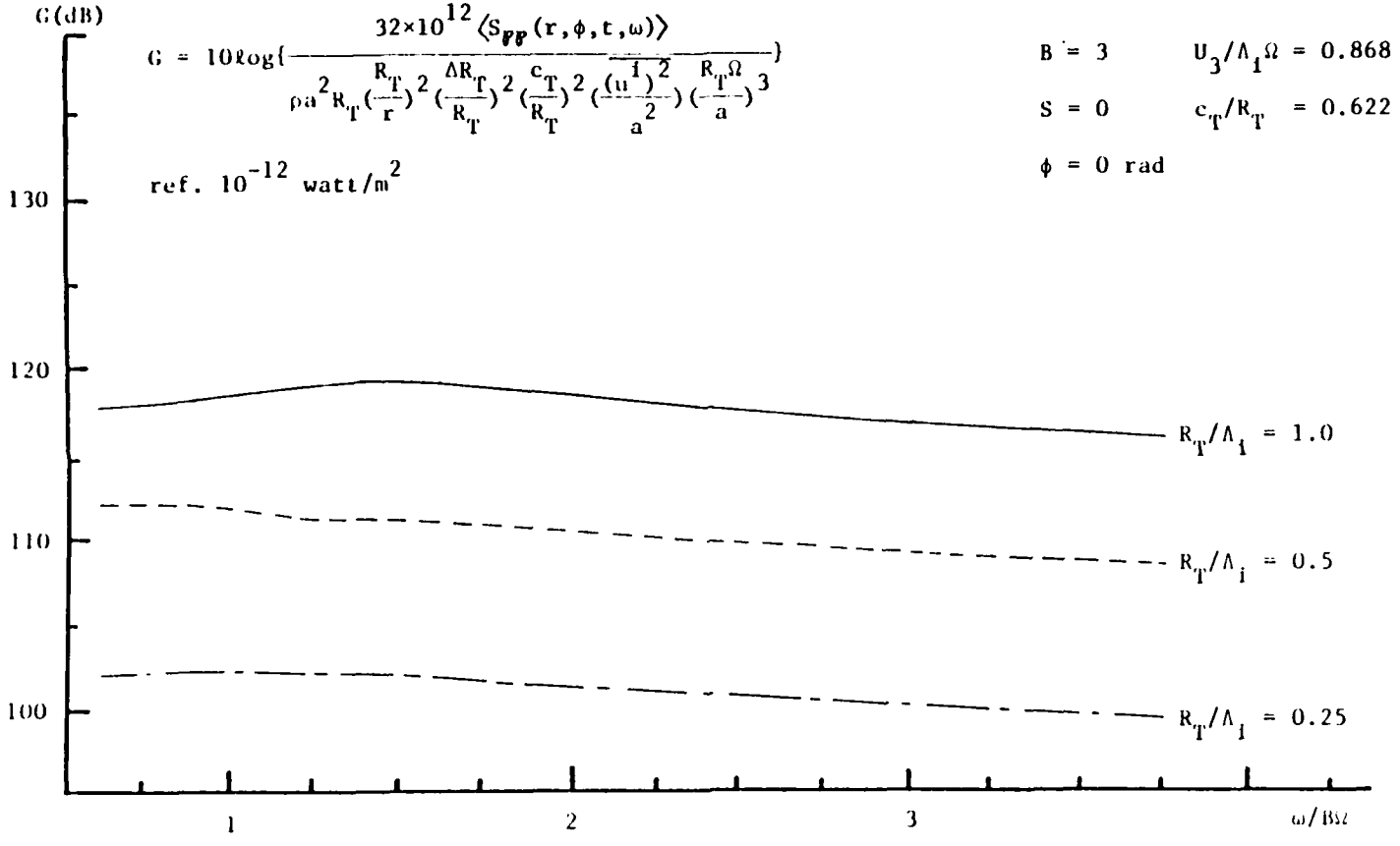

Fig. 5. Non-Dimensionalized $\langle S_{\phi\phi}(r,\phi,t,\omega)\rangle$ for B = 3 and $U_3/\Lambda_1\Omega$ = 0.868

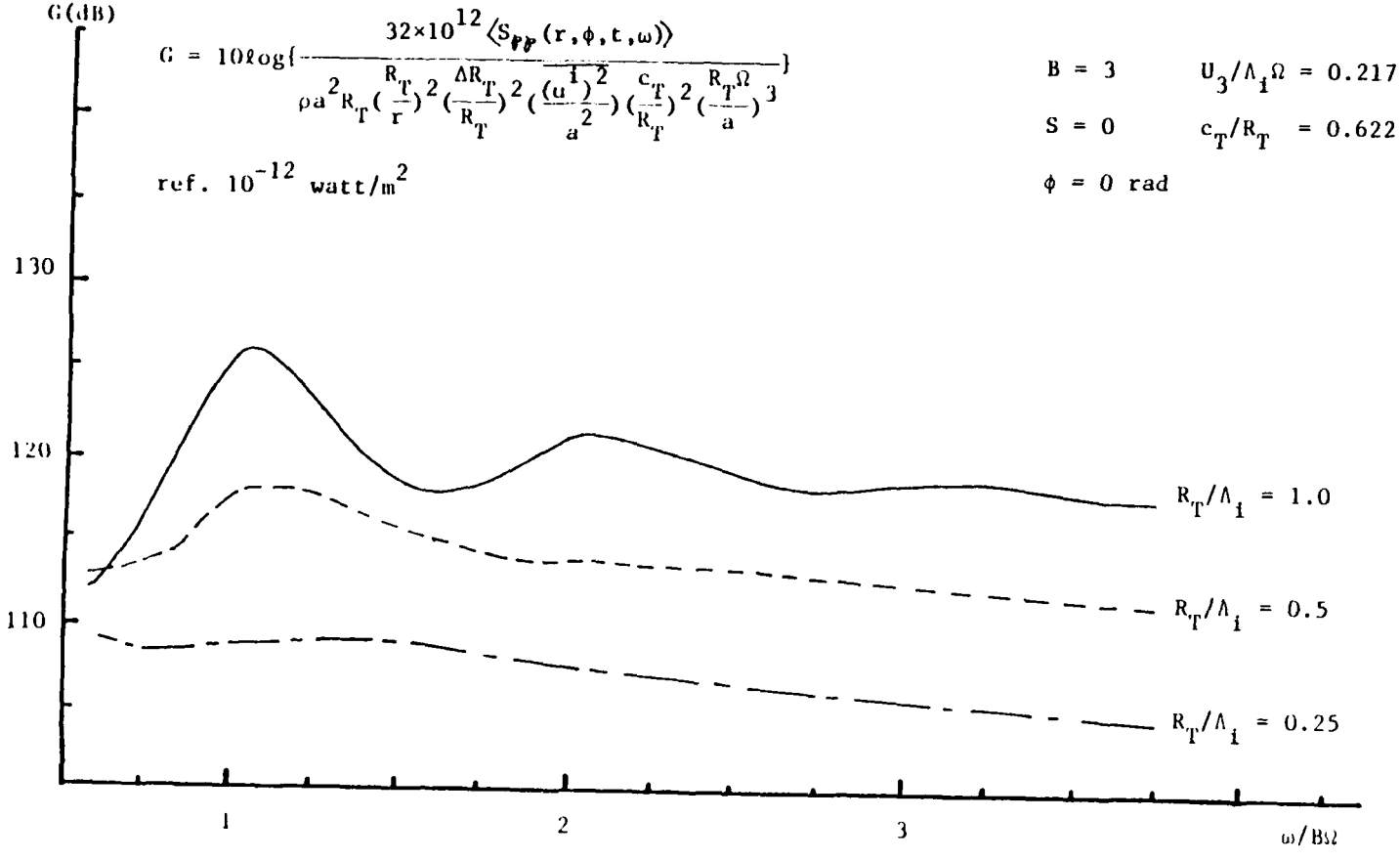

Fig. 6. Non-Dimensionalized $\langle S_{pp}(r,\phi,t,\omega)\rangle$ for B = 3 and $U_3/\Lambda_i\Omega = 0.217$

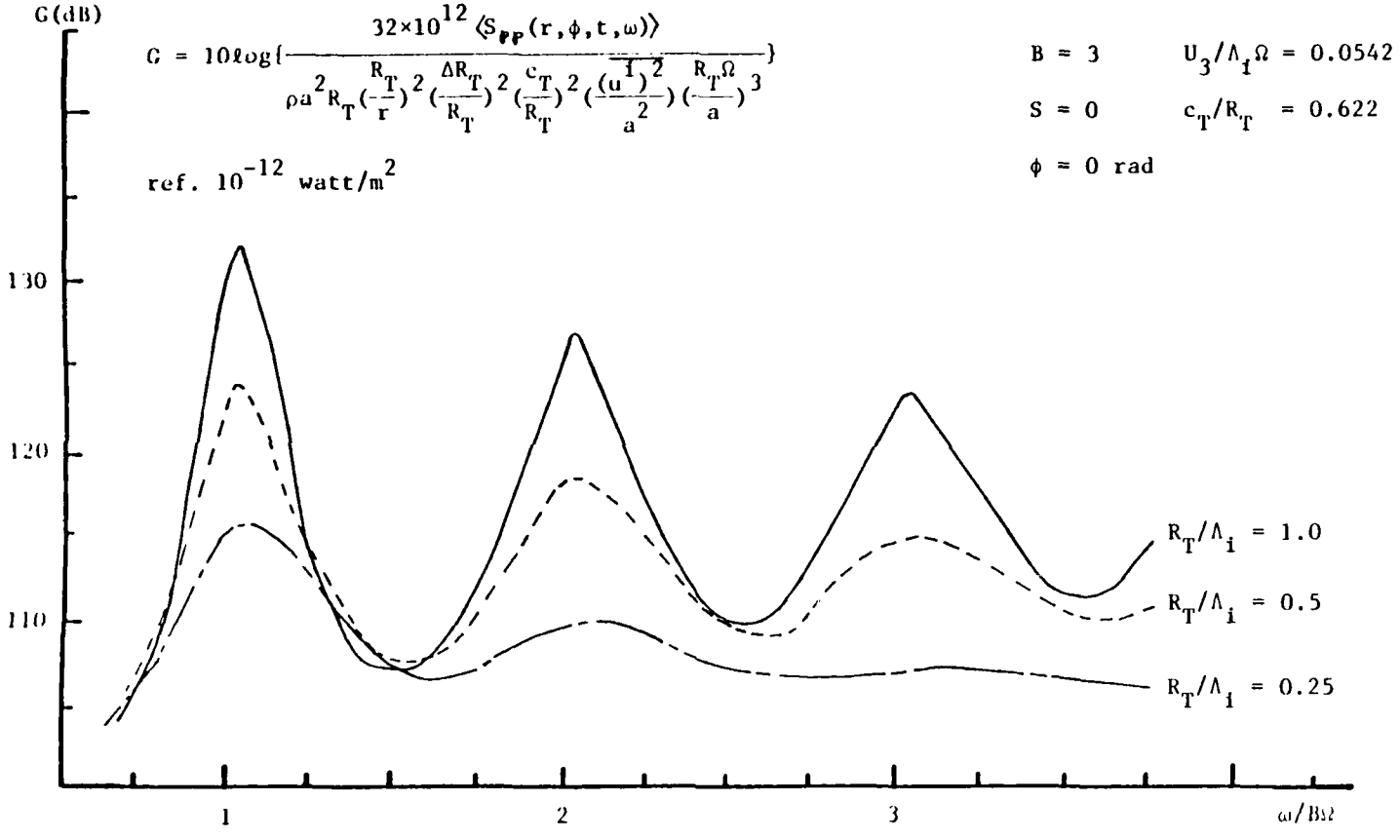

Fig. 7. Non-Dimensionalized $\langle S_{pp}(r,\phi,t,\omega)\rangle$ for B = 3 and $U_3/\Lambda_1\Omega$ = 0.0542

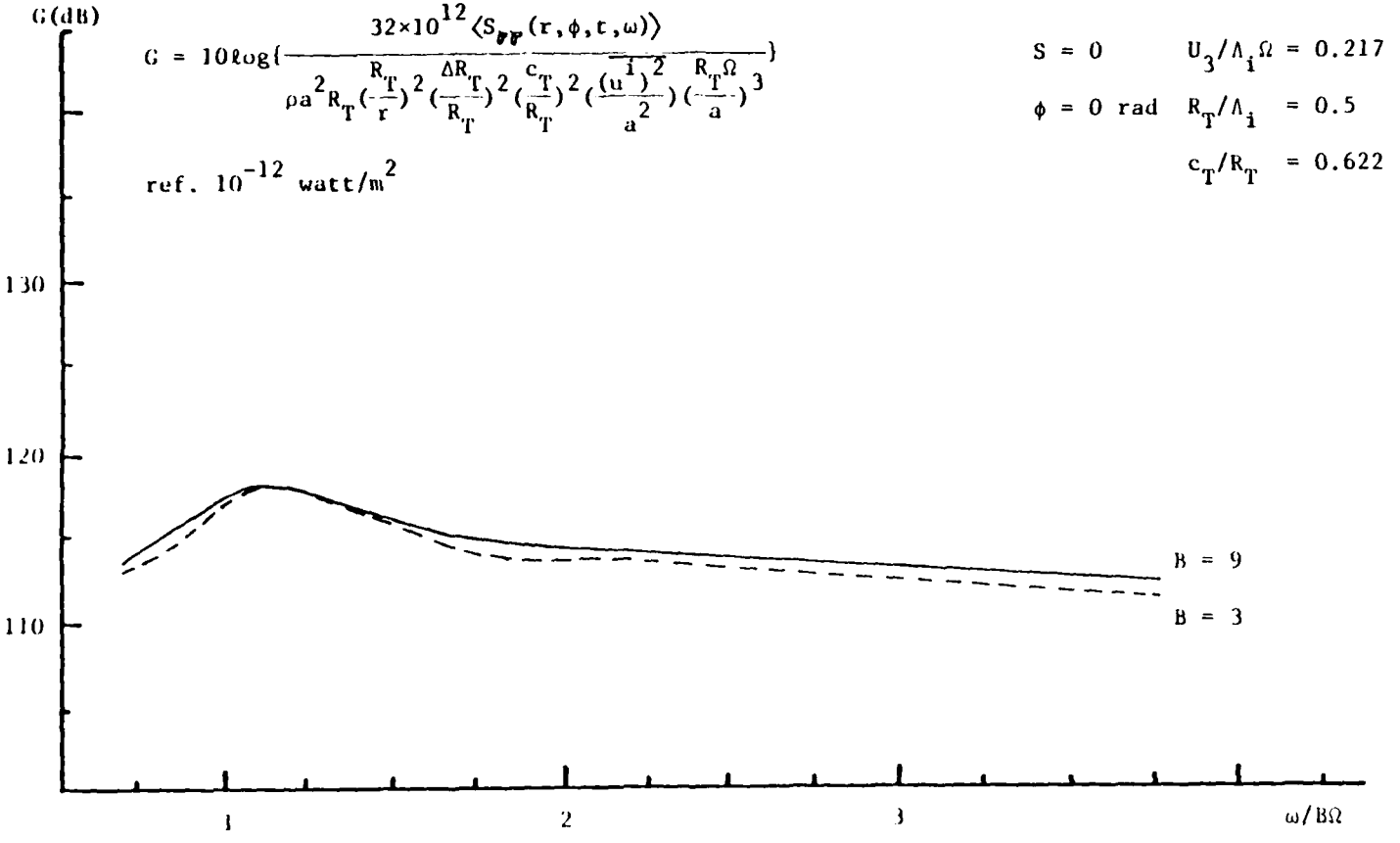

Fig. 8. Blade Number Dependence of Non-Dimensionalized $\langle S_{pp}(r,\phi,t,\omega)\rangle$ for $U_3/\Lambda_i\Omega = 0.217$ and $R_T/\Lambda_i = 0.5$

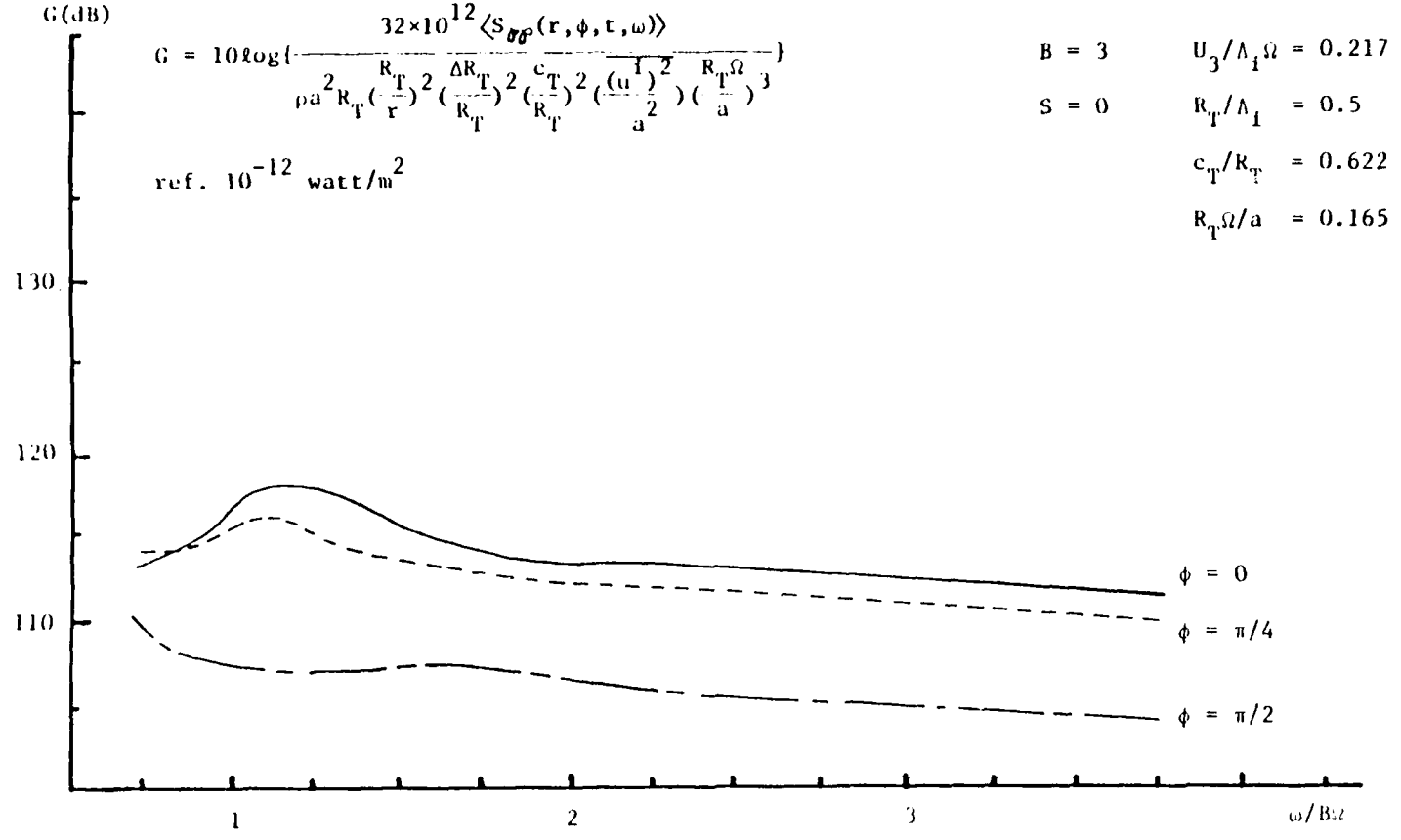

Fig. 9. ϕ-Dependence of Non-Dimensionalized $\langle S_{\theta\theta}(r,\phi,t,\omega)\rangle$ for B = 3, $U_3/\Lambda_1\Omega = 0.217$, and $R_T/\Lambda_1 = 0.5$

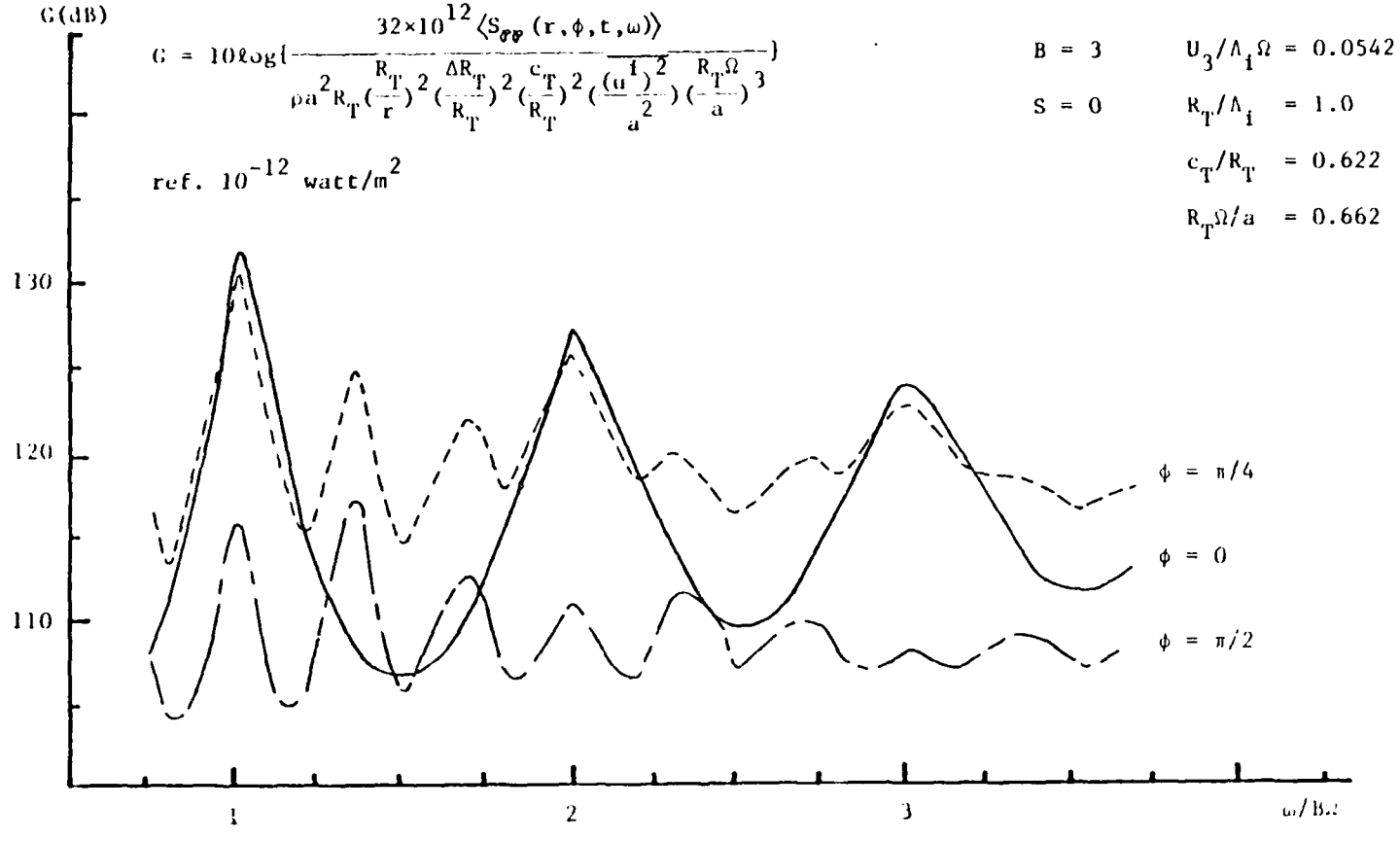

Fig. 10. ϕ-Dependence of Non-Dimensionalized $\langle S_{\sigma\sigma}(r,\phi,t,\omega)\rangle$ for B = 3, $U_3/\Lambda_1\Omega = 0.0542$, and $R_T/\Lambda_1 = 1.0$

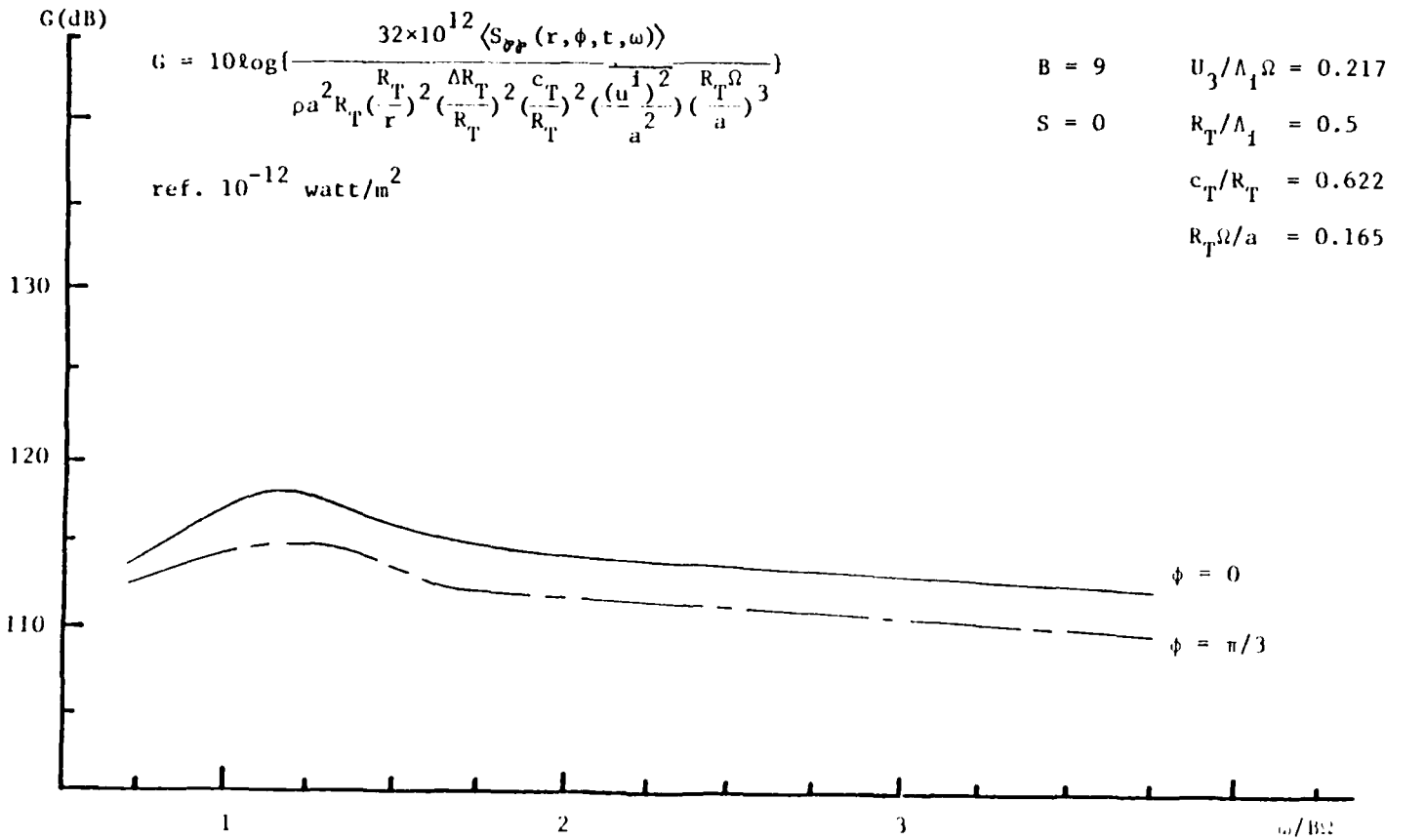

Fig. 11. ϕ-Dependence of Non-Dimensionalized $\langle S_{\gamma\gamma}(r,\phi,t,\omega)\rangle$ for B = 9, $U_3/\Lambda_1\Omega = 0.217$, and $R_T/\Lambda_1 = 0.5$

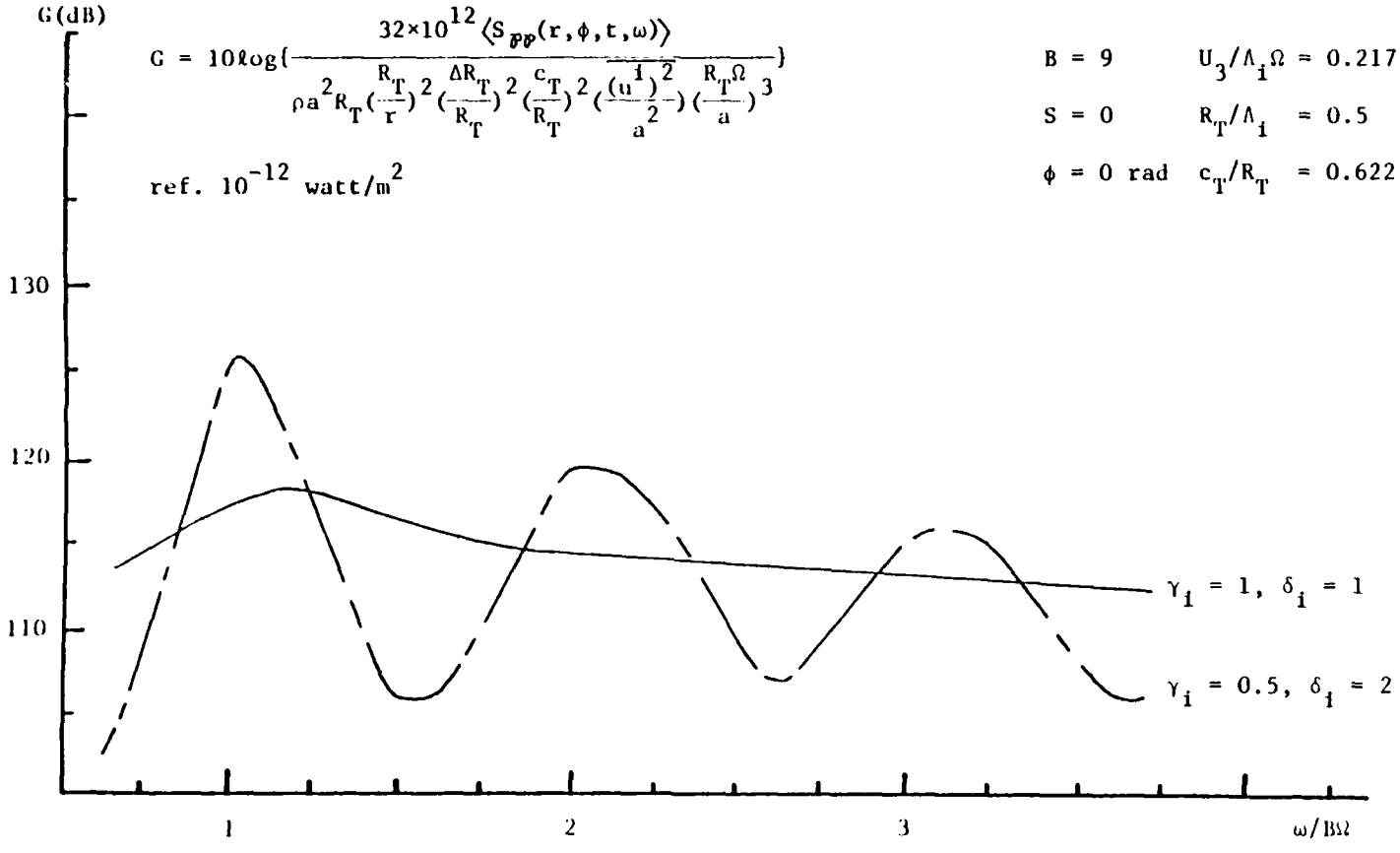

Fig. 12. Turbulence Elongation and Contraction Effect on Non-Dimensionalized $\langle S_{pp}(r,\phi,t,\omega)\rangle$

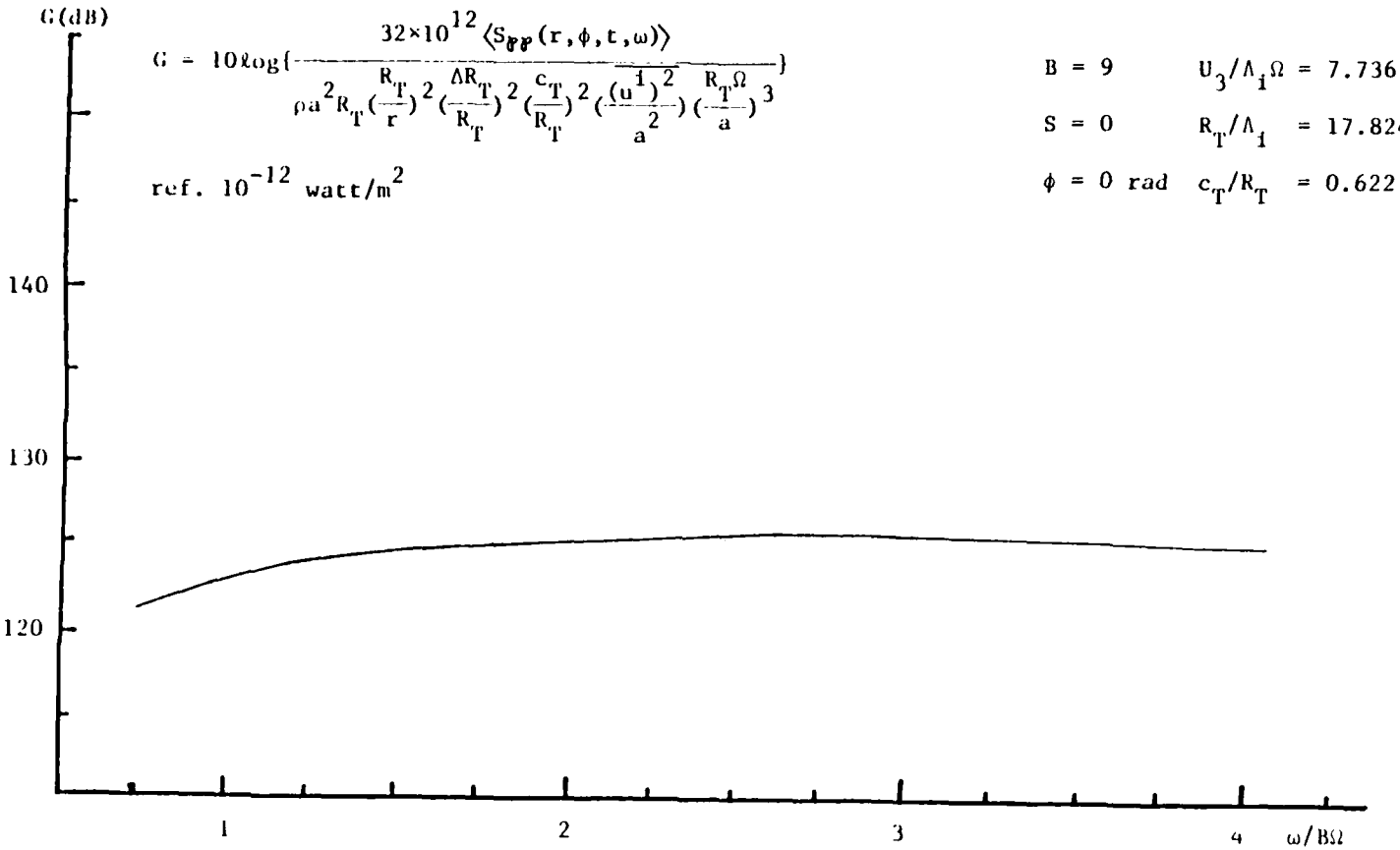

Fig. 13. Non-Dimensionalized $\langle S_{\theta\theta}(r,\phi,t,\omega)\rangle$ for B = 9, $U_3/\Lambda_1\Omega = 7.736$, S = 0, and $R_T/\Lambda_1 = 17.824$

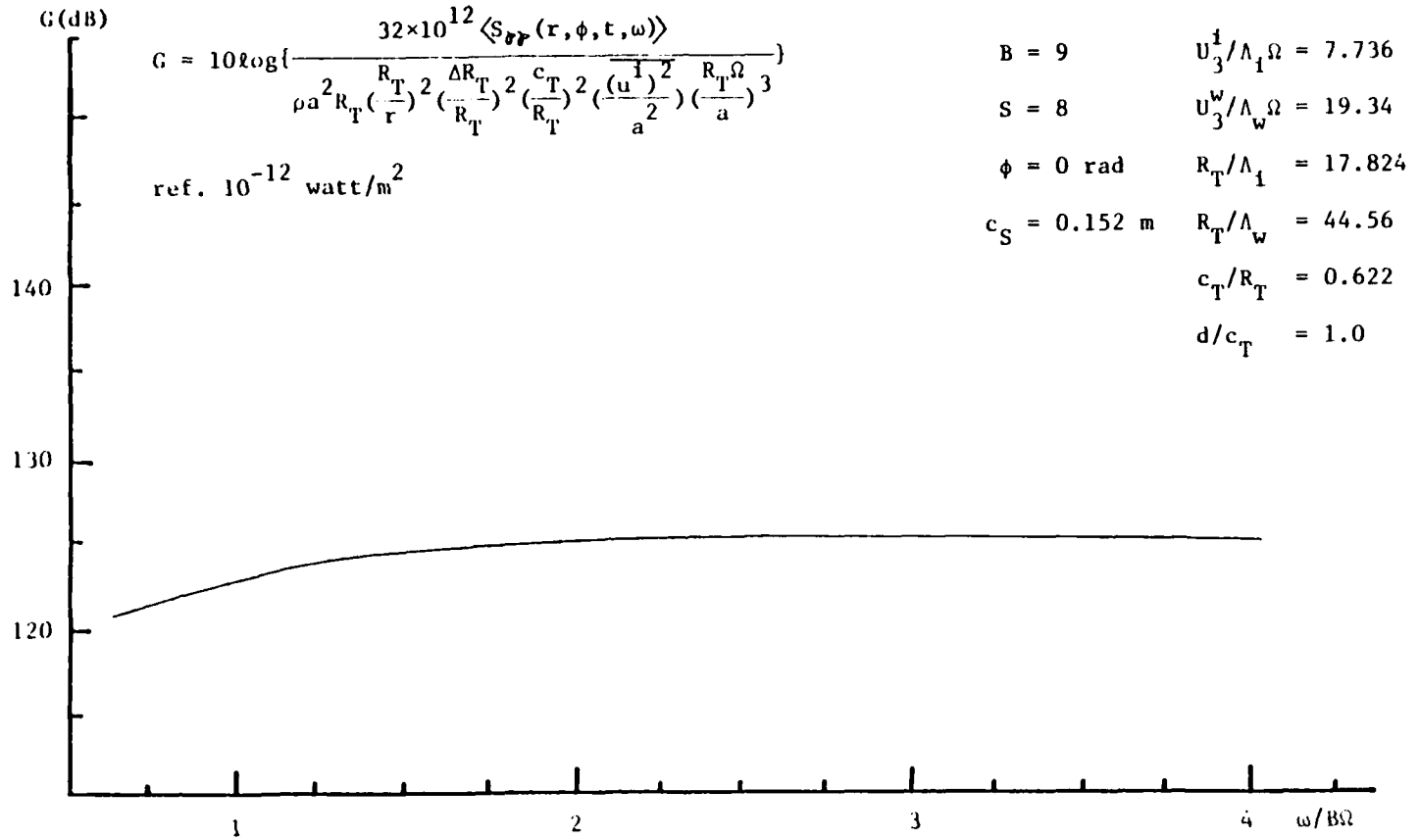

Fig. 14. Non-Dimensionalized $\langle S_{rr}(r,\phi,t,\omega)\rangle$ for B = 9, and S = 8

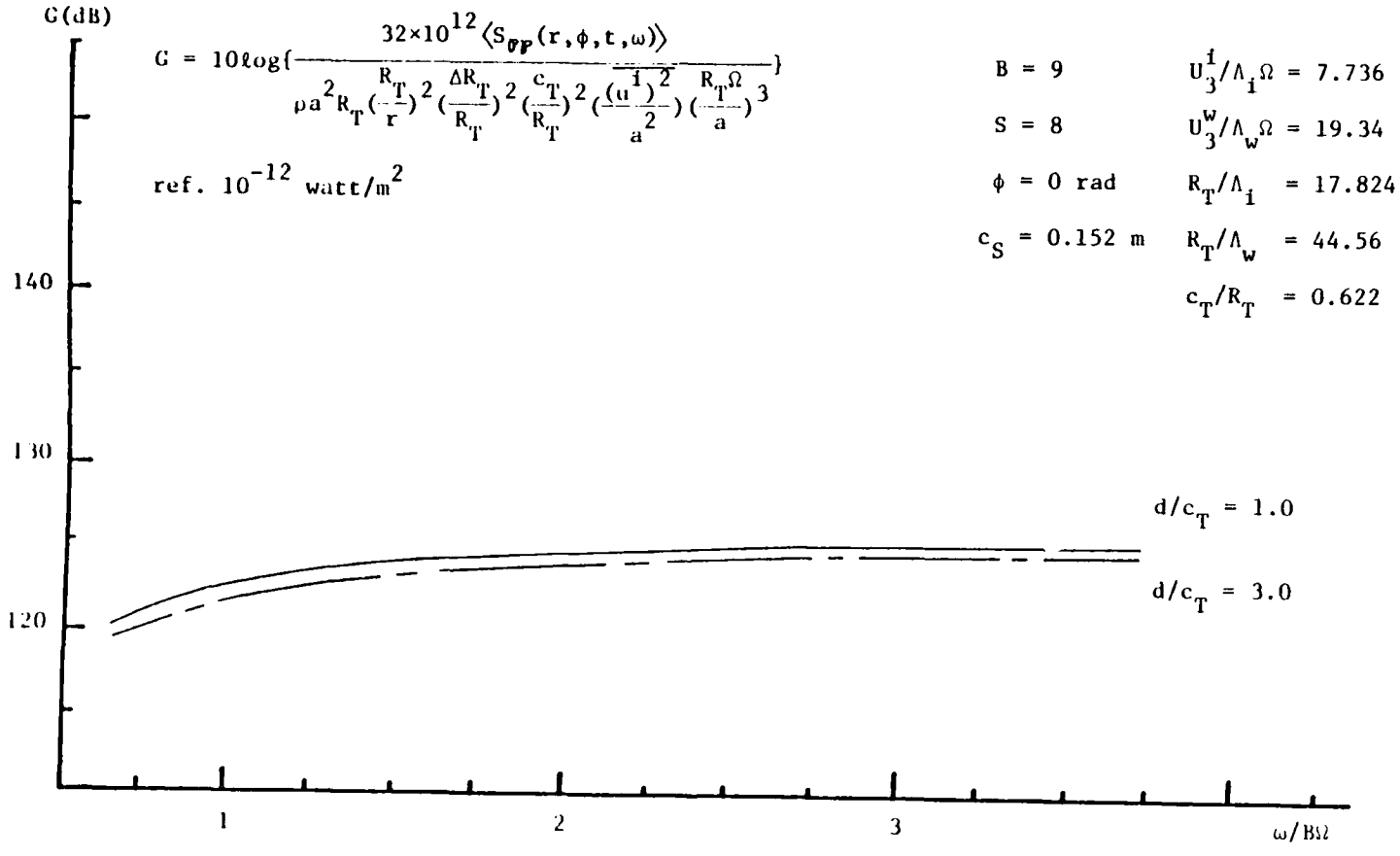

Fig. 15. Strut-Rotor Spacing Dependence of Non-Dimensionalized $\langle S_{pp}(r,\phi,t,\omega)\rangle$

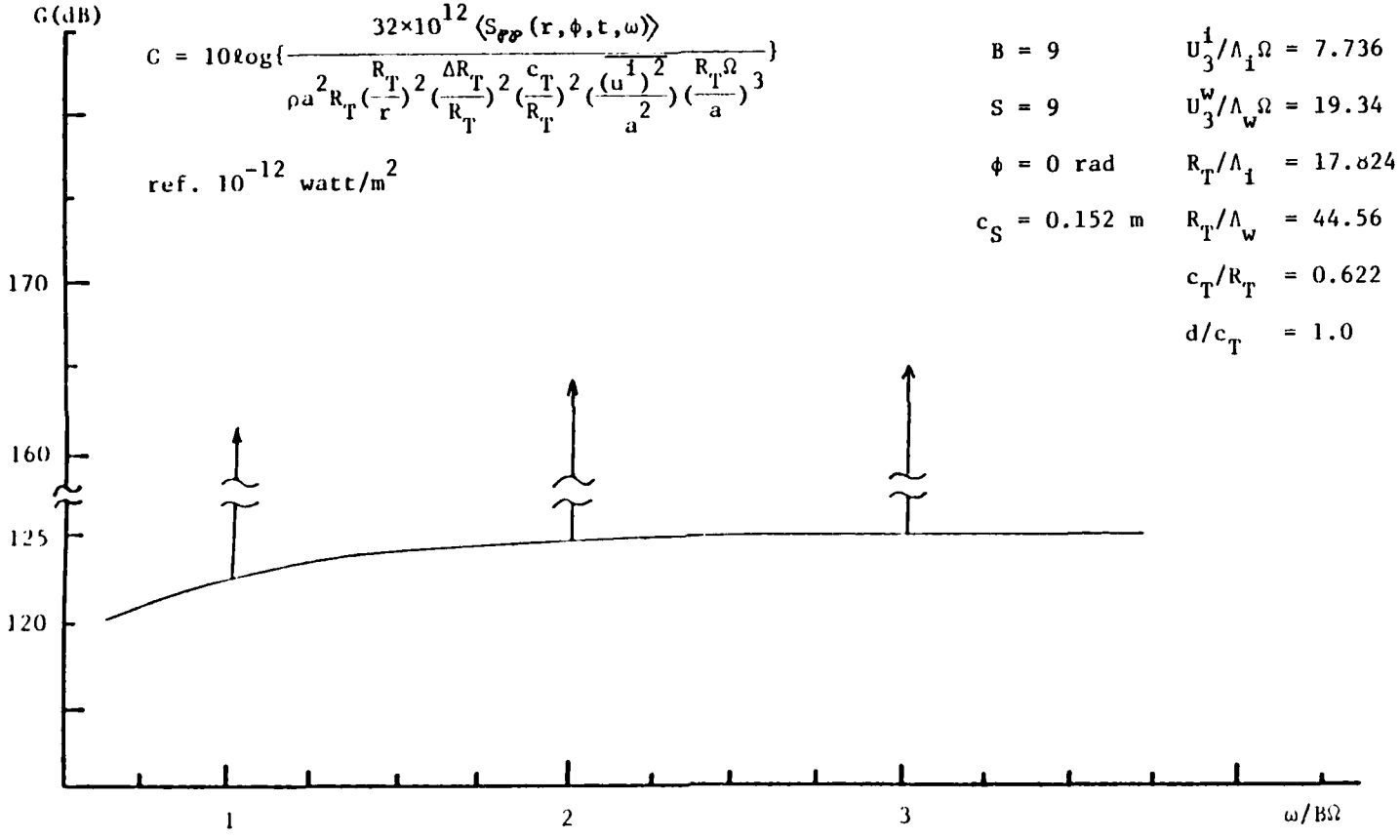

Fig. 16. Non-Dimensionalized $\langle S_{pp}(r,\phi,t,\omega)\rangle$ for B = 9, and S = 9

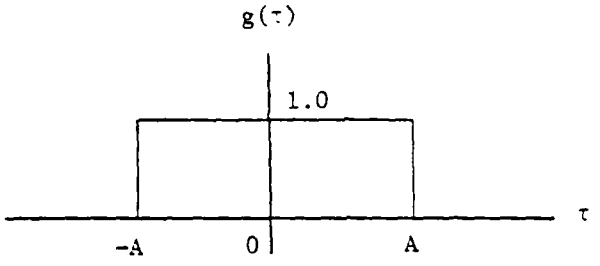

where

$A = 0.68c\{C_D(x/c-0.35)\}^{1/2}/S\Omega$

C_D = airfoil profile drag coefficient

c = airfoil chord length

x = coordinate along airfoil measured from midchord

Fig. 17. Wake Position Function Profile

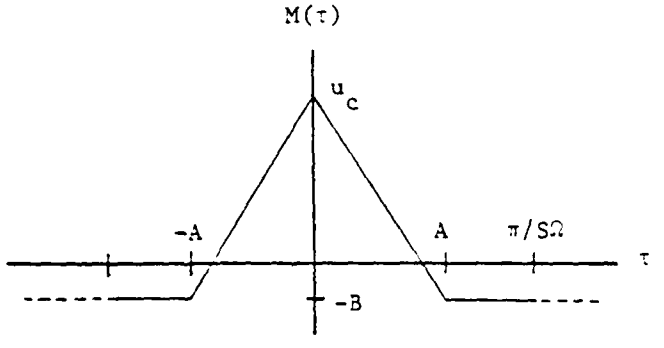

where

$u_c = U_3(4.84C_D^{1/2})\cos\beta/(x/c-0.2)$

$A = 0.68c\{C_D(x/c-0.35)\}^{1/2}/S\Omega$

$B = 2Au_c/(A+2\pi/S\Omega)$

c = airfoil chord length

C_D = airfoil profile drag coefficient

x = coordinate along airfoil measured from midchord

Fig. 18. Mean Flow Deficit Profile

CHAPTER VII

CONCLUSIONS

The time averaged intensity density function of the acoustic radiation from rotating blades was derived by replacing blades with rotating dipoles. The following conclusions can be drawn from the derivation:

1. The rectilinear model of a rotating blade row is applicable only for the frequency range such that $\omega >> \Omega$; see Eq. (2.25).
2. The effect of the variation of the distance between the observer and rotating dipoles can be neglected when $R_T \Omega \sin\theta/a << 1$; see Eq. (2.26) through Eq. (2.28). However, care must be taken as exhibited in Fig. 10.
3. The retarded time difference of the lift among blades and its derivative can be neglected when the dipole source dominates over other sources, the speed of the rotor is low, and/or the aspect ratio is low; see Eq. (5.5) and (5.6).
4. Two non-dimensional parameters, $U_3/\Lambda_i\Omega$ and R_T/Λ_i, govern the profile of the noise spectrum. As $U_3/\Lambda_i\Omega$ decreases, the level of the blade-passing frequency and its multiples increases, and as R_T/Λ_i increases the level also increases; see Figs. 5, 6, and 7.
5. The non-dimensionalized time average acoustic intensity density function is proportional to $(\overline{(u^2)^2}/a^2)(R_T\Omega/a)^3$ under the condition that other non-dimensional parameters are fixed; see

Eq. (5.22).

6. The effect of the wake turbulence can be reduced by reducing the wake width, increasing $U_3^w/\Lambda_w\Omega$, decreasing R_T/Λ_w, decreasing the number of struts, and reducing the ratio, $\overline{(u^w)^2}/\overline{(u^i)^2}$; see Eq. (5.22).

7. The number of struts and rotor blades should be chosen so that the least common multiple of S and B multiplied by Ω is in the cutoff range of the Sears' function in order to minimize the effect of the mean flow deficit; see Eq. (5.22).

8. The acoustic intensity at the off-angle from the rotor axis is not stationary even if the inflow turbulence is frozen and homogeneous; see Eq. (5.11). The acoustic intensity from the rotor with struts is not stationary even at the rotor axis; see Eq. (5.22).

9. Increasing B, and/or increasing Ω under the condition that $U_3/\Lambda_i\Omega$ is fixed increases the bandwidth of the peak of the blade-passing frequency and its multiples; see Feg. 8.

10. To find the effect of the rotor strut spacing on $\langle S_{pp}(r,\phi,t,\omega)\rangle$, consideration of the wake properties and mean flow deficit profile with respect to the spacing is necessary.

11. As was derived in Eq. (5.22), $\langle S_{pp}(r,\phi,t,\omega)\rangle$ is expressed by the terms due to the inflow turbulence and wake turbulence, and the term due to the mean flow deficit. Hence, we can deal with the $\langle S_{pp}(r,\phi,t,\omega)\rangle$ due to the inflow turbulence, the wake turbulence, and mean flow deficit separately, although this separation is hypothetical.

REFERENCES

1. Kemp, N. H., and Sears, W. R., "Aerodynamic Interference between Moving Blade Rows," J. Aeronautical Sciences, Vol. 20, No. 9, 1953, pp. 585-597.
2. Lighthill, M. J., "On Sound Generated Aerodynamically--I," Proc. Roy. Soc. London, 211A, 1952, pp. 564-587.
3. Curle, N., "The Influence of Solid Boundaries Upon Aerodynamic Sound," Proc. Roy. Soc. London, A231, 1955, pp. 505-514.
4. Doak, P. E., "Acoustic Radiation from a Turbulent Fluid Containing Foreign Bodies," Proc. Roy. Soc. London, 254A, 1960, pp. 129-145.
5. Ffowcs Williams, J. E., and Hawkings, D. L., "Sound Generation by Turbulence and Surfaces in Arbitrary Motion," Phil. Trans. Roy. Soc. London, 264A, 1969, pp. 321-342.
6. Goldstein, M. E., Aeronautics, NASA SP-346, 1974.
7. Lowson, M. V., "Sound Field for Singularities in Motion," Proc. Roy. Soc. London, A286, 1965, pp. 559-572.
8. Homicz, G. F., Broadband and Discrete Frequency Noise Radiation from Subsonic Rotors, Ph.D. Thesis, Cornell University, 1973.
9. Gutin, L., On the Sound Field of a Rotating Propeller, NACA TM 1195, 1948.
10. Wright, S. E., "Sound Radiation from a Lifting Rotor Generated by Asymmetric Disc Loading," J. Sound and Vib., Vol. 9, No. 2, 1969, pp. 223-240.

11. Wright, S. E., "Discrete Radiation from Rotating Periodic Sources," J. Sound and Vib., Vol. 17, No. 4, 1971, pp. 437-498.

12. Ffowcs Williams, J. E., and Hawkings, D. L., "Theory Relating to the Noise of Rotating Machinery," J. of Sound and Vib., Vol. 10, No. 1, 1969, pp. 10-21.

13. Lowson, M. V., and Ollerhead, J. B., "A Theoretical Study of Helicopter Rotor Noise," J. Sound and Vib., Vol. 9, No. 2, 1969, pp. 197-222.

14. Morfey, C. L., and Tanna, H. K., "Sound Radiation from a Point Force in Circular Motion," J. Sound and Vib., Vol. 15, No. 3, 1971, pp. 325-351.

15. Mani, R., "Noise due to Interaction of Inlet Turbulence with Isolated Stators and Rotors," J. Sound and Vib., Vol. 17, No. 2, 1971, pp. 251-260.

16. Hanson, D. B., "A Study of Subsonic Fan Noise Sources," Progress in Astronautics and Aeronautics, Vol. 44, AIAA, 1976.

17. Amiet, R. K., "Noise Produced by Turbulent Flow into a Propeller or Helicopter Rotor," AIAA Paper No. 76-560, 1976.

18. Aravamudan, K. S., and Harris, W., "Low-frequency Broadband Noise Generated by a Model Rot r," J. Acoust. Soc. Am., Vol. 66, No. 2, 1979, pp. 522-533.

19. Mani, R., "Discrete Frequency Noise Genegation by Axial Flow Fan Blade Row," J. Basic Engng., Vol. 92, 1970, pp. 37-43.

20. Sevik, M. M., "The Response of a Propulsor to Random Velocity Fluctuations," ORL, Serial No. N00017-70-C-1407-2, 1970.

21. Sears, W. R., "Some Aspects of Non-Stationary Airfoil Theory and Its Practical Application," J. Aeronautical Sciences, Vol. 8,

No 3, 1941, pp. 104-108.

22. Kelly, J. C., Broad Band Fan Noise due to Vortex Shedding, Rolls-Royce Rep. RR(OH)400, 1969.

23. McCroskey, W. J., "Some Current Research in Unsteady Fluid Dynamics," Trans. of ASME, J. Fluids Eng., 1977, pp. 8-38.

24. Jackson, R., Graham, J. M. R., and Maull, D. J., "The Lift on a Wing in a Turbulent Flow," Aeronautical Quaterly, Vol. 24, 1973, pp. 155-166.

25. Filotas, L. T., Theory of Airfoil Response in a Gusty Atmosphere, Part I--Aerodynamic Transfer Function; Part II--Response to Discrete Gusts or Continuous Turbulence, UTIA Rep. No. 139, 141, 1969.

26. Graham, F. M. R., "Lifting Surface Theory for the Problem of an Arbitrarily Yawed Sinusoidal Gust Incident on a Thin Aerofoil in Incompressible Flow," Aeronautical Quaterly, Vol. 21, 1970, pp. 182-198.

27. Amiet, R. K., "Acoustic Radiation from an Airfoil in a Turbulent Flow," J. Sound and Vib., Vol. 41, No. 4, 1975, pp. 407-420.

28. Morse, P. M., and Ingard, K. U., Theoretical Acoustics, McGraw-Hill, 1968.

29. Lowson, M. V., "Fundamental Considerations of Noise Radiation by Rotary Wings," AGARD Conference Pre-print No. 111 on Aerodynamics of Rotary Wings., 1972.

30. Leverton, J. W., "Noise of Rotorcraft," Westland Aircraft, RF 365, 1969.

31. Sevik, M. M., "Sound Radiation from a Subsonic Rotor Subjected to Turbulence," NASA SP 304, Part II, 1970, pp. 493-508.

32. Robins, B., and Lakshminarayana, B., "Effect of Inlet Turbulence on Compressor Noise," J. of Aircraft, Vol. 11, 1974, pp. 273-281.

33. Lane, F., Broadband Noise Generated by Turbulent Inflow to Rotor or Stator Blades in an Annular Duct, NASA TR-4, 1975.

34. Farassat, F., Theory of Noise Generation from Moving Bodies with an Application to Helicopter Rotors, NASA TR-451, 1975.

35. Liepmann, H. W., "On the Application of Statistical Concepts to the Buffeting Problem," J. Aeronautical Sciences, Vol. 19, No. 12, 1952, pp. 793-800.

36. Giesing, J. P., Rodden, W. P., and Stahl, B., "Sears Function and Lifting Surface Theory for Harmonic Gusts," J. of Aircraft, Vol. 7, 1970, pp. 252-255.

37. Kemp, N. H., and Sears, W. R., "The Unsteady Forces Due to Viscous Wakes in Turbomachines," J. Aeronautical Sciences, Vol. 22, 1955, pp. 478-483.

38. Von Karman, T., and Howarth, L., "On the Statistical Theory of Isotropic Turbulence," Proc. Roy. Soc. London, 164A, 1938, pp. 192-215.

39. Panchev, S., Random Functions and Turbulence, Pergamon Press, 1971, p. 105.

40. Ribner, H. S., and Tucker, M., Spectrum of Turbulence in a Contacting Stream, NACA Report 1113, 1952.

41. Chandrasekhar, S., "The Theory of Axisymmetric Turbulence," Philos. Trans. Roy. Soc. London, 242A, 1950, pp. 557-577.

42. Kershen, E. J., and Gliebe, P. R., "Noise Caused by the Interaction of a Rotor with Anisotropic Turbulence," AIAA J., Vol. 19, No. 6, 1981, pp. 717-723.

AD-A129 757 ROTOR NOISE DUE TO BLADE-TURBULENCE INTERACTION(U) 2/2
PENNSYLVANIA STATE UNIV UNIVERSITY PARK APPLIED
RESEARCH LAB K ISHIMARU 25 JAN 83 ARL/PSU/TM-83-27
UNCLASSIFIED N00024-79-C-6043 F/G 20/1 NL

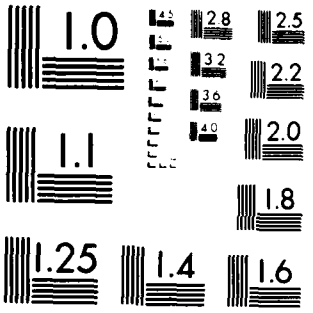

43. Lansing, D. L., "Exact Solution for Radiation of Sound From a Semi-infinite Circular Duct with Application to Fan and compressor Noise," Analytic Methods in Aircraft Aerodynamics, NASA SP-228, 1970.

44. Raj, R., and Lakshminarayana, B., "Characteristic of the Wake Behind a Cascade of Airfoils," J. Fluid Mech., Vol. 61, No. 4, 1973, pp. 707-730.

APPENDIX I

Given Eq. (2.17) as follows:

$$(r,\phi,t) = -\frac{1}{4\pi}\int_{-\infty}^{\infty}\sum_{m=1}^{B}\sum_{n=1}^{N}(\vec{\ell}_{mn}\cdot\nabla_o D_{mn})\Delta R_n\left\{\frac{\delta'(\tau-t+D_{mn}/a)}{aD_{mn}} - \frac{\delta'(\tau-t+D_{mn}/a)}{D_{mn}^2}\right\}d\tau \ , \tag{AI.1}$$

where

$$D_{mn} \simeq r - R_n\sin\theta\cos(\Omega\tau + \phi_m) \ , \tag{AI.2}$$

and integrating Eq. (AI.1) with respect to τ, one obtains

$$(r,\phi,t) = \frac{1}{4\pi}\sum_{m=1}^{B}\sum_{n=1}^{N}\left\{\frac{\Delta R_n}{1+\frac{\partial D_{mn}}{a\partial\tau}}\left\{\frac{\partial}{\partial\tau}\left(\frac{g_{mn}}{a(1+\frac{\partial D_{mn}}{a\partial\tau})D_{mn}}\right) + \frac{g_{mn}}{D_{mn}^2}\right\}\right\} \ , \tag{AI.3}$$

where

$$g_{mn} = \ell_{mn}^{\theta}\frac{\partial D_{mn}}{R_n\partial\phi} + \ell_{mn}^{Z}\frac{\partial D_{mn}}{\partial Z} \ , \tag{AI.4}$$

and the relation, $d\{\delta(\gamma(\tau))\}/d\gamma = (d\delta/d\tau)(d\tau/d\gamma)$, is used. Considering the terms in the parenthesis of Eq. (AI.3), one obtains the following equation:

$$\frac{\partial}{\partial\tau}\left(\frac{g_{mn}}{a(1+\frac{\partial D_{mn}}{a\partial\tau})D_{mn}}\right) + \frac{g_{mn}}{D_{mn}^2} = \frac{\partial}{r\partial\tau}\left\{\frac{g_{mn}}{a(1+\frac{\partial D_{mn}}{a\partial\tau})}\right\} - \frac{g_{mn}}{r^2a(1+\frac{\partial D_{mn}}{a\partial\tau})}\frac{\partial D_{mn}}{\partial\tau} + \frac{g_{mn}}{r^2} \ , \tag{AI.5}$$

where D_{mn} is approximated by r, due to the assumption that $R_n << r$ for all $n = 1,2,\ldots,N$ and because the time history of the pressure is not sought. Taking the τ-Fourier transform of Eq. (AI.5) and taking the ratio of the 1^{st} and 3^{rd} terms yields

$$\frac{-\frac{j\omega}{ar}\{G(\omega)*A(\omega)\}}{\frac{G(\omega)}{r^2}},$$

where $G(\omega) = \mathcal{F}\{g_{mn}(\tau)\}$ and $A(\omega) = \mathcal{F}\{1/(1+\frac{1}{a}\frac{\partial D_{mn}}{\partial \tau})\}$. Now, by utilizing a Taylor expansion on A, one obtains

$$\{1 + \frac{\partial D_{mn}}{a\partial\tau}\}^{-1} = 1 - \frac{\partial D_{mn}}{a\partial\tau} + \left(\frac{\partial D_{mn}}{a\partial\tau}\right)^2 + \ldots\ldots$$

The above equation shows that the steady state component has a magnitude "1". Therefore, because $\partial D_{mn}/a\partial\tau << 1$ (since a low speed rotor is considered here), $G(\omega)*A(\omega) = G(\omega)$ for all ω. Hence, the absolute value of the ratio of the 1^{st} and 3^{rd} terms becomes $\omega r/a$. If $\omega r/a >> 1$, the 3^{rd} term is negligible. The condition $\omega r/a >> 1$ defines the acoustic far field.

APPENDIX II

Lowson [7] derived the following Fourier coefficients of the amplitude modulation for 3^{rd} and 4^{th} terms in Eq. (2.25), under the condition $\phi_m = 0$,

$$\frac{\cos\Omega(t - D_{mn}/a)}{\left(1 + \frac{R_n\Omega}{a}\sin\phi\ \sin\Omega(t - D_{mn}/a)\right)^3} = \sum_{p=-\infty}^{\infty} \frac{-jpJ_p(p\frac{R_n\Omega}{a}\sin\phi)}{\frac{R_n\Omega}{a}\sin\phi} \times e^{jp(\Omega t + \pi/2)} . \quad \text{(AII.1)}$$

Taking the phase ϕ_m, of the amplitude modulation in Eq. (2.25) into account yields

$$\frac{\cos\{\Omega(t - D_{mn}/a) + \phi_m\}}{\left(1 + \frac{R_n\Omega}{a}\sin\phi\ \sin\{\Omega(t - D_{mn}/a) + \phi_m\}\right)^3} = \sum_{p=-\infty}^{\infty} \frac{-jpJ_p(p\frac{R_n\Omega}{a}\sin\phi)}{\frac{R_n\Omega}{a}\sin\phi} \times e^{jp(\Omega t + \pi/2 + \phi_m)} . \quad \text{(AII.2)}$$

Now, consider the Fourier coefficient of the other amplitude modulation in Eq. (2.25), for instance, the Fourier coefficient of $\{1 + (R_n\Omega/a)\sin\phi\ \sin\{\Omega(t - D_{mn}/a) + \phi_m\}\}^{-2}$. Taking the time derivative of $\{1 + (R_n\Omega/a)\sin\phi\ \sin\{\Omega(t - D_{mn}/a) + \phi_m\}\}^{-1}$ yields

$$\frac{d}{dt}\{1 + (R_n\Omega/a)\sin\phi\ \sin\gamma\}^{-1} = -\frac{\Omega^2 R_n \sin\phi\ \sin\gamma}{a\left(1 + \frac{R_n\Omega}{a}\sin\phi\ \sin\gamma\right)^3} , \quad \text{(AII.3)}$$

where the following relations are used:

$$\frac{d}{dt} = \frac{d\gamma}{dT}\frac{dT}{dt}\frac{d}{d\gamma} , \tag{AII.4}$$

$$\gamma = \Omega(t - D_{mn}/a) + \phi_m , \tag{AII.5}$$

and

$$T = \Omega(t - r/a) + \phi_m = \gamma - \frac{R_n\Omega}{a}\sin\phi\cos\gamma . \tag{AII.6}$$

By comparing Eq. (AII.2) with Eq. (AII.3), one obtains the following expansion:

$$\left(1 + \frac{R_n\Omega}{a}\sin\phi\,\sin\{\Omega(t - D_{mn}/a) + \phi_m\}\right)^{-1} = \sum_{p=-\infty}^{\infty} J_p\left(p\frac{R_n\Omega}{a}\sin\phi\right) \times e^{jp(\Omega t + \pi/2 + \phi_m)} , \tag{AII.7}$$

where the steady state component can be computed by

$$\frac{\Omega}{2\pi}\int_0^{2\pi/\Omega}\left(1 + \frac{R_n\Omega}{a}\sin\phi\,\sin\gamma\right)^{-1}dt = 1 , \tag{AII.8}$$

since $d\gamma = \left(1 + \frac{R_n\Omega}{a}\sin\phi\,\sin\gamma\right)^{-1}dt$.

Therefore, one obtains

$$\left(1 + \frac{R_n\Omega}{a}\sin\phi\,\sin\{\Omega(t - D_{mn}/a) + \phi_m\}\right)^{-2} = \sum_{p=-\infty}^{\infty}\sum_{q=-\infty}^{\infty} J_p\left(p\frac{R_n\Omega}{a}\sin\phi\right)J_q\left(q\frac{R_n\Omega}{a}\sin\phi\right)e^{j(p+q)(\Omega t + \pi/2 + \phi_m)} . \tag{AII.9}$$

Now, consider the Fourier coefficient of $\sin\{\Omega(t-D_{mn}/a)+\phi_m\}/\left(1+\frac{R_n\Omega}{a}\sin\phi\ \sin\{\Omega(t-D_{mn}/a)+\phi_m\}\right)^2$. Since it can be expressed by

$$\frac{\sin\{\Omega(t-D_{mn}/a)+\phi_m\}}{1+\frac{R_n\Omega}{a}\sin\phi\sin\{\Omega(t-D_{mn}/a)+\phi_m\}}\cdot\frac{1}{1+\frac{R_n\Omega}{a}\sin\phi\sin\{\Omega(t-D_{mn}/a)+\phi_m\}},$$

the Fourier coefficient can be obtained through coefficients for each term in the above.

Taking the time derivative of $\sin\{\Omega(t-D_{mn}/a)+\phi_m\}/\left(1+\frac{R_n\Omega}{a}\sin\phi\ \sin\{\Omega(t-D_{mn}/a)+\phi_m\}\right)$ yields

$$\frac{d}{dt}\left(\frac{\sin\gamma}{1+\frac{R_n\Omega}{a}\sin\phi\sin\gamma}\right)=\frac{\Omega\cos\gamma}{\left(1+\frac{R_n\Omega}{a}\sin\phi\sin\gamma\right)^3}, \qquad \text{(AII.10)}$$

where Eq. (AII.4), Eq. (AII.5), and Eq. (AII.6) are utilized.

By comparing Eq. (AII.10) with Eq. (AII.2), the following expansion can be obtained:

$$\frac{\sin\gamma}{1+\frac{R_n\Omega}{a}\sin\phi\sin\gamma}=\sum_{p=-\infty}^{\infty}-\frac{J_p(p\frac{R_n\Omega}{a}\sin\phi)}{\frac{R_n\Omega}{a}\sin\phi}e^{jp(\Omega t+\pi/2+\phi_m)}\times$$

$$(\delta_{0p}-1), \qquad \text{(AII.11)}$$

where the steady state component is obtained by

$$\frac{\Omega}{2\pi}\int_0^{2\pi/\Omega}\frac{\sin\gamma}{1+\frac{R_n\Omega}{a}\sin\phi\sin\gamma}dt=\frac{1}{2\pi}\int_0^{2\pi}\sin\gamma d\gamma=0. \qquad \text{(AII.12)}$$

Therefore, utilizing Eq. (AII.9) and Eq. (AII.12), the following expansion is obtained:

$$\frac{\sin\{\Omega(t - \frac{D_{mn}}{a}) + \phi_m\}}{\left(1 + \frac{R_n\Omega}{a}\sin\phi \sin\{\Omega(t - \frac{D_{mn}}{a}) + \phi_m\}\right)^2} = \sum_{p=-\infty}^{\infty} \sum_{q=-\infty}^{\infty} \frac{\delta_{op} - 1}{\frac{R_n\Omega}{a}\sin\phi} \times$$

$$J_p(p\frac{R_n\Omega}{a}\sin\phi)J_q(q\frac{R_n\Omega}{a}\sin\phi)e^{j(p+q)(\Omega t+\phi_m+\frac{\pi}{2})} .$$

(AII.13)

APPENDIX III

The expected value of $\mathrm{Rect}(\frac{t+b}{w})$ is computed by the following integration:

$$g(t) = \int_{-\infty}^{\infty}\int \mathrm{Rect}(\frac{t+b}{w})p_r(b)p_r(w)dbdw \ , \qquad \text{(AIII.1)}$$

where

$$p_r(b) = \begin{cases} \frac{1}{2\Delta} & |b| \leq \Delta \\ 0 & \text{otherwise} \ , \end{cases} \qquad \text{(AIII.2)}$$

$$p_r(w) = \begin{cases} \frac{1}{\Delta_2 - \Delta_1} & \Delta_1 \leq w \leq \Delta_2 \\ 0 & \text{otherwise} \ , \end{cases} \qquad \text{(AIII.3)}$$

and b and w are random variables for the position and width of Rect(t), respectively.

Integrating with respect to b and w, one obtains

$$g(t) = \begin{cases} 0 & |t| \geq \Delta_2+\Delta \\ \frac{1}{4\Delta(\Delta_2 - \Delta_1)}(\Delta_2 - |t| + \Delta)^2 & \Delta_2+\Delta \geq |t| \geq \Delta_2-\Delta \\ \frac{1}{\Delta_2-\Delta_1}\{2\Delta + \frac{1}{2}(\Delta_2-|t|-\Delta)\frac{1}{2\Delta} - \frac{1}{2}\}(|t|+3\Delta-\Delta_2) & \\ & \Delta_2-\Delta \geq |t| \geq \Delta_2-3\Delta \\ 1 & |t| \leq \Delta_2-3\Delta \ , \end{cases} \qquad \text{(AIII.4)}$$

where $\Delta_2 - \Delta_1 = 2\Delta$ is assumed.

Now, consider the special case such that $p_r(b) = \delta(b)$ and $p_r(w) = \delta(w - w_c)$. Then, g(t) becomes

$$g(t) = \text{Rect}(t/w_c) \ . \qquad \text{(AIII.5)}$$

Eq. (AIII.5) represents the case where Rect(t) is a deterministic function whose width and position are $2w_c$ and zero in the time axis, respectively.

DISTRIBUTION LIST FOR UNCLASSIFIED ARL TM 83-27 by K. Ishimaru, dated January 25, 1983.

Commander
Naval Sea Systems Command
Department of the Navy
Washington, DC 20362
Attn: Library
Code NSEA-09G32
(Copy Nos. 1 and 2)

Naval Sea Systems Command
Attn: S. M. Blazek
Code NSEA-55N
(Copy No. 3)

Naval Sea Systems Command
Attn: A. R. Paladino
Code NSEA-55N
(Copy No. 4)

Naval Sea Systems Command
Attn: F. B. Peterson
Code 56X
(Copy No. 5)

Naval Sea Systems Command
Attn: T. E. Peirce
Code NSEA-63R31
(Copy No. 6)

Commanding Officer
Naval Underwater Systems Center
Newport, RI 02840
Attn: B. J. Myers
Code 36311
(Copy No. 7)

Naval Underwater Systems Center
Attn: Library
Code 54
(Copy No. 8)

Naval Underwater Systems Center
Attn: P. Corriveau
Code 3634
(Copy No. 9)

Officer-in-Charge
David W. Taylor Naval Ship R&D Center
Department of the Navy
Annapolis Laboratory
Annapolis, MD 21402
Attn: J. V. Pierpoint
Code 2741
(Copy No. 10)

David W. Taylor Naval Ship R&D Center
Attn: J. W. Henry
Code 2741
(Copy No. 11)

Commander
David W. Taylor Naval Ship R&D Center
Department of the Navy
Bethesda, MD 20084
Attn: W. B. Morgan
Code 15
(Copy No. 12)

David W. Taylor Naval Ship R&D Center
Attn: Library
Code 1505
(Copy No. 13)

David W. Taylor Naval Ship R&D Center
Attn: J. H. McCarthy
Code 154
(Copy No. 14)

David W. Taylor Naval Ship R&D Center
Attn: M. M. Sevik
Code 19
(Copy No. 15)

David W. Taylor Naval Ship R&D Center
Attn: W. K. Blake
Code 1905
(Copy No. 16)

David W. Taylor Naval Ship R&D Center
Attn: F. S. Archibald
Code 1942
(Copy No. 17)

David W. Taylor Naval Ship R&D Center
Attn: J. T. Shen
Code 194
(Copy No. 18)

David W. Taylor Naval Ship R&D Center
Attn: A. F. Kilcullen
Code 1962
(Copy No. 19)

DISTRIBUTION LIST FOR UNCLASSIFIED ARL TM 83-27 by K. Ishimaru, dated January 25, 1983.

Office of Naval Research
Department of the Navy
800 N. Quincy Street
Arlington, VA 22217
Attn: R. Whitehead
Code 432F
(Copy No. 20)

Office of Naval Research
Attn: M. M. Reischman
(Copy No. 21)

Defense Technical Information Center
5010 Duke Street
Cameron Station
Alexandria, VA 22314
(Copy Nos. 22 to 27)

Applied Research Laboratory
The Pennsylvania State University
Post Office Box 30
State College, PA 16801
Attn: R. E. Henderson
(Copy No. 28)

Applied Research Laboratory
Attn: B. E. Robbins
(Copy No. 29)

Applied Research Laboratory
Attn: G. C. Lauchle
(Copy No. 30)

Applied Research Laboratory
Attn: J. A. Macaluso
(Copy No. 31)

Applied Research Laboratory
Attn: J. M. Lawther
(Copy No. 32)

Applied Research Laboratory
Attn: S. Hayek
(Copy No. 33)

Applied Research Laboratory
Attn: W. C. Zierke
(Copy No. 34)

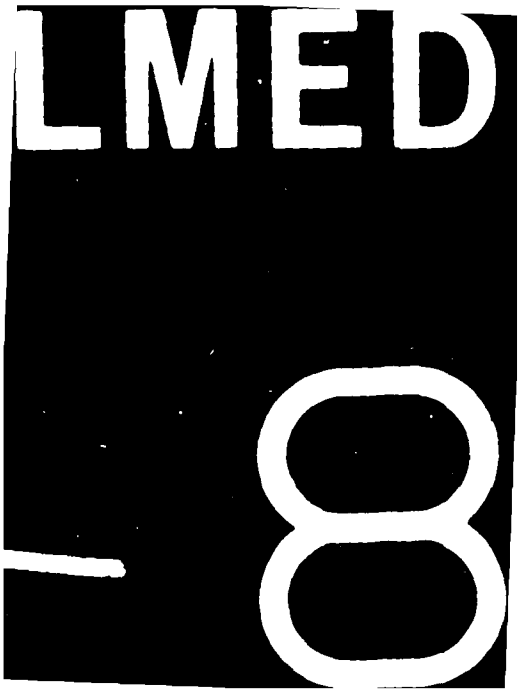
LMED
8